ฤทธิ์ของสารสกัดจากดอกอัญชันในการป้องกันการเกิดไกลเคชันของโปรตีน ความเสียหายออกซิเดชัน ของดีเอ็นเอ และการสร้างเซลล์ไขมันที่ถูกเหนี่ยวนำด้วยเมทิลไกลออกซอล

นายปรมินทร์ ฉายารัตนศิลป์

วิทยานิพนธ์นี้เป็นส่วนหนึ่งของการศึกษาตามหลักสูตรปริญญาวิทยาศาสตรดุษฎีบัณฑิต
สาขาวิชาชีวศาสตร์ทางสัตวแพทย์ ภาควิชากายวิภาคศาสตร์
คณะสัตวแพทยศาสตร์ จุฬาลงกรณ์มหาวิทยาลัย
ปีการศึกษา 2559

PREVENTIVE EFFECTS OF *CLITORIA TERNATEA* EXTRACT ON METHYLGLYOXAL-INDUCED PROTEIN GLYCATION, OXIDATIVE DNA DAMAGE AND ADIPOGENESIS

Mr. Poramin Chayaratanasin

A Dissertation Submitted in Partial Fulfillment of the Requirements
for the Degree of Doctor of Philosophy Program in Veterinary Biosciences
Department of Veterinary Anatomy
Faculty of Veterinary Science
Chulalongkorn University
Academic Year 2016

Thesis Title	PREVENTIVE EFFECTS OF *CLITORIA TERNATEA* EXTRACT ON METHYLGLYOXAL- INDUCED PROTEIN GLYCATION, OXIDATIVE DNA DAMAGE AND ADIPOGENESIS
By	Mr. Poramin Chayaratanasin
Field of Study	Veterinary Biosciences
Thesis Advisor	Associate Professor Sirichai Adisakwattana, Ph.D.
Thesis Co-Advisor	Nipattra Suanpairintr, Ph.D.
	Associate Professor Manuel Alejandro Barbieri, Ph.D.

Accepted by the Faculty of Veterinary Science, Chulalongkorn University in Partial Fulfillment of the Requirements for the Doctoral Degree

.....Dean of the Faculty of Veterinary Science
(Professor Roongroje Thanawongnuwech, Ph.D.)

THESIS COMMITTEE

.....Chairman
(Associate Professor Meena Sarikaputi, Ph.D.)

.....Thesis Advisor
(Associate Professor Sirichai Adisakwattana, Ph.D.)

.....Thesis Co-Advisor
(Nipattra Suanpairintr, Ph.D.)

.....Thesis Co-Advisor
(Associate Professor Manuel Alejandro Barbieri, Ph.D.)

.....Examiner
(Associate Professor Sutthasinee Poonyachoti, Ph.D.)

.....Examiner
(Assistant Professor Sirakarnt Dhitavat, Ph.D.)

.....External Examiner
(Associate Professor Supatra Srichairat, Ph.D.)

ปรมินทร์ ฉายารัตนศิลป์ : ฤทธิ์ของสารสกัดจากดอกอัญชันในการป้องกันการเกิดไกลเคชันของโปรตีน ความเสียหายออกซิเดชันของดีเอ็นเอ และการสร้างเซลล์ไขมันที่ถูกเหนี่ยวนำด้วยเมทิลไกลออกซอล (PREVENTIVE EFFECTS OF *CLITORIA TERNATEA* EXTRACT ON METHYLGLYOXAL-INDUCED PROTEIN GLYCATION, OXIDATIVE DNA DAMAGE AND ADIPOGENESIS) อ.ที่ปรึกษาวิทยานิพนธ์หลัก: รศ. ดร. สิริชัย อดิศักดิ์วัฒนา , อ.ที่ปรึกษาวิทยานิพนธ์ร่วม: ดร. นิภัทรา สวนไพรินทร์, มานูเอล อะลีฮันโดร บาบีเอรี่, 160 หน้า.

การศึกษานี้มีวัตถุประสงค์เพื่อศึกษาฤทธิ์ของสารสกัดจากดอกอัญชันในการต้านปฏิกิริยาไกลเคชั่นที่เกิดในโปรตีนอัลบูมินจากซีรัมของวัว การเกิดออกซิเดชั่นของดีเอ็นเอ และการเกิดอะดิโพเจนนิซิสเซลล์ไขมันจากการเหนี่ยวนำด้วยเมทิลไกลออกซอล ผลการศึกษาพบว่าสารสกัดจากดอกอัญชันประกอบด้วยสารโพลีฟีนอลที่สำคัญได้แก่ เทอร์นาทิน อนุพันธ์ของเดลฟินิดิน ควอเซติน-3-รูติโนไซด์ อะพิเจนนิน-7-นีโอเฮสเพอริโดไซด์ คาเอมเฟอรอล-3-รูติโนไซด์ คาเทชิน-7-กลูโคไซด์ และไซรินเจติน-3-กลูโคไซด์ สารสกัดจากดอกอัญชันที่ความเข้มข้น 250-1,000 ไมโครกรัมต่อมิลลิลิตรสามารถยับยั้งการเหนี่ยวนำของเมทิลไกลออกซอลและน้ำตาลฟรุกโตสในการสร้างสารประกอบเชิงซ้อนในขั้นตอนสุดท้ายของปฏิกิริยาไกลเคชั่นทั้งชนิดที่เรืองแสงและไม่เรืองแสง การเกิดฟรุกโตซามีน โครงสร้างอะไมลอยด์ครอสเบต้า ปฏิกิริยาออกซิเดชั่นโดยลดการเติมหมู่คาร์บอนิลและลดการสูญเสียหมู่ไทออลในโปรตีนจากการเหนี่ยวนำด้วยเมทิลไกลออกซอลและน้ำตาลฟรุกโตส นอกจากนี้ยังสามารถยับยั้งความเสียหายออกซิเดชั่นของดีเอ็นเอโดยผ่านการยับยั้งการเกิดอนุมูลอิสระซุปเปอร์ออกไซด์และไฮดรอกซิลจากระบบของเมทิลไกลออกซอลและไลซีนและระบบเอเอพีเอช กลไกในการยับยั้งปฏิกิริยาไกลเคชั่นของสารสกัดดอกอัญชันคือการจับกับสารประกอบคาร์บอนิลและขจัดอนุมูลอิสระ สารสกัดจากดอกอัญชันที่ความเข้มข้น 500-1,000 ไมโครกรัมต่อมิลลิลิตร สามารถยับยั้งกระบวนการอะดิโพเจนนิซิสที่เหนี่ยวนำด้วยเมทิลไกลออกซอลในระยะต้นของเซลล์ไขมันชนิด 3T3-L1 โดยผ่านการลดการสร้างของเซลล์ไขมันซึ่งกระตุ้นผ่านทาง Akt และ ERK1/2 ส่วนในระยะท้ายของกระบวนการอะดิโพเจนนิซิสนั้น สารสกัดจากดอกอัญชันสามารถลดอะดิโพเจนนิก ทรานคริปชั่นแฟคเตอร์ (adipogenic transcription factors) ได้แก่ PPARγ และ C/EBPα ส่งผลให้มีการลดลงของเอนไซม์ที่ใช้ในการสร้างไขมันไตรกลีเซอไรด์ได้แก่ FAS และ ACC และมีผลให้การสะสมของไขมันไตรกลีเซอไรด์ในเซลล์ไขมันที่โตเต็มวัยลดลง ในเซลล์ไขมันที่ไม่ได้มีการเหนี่ยวนำจากเมทิลไกลออกซอล สารสกัดจากดอกอัญชันที่ความเข้มข้น 500-1,000 ไมโครกรัมต่อมิลลิลิตรสามารถยับยั้งการสร้างเซลล์ไขมันผ่านทาง Akt และ ERK1/2 ในระยะต้นร่วมกับการลดลงของการแสดงออกของยีนที่เกี่ยวข้องกับการสร้างเซลล์ไขมัน PPARγ และ C/EBPα ในระยะท้ายของกระบวนการอะดิโพเจนนิซิส นอกจากนี้สารสกัดจากดอกอัญชันยังสามารถเพิ่มการสลายไขมันในเซลล์ไขมันที่โตเต็มวัย ในการยับยั้งกระบวนการอะดิโพเจนนิซิสที่เหนี่ยวนำด้วยเมทิลไกลออกซอลของสารสกัดจากดอกอัญชันเกิดจากความสามารถในการควบคุม Akt และ ERK1/2 อะดิโพเจนนิก ทรานคริปชั่นแฟคเตอร์ และความสามารถในการดักจับสารเมทิลไกลออกซอลโดยตรงจากการศึกษานี้พบว่าสารสกัดจากดอกอัญชันมีศักยภาพในการนำมาเป็นสารป้องกันปฏิกิริยาไกลเคชั่นและกระบวนการอะดิโพเจนนิซิส ได้

ภาควิชา กายวิภาคศาสตร์ ลายมือชื่อนิสิต .....

สาขาวิชา ชีวศาสตร์ทางสัตวแพทย์ ลายมือชื่อ อ.ที่ปรึกษาหลัก .....

ปีการศึกษา 2559 ลายมือชื่อ อ.ที่ปรึกษาร่วม .....

ลายมือชื่อ อ.ที่ปรึกษาร่วม .....

5375961131 : MAJOR VETERINARY BIOSCIENCES
KEYWORDS: KEYWORDS: CLITORIA TERNATEA EXTRACT, METHYLGLYOXAL, PROTEIN GLYCATION, OXIDATIVE DNA DAMAGE, ADIPOGENESIS

PORAMIN CHAYARATANASIN: PREVENTIVE EFFECTS OF *CLITORIA TERNATEA* EXTRACT ON METHYLGLYOXAL-INDUCED PROTEIN GLYCATION, OXIDATIVE DNA DAMAGE AND ADIPOGENESIS. ADVISOR: ASSOC. PROF. SIRICHAI ADISAKWATTANA, Ph.D., CO-ADVISOR: NIPATTRA SUANPAIRINTR, Ph.D., ASSOC. PROF. MANUEL ALEJANDRO BARBIERI, Ph.D., 160 pp.

This study was aimed to determine the inhibitory effects of *Clitoria ternatea* extract (CTE) on glycation of BSA, oxidative DNA damage, and adipogenesis mediated by methylglyoxal (MG). The results showed that polyphenols in CTE identified by LC-MS/MS were ternatins, delphinidin derivatives, quercetin-3-rutinoside, apigenin-7-*O*-neohesperidoside , Kaemferol-3-*O*-rutinoside, (+)-catechin-7-*O*-b-glucoside, and syringetin-3-*O*-glucoside. CTE (250-1,000 µg/mL) significantly inhibited fructose- and MG-induced formation of fluorescent, non-fluorescent AGEs, fructosamine, amyloid cross β structure, protein carbonyl content and preventing free thiol depletion in BSA system. CTE (250-1,000 µg/mL) suppressed oxidative DNA strand breakage through inhibition of superoxide anion and hydroxyl radical production in 2,2'- Azobis(2-amidinopropane) dihydrochloride (AAPH) and MG/lysine system. The mechanisms of anti-glycation of CTE are a direct carbonyl trapping ability and free radical scavenging activity. In early phase, CTE (500-1,000 µg/mL) inhibited MG-mediated adipogenesis through suppression of cell proliferation related to Akt and ERK1/2 signaling pathway in 3T3-L1 preadipocytes. In late stage of adipogenesis, CTE inhibited MG-induced expression of adipogenic transcription factors including PPARγ and C/EBPα and subsequently down-regulation of fatty acid synthase (FAS) and acetyl-CoA carboxylase (ACC), causing the reduction of TG accumulation in mature adipocytes. When the cells were incubated without MG, CTE (500-1,000 µg/mL) treatment markedly decreased cell differentiation through Akt and ERK1/2 signaling pathway in the early stage of adipogenesis together with suppression of mRNA expression of adipogenic genes (PPARγ and C/EBPα) in late stage of adipogenesis. Furthermore, CTE could enhance lipolysis in mature adipocytes. The inhibition of MG-induced adipogenesis by CTE was due to its effects on the regulation of Akt and ERK1/2 signaling pathway and adipogenic transcription factors and the direct MG trapping ability. This study indicates that CTE can be a potential candidate for the prevention of protein glycation and adipogenesis.

Department:	Veterinary Anatomy	Student's Signature	.....
Field of Study:	Veterinary Biosciences	Advisor's Signature	.....
Academic Year:	2016	Co-Advisor's Signature	.....
		Co-Advisor's Signature	.....

ACKNOWLEDGEMENTS

Firstly, I would like to express my sincere appreciation to my thesis advisor, Assoc. Prof. Sirichai Adisakwattana, for his patience, encouragement and support throughout my Ph.D. study. His guidance helped me all the time, not only research perspective but also many other perspectives of my life. I could not have imagined achieving this long and rough journey to Ph. D. without all the support that I have always received from him.

In my unforgettable memories, I would like to express my special appreciation and grateful thanks to Assoc. Prof. Sirintorn Yibchokanun, for providing me this opportunity and granting me the capability to achieve this successful. Although you have passed away, your almighty love always keeps warm in my heart forever. I would like to thanks for loving me.

I would like to thank Assis. Prof. Dr. Manuel Alejandro Barbieri, my co-advisor, who provided me an opportunity to access the laboratory and research facilities at Florida international university (FIU), USA. In addition, I would like to thank Dr. Nipattra Suanpairintr, my co-advisor, for encouragement.

Moreover, my sincere thank go to Prof. Dr. Sanipa Suradhat and her team for providing me the access to Flow cytometer facilities.

Finally, I am also greatful to all committee members, labmates in Dr. Adisakwattana's research group and Dr. Barbieri's research group, and my family for supporting me.

PC was supported by H.M. the king's 72nd Birthday Scholarship, Graduate School, Chulalongkorn University and Royal Golden Jubilee Ph. D. program Scholarship (PHD/0005/2555), the Thailand Research Fund (TRF), and the Overseas Research Experience Scholarship for Graduate Student, Graduate school, Chulalongkorn University. This research was supported by Grant for International Research Integration: Chula Research Scholar, Ratchadaphiseksomphot Endowment Fund, The Asia Research Center, Chulalongkorn University.

CONTENTS

Page

LIST OF FIGURES

LIST OF TABLES

CHAPTER I

INTRODUCTION

Background and significance of this study

Diabetes Mellitus (DM) is a group of metabolic diseases characterized by hyperglycemia, dyslipidemia, and abnormal protein metabolism that result from defects in both insulin secretion and/or insulin action. Chronic hyperglycemia is a major cause of complications of diabetes through 5 major mechanisms including polyol pathway, the formation of advanced glycation end products (AGEs), increased expression of AGEs receptor, Protein kinase C isoform activation and hexosamine pathway (Stitt, 2001; Giacco and Brownlee, 2010). In general, non-enzymatic glycation is a complex series of reactions between the carbonyl group of reducing sugars (glucose, fructose, and ribose) and the amino group of proteins. Consequently, a reversible structure called as an unstable Schiff's base is formed and spontaneously rearranged into an Amadori product such as fructosamine. During the propagation reaction, the Amadori products react with the amino acids to form irreversible AGEs, including fluorescent and crosslinking AGEs (such as pentosidine and imidazolones) and non-fluorescent and non-crosslinking AGEs (such as N^{ε}-CML) (Singh et al., 2001;

Wu et al., 2011). The accumulation of AGEs in living organisms also contributes to functional modifications of tissue proteins, resulting in the progress of normal aging and the pathogenesis of age-related diseases, such as diabetes, cardiovascular diseases, and Alzheimer's disease (Basta et al., 2004; Ahmed, 2005; Ramasamy et al., 2005; Goh and Cooper, 2008). Fructose is one of the most common reducing monosaccharides found in blood circulation. Evidence supports that high fructose overconsumption has been associated with an increased risk of developing long-term diabetic complications (Bell et al., 2000; Tappy and Le, 2010). Intracellular fructose is increased in a number of tissues in diabetic patients via the polyol pathway, resulting in glycation production approximately 10 times faster than glucose (Suarez et al., 1991). Therefore, there has been serious concern regarding the critical role of dietary fructose in metabolic diseases. Scientists are developing an alternative approach to preventing progression of diabetic complications through the reduction of AGE formation. Aminoguanidine (AG), a well-known antiglycating agent, inhibits the formation of AGEs and prevents the development of diabetic complications in animal models of diabetes. Nevertheless, aminoguanidine has been terminated due to serious adverse effects such as myocardial infarction, congestive heart failure, atrial fibrillation, anemia, and gastrointestinal disturbance (Thornalley, 2003b; Friedman, 2010). There has been a great deal of interest in using plant-based foods for prevention and amelioration of AGE-mediated diabetic complications (Wu et al., 2011; Ramkissoon et al., 2013).

The scientific evidence indicates that highly reactive dicarbonyl compound, namely methylglyoxal (MG), is a reactive precursor to produce AGEs associated with diabetic complications such as nephropathy, neurodegenerative disease and atherosclerosis (Jagt, 2008). In both type I and type II diabetic patients, MG is found in 2-6 fold higher plasma level (Brownlee et al., 1988; Wu and Chan, 2007). Due to their greater amount of dicarbonyl compounds and reactive oxygen species (ROS) formation during glycation and autoxidation, these intermediates are a predominant factor relating to acceleration of AGEs production (Suarez et al., 1989; Schalkwijk et al., 2004; Hori et al., 2012). Non-enzymatic crosslinking of MG with lysine or arginine residues of proteins during AGEs formation is able to generate reactive oxygen species (ROS) including superoxide and hydroxyl radical (Kang, 2003b). It is supposed to be a causative factor mediated an oxidative modification and subsequent damage on cellular components including proteins (Desai et al., 2010) and DNA (Kang, 2003a; Suji and Sivakami, 2007). The oxidative stress also plays an essential role in diabetic complications (Kawahito et al., 2009). Besides, the eveidence also supported that MG could mediated adipogenesis via Akt signaling pathway resulting in cell proliferation (Jia et al., 2012). Increased of number and size of adipocytes contributes to the obesity which is preliminary factor for insulin resistance. Therefore, there has been seriously concerned regarding the critical role of dicarbonyl compound and free radical generated in glycation reaction and adipogenesis.

Clitoria ternatea L. (family: Fabaceae) or butterfly-pea is a famous traditional plant that has been used for centuries in traditional medicine. In Asian and America, it is commonly recommended for the treatment of snakebite, scorpion sting, chronic bronchitis, indigestion, constipation, fever, arthritis, eye ailments, sore throat, skin diseases, rheumatism, syphilis, eye and ear-diseases (Mukherjee et al., 2008). The main phytochemical components of *Clitoria ternatea* extract (CTE) are delphinidin-derived anthocyanins including delphinidin-3,5-glucoside, delphinidin-3β-glucoside and six major delphinidin-based ternatins (ternatins A1, A2, B1, B2, D1 and D2) (Terahara et al., 1990; Terahara et al., 1996). CTE has been reported to possess many pharmacological effects such as anti-microbial, anti-platelet aggregation, anti-inflammatory, anti-pyretic, and anti-helmintic activities (Mukherjee et al., 2008; Gupta et al., 2010). In addition, CTE exerts anti-hyperglycemic and anti-hyperlipidemic effects in alloxan-induced diabetic rats (Daisy and Rajathi, 2009; Daisy et al., 2009). To the best our knowledge, there have been many studies demonstrating the anti-diabetic activity of CTE; however, the studies regarding the effect of CTE on anti-glycation activity remain unknown. Therefore, it would be interesting to examine the effect of CTE against bovine serum albumin (BSA) in fructose and MG-induced non-enzymatic glycation. Moreover, the study investigated the effect of CTE on 2,2'-Azobis(2-amidinopropane) dihydrochloride (AAPH) and MG-induced oxidative damages of DNA. Antioxidant activity of CTE was also determined in various *in vitro* models. The inhibitory effects of CTE and its underlying cellular mechanisms on the adipogenesis and lipid accumulation were also been

investigated by using 3T3-L1 cells This work would provide more fundamental and scientific information for further development of nutraceutical and functional foods of diabetic patients to prevent the complications.

Objectives of the present study

1. To study the preventive effect of CTE on glycation of bovine serum albumin (BSA) induced by fructose and methylglyoxal *in vitro*
2. To determine the antioxidant effects of CTE
3. To investigate the preventive effect of CTE on oxidative damage of DNA induced by 2,2'-Azobis (2-amidinopropane) dihydrochloride (AAPH) and methylglyoxal *in vitro*
4. To explore the preventive effect of CTE on adipogenesis *in vitro*
5. To explore the preventive effect of CTE on methylglyoxal mediated adipogenesis *in vitro*

Hypotheses of this study

1. CTE could prevent fructose- and MG-induced glycation of bovine serum albumin (BSA) by reducing the formation of AGEs and the oxidative-dependent protein damage.
2. CTE could directly trap to reactive carbonyl compound and scavenge reactive oxygen species via the capacity to scavenge DPPH, TEAC, FRAP, HRSA, SRSA and FICP

3. CTE could prevent oxidative DNA damage induced by AAPH and MG/lysine system through reducing ROS generation and DNA strand break.
4. CTE could prevent adipogenesis by reducing Akt and ERK phosphorylation, subsequently inhibit preadipocyte proliferation and differentiation whereas CTE could enhance the lipolysis of preadipocyte.
5. CTE could prevent MG-induced adipogenesis by inhibiting the phosphorylation of Akt and contributing to suppress preadipocyte cell proliferation, differentiation and stimulation of lipolysis.

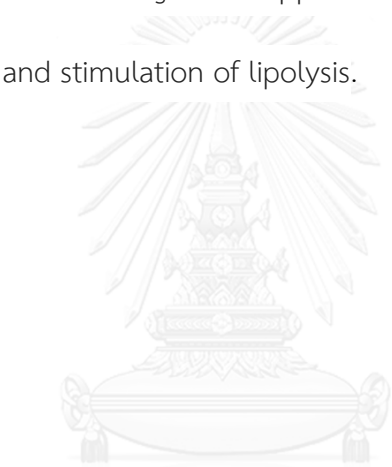

CHAPTER II

LITERATURE REVIEW

2.1 Glycation and its mechanisms

Hyperglycemia plays a major role in the progression of diabetic complications *via* protein glycation which causes various types of protein and chemical modifications, resulting in the generation of irreversible heterogeneous byproducts termed advanced glycation end products (AGEs) (Singh et al., 2001). AGEs formation could be occurred through the glycation reaction as shown in Figure 1. In the early stage of glycation, protein glycation involves a series complex reaction that occurs between reducing sugars (glucose and fructose) and amino acids or protein, which produces an unstable Schiff's base. It has been found that rate of fructose in intracellular glycation production is faster than that of glucose because fructose-induced protein glycation is a predominant source of reactive oxygen species (ROS) and reactive carbonyl species (RCS) generated by both non-oxidative and oxidative pathways (glycoxidation) (Suarez et al., 1989; Ruderman et al., 1992). Then, the Schiff's base can be turned into an Amadori product such as fructosamine. Fructosamine is clinically used as an indicator for short-term control of blood sugar in diabetic patients, the reduction of fructosamine is hence a therapeutic way to delay incidence of vascular complications (Shield et al.,

1994; Ardestani and Yazdanparast, 2007). During the propagation reaction, the Amadori products react with the amino acids to form irreversible AGEs. The production of N^{ε}-(carboxymethyl)lysine (CML) is one of well-known AGEs formed either from oxidative breakdown of Amadori products or polyol pathway mediated by α-oxoaldehydes such as glyoxal, methylglyoxal, and 3-deoxyglucosone (Singh et al., 2001). Previous studies show that MG can also react with the amino groups of long-lived proteins to produce non-enzymatic cross-links or AGEs (Wu et al., 2011).

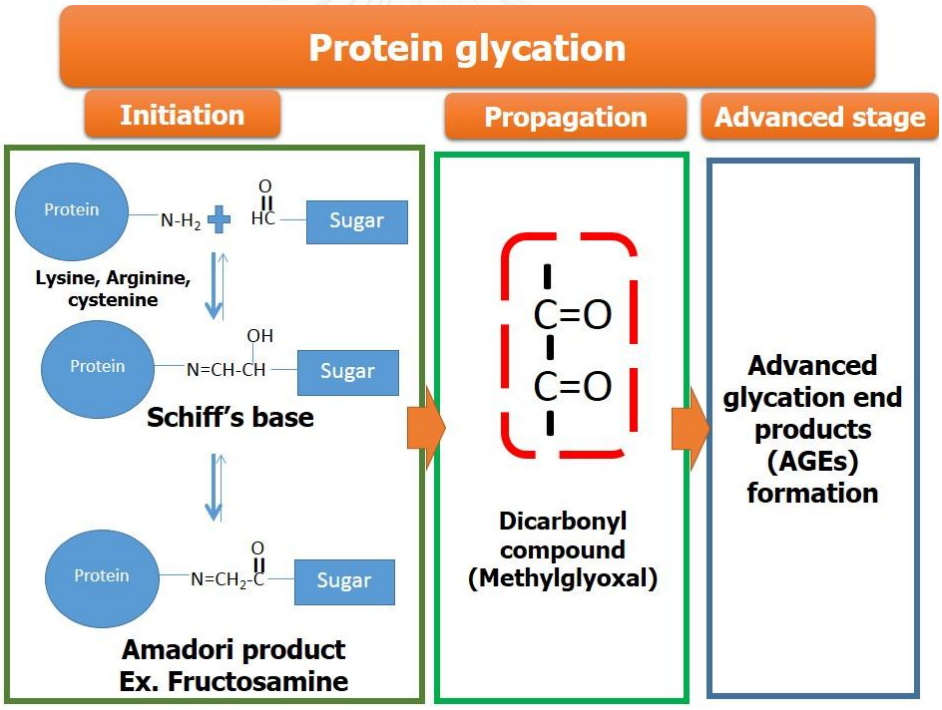

Figure 1 Chemical glycation pathways leading to AGEs formation, modified from (Wu et al., 2011).

2.2 Effect of protein glycation and AGEs related to diabetic complications

The accumulation of AGEs in living organisms also contributes to functional and structural modifications of tissue proteins resulting in the progress of normal aging and the pathogenesis of age-related diseases, such as diabetes, cardiovascular diseases, and Alzheimer's disease (Basta et al., 2004; Goh and Cooper, 2008) The chemical nature of AGEs *in vivo* is largely unknown, but there is a growing population of structurally defined AGE adducts such as pyrraline, pentosidine, N□-carboxy-methyl lysine (CML) and crossline that are found to be elevated in diabetic tissues as illustrated in Figure 2 (Dyer et al., 1993; McCance et al., 1993; Stitt, 2001). The most found chemically characterized AGEs in humans are pentosidine and CML (Price et al., 2001). AGEs can act as mediators and initiate a wide range of abnormal responses in cells and tissues involving accumulation of extra-cellular matrix, initiation of apoptosis, and decrease of solubility, elasticity and enzymatic affinities in long-living proteins such as collagen (Dunn et al., 1989). The glycation of lens crystallines induces conformational changes and increased glycation of Na^+-K^+ ATPase which reduces its activity, thus altering intracellular ion concentration and subsequent water movement via osmosis results in the cataract formation in diabetic patients (Cheng and Gonzalez, 1986). Circulating proteins in blood, modified by AGE precursors, can bind to AGE receptors and activate them leading to the production of inflammatory cytokines (Wu et al., 2011; Gaens et al., 2013). AGEs are also toxic to pericytes possessing AGE receptors, and damage to pericytes in diabetic retinopathy (Zong et al., 2011).

Furthermore, the levels of AGEs are correlated to the obesity which is the risk factor for insulin resistance (Uribarri et al., 2015). Activation of IGF-1 receptors by AGEs promoted the differentiation of 3T3-L1 via Akt pathway (Yang et al., 2013). Receptor for AGEs (RAGE) have found to be involved in adipocyte hypertrophy and insulin sensitivity associated with attenuation of insulin-stimulating signaling and glucose uptake in 3T3-L1 cells and mice (Monden et al., 2013).

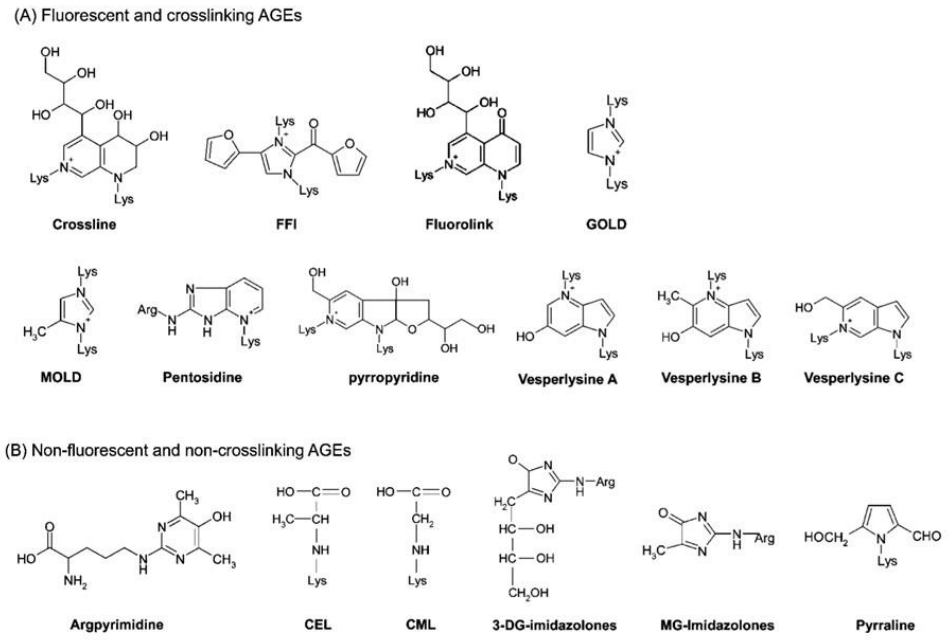

Figure 2 Chemical structures of two types of AGEs: fluorescence AGEs (A) and non-fluorescence AGEs (B) (Wu et al., 2011).

2.3 Methylglyoxal (MG)

MG is a reactive carbonyl compound which is composed of two carbonyl groups in the molecule (see structure of MG in Figure 3). MG is produced endogenously from glycolysis, protein and fatty acid metabolism. MG also found exogenously dietary intake such as brewed coffee, milk, bakery products and honey (Hayashi and Shibamoto, 1985). Glycolysis is supposed to be mainly process for MG synthesis. During glycolysis, MG synthase converts dihydroxyacetone phosphate (DHAP), which is triose phosphate intermediate, into MG particularly in inadequate inorganic phosphate condition (Figure 4) (Nemet et al., 2006). Other sources of MG are proposed to derive from intermediates of protein and fatty acid metabolism such as L-threonine and glycine, and acetone respectively (Figure 5) (Desai et al., 2010). MG is also produced from by Semicarbazide-sensitive (SSAO), which catalyzes breakdown of aminoacetone to MG and by acetone and acetol mono-oxygenase (AMO) which converts acetone to acetol and acetol to MG (Beisswenger et al., 2003). In hyperglycemia, MG is synthesized by fructose produced from glucose through polyol pathway or autoxidation of sugar, oxidation of Schiff's base and Amadori products (Chang and Wu, 2006).

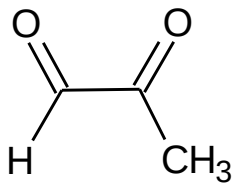

Methylglyoxal

Figure 3 Chemical structures of methylglyoxal (Wang and Ho, 2012).

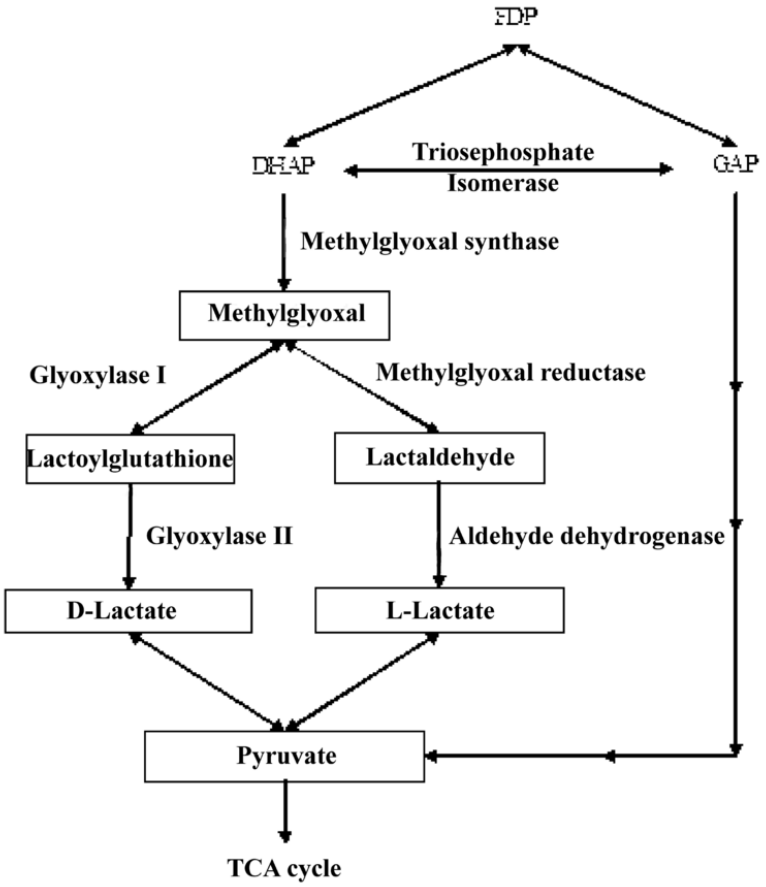

Figure 4 The production of methylglyoxal from glycolysis. FDP: fructose 1,6-diphosphate, DHAP: dihydroxyacetone phosphate, GAP: glyceraldehyde 3-phosphate, TCA cycle: tricarboxylic acid cycle or the Krebs cycle (Hasim et al., 2014).

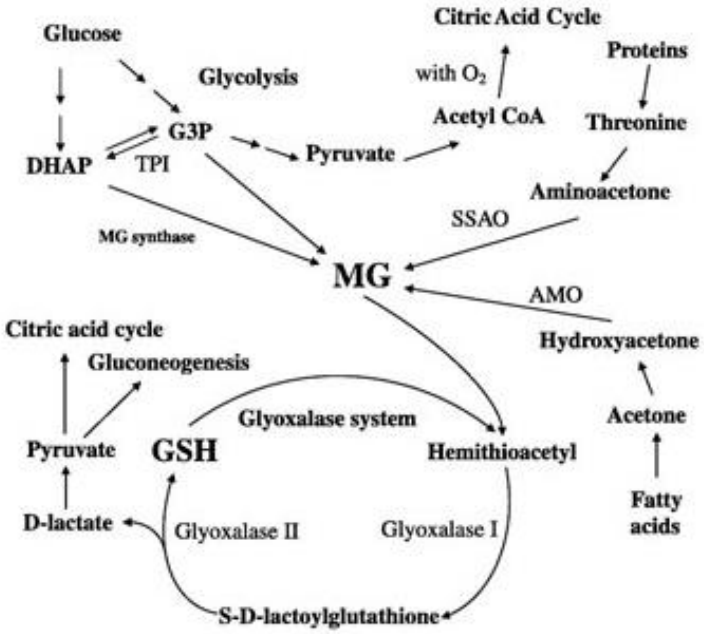

Figure 5 The production of methylglyoxal and detoxification from other mechanisms including carbohydrate, protein and lipid metabolism. AMO: acetone monooxygenase, DHAP: dihydroxyacetone phosphate, G3P: Glyceroldehyde 3-phosphate, SSAO: semicarbazide-sensitive amine oxidase, TPI: triosephosphate isomerase (Chang and Wu, 2006).

When MG is produced, the removal of MG is catalyzed by glyoxylase system (Figure 6). Glyoxylase system consists of glyoxylase I and glyoxylase II contributing to MG degradation to D-lactic acid. MG first non-enzymatically reacts with reduced glutathione (GSH) resulting in hemithioacetal formation which is substrate for glyoxylase I and then D-lactic acid degradation by glyoxylase II. D-lactate can eventually be metabolized further to pyruvate for the citric acid cycle. As a result, GSH

and GSH-related enzyme including glutathione peroxidase and glutathione reductase play a major role in MG catabolism through GSH-dependent glyoxylase system to keep MG in low levels (Jagt, 2008). It has been found that plasma levels of MG in diabetic patients increase 2-6 fold compared to healthy people (Brownlee et al., 1988; Wu and Chan, 2007). A recent study demonstrated that MG accumulation and malfunction of glyoxylase system were correlated with several metabolic diseases such as diabetes, cardiovascular disease, cancer and disorders of the central nervous system (Maessen et al., 2015). Decreased MG degradation was due to defect of glyoxalase-1 and subsequently reduced glutathione activities contributed to increase glycation and tissue damage related to aging process and oxidative stress formation (Thornalley, 2003a). On the other hands, overexpression of glyoxalase-1 appeared to decrease hyperglycemia-induced MG accumulation (Shinohara et al., 1998; Schlotterer et al., 2009). Furthermore, high levels of reduced glutathione resultes in degradation of MG via glyoxalase system (Ferguson and Booth, 1998). In hyperglycemic condition, increased polyol pathway causes the competitive usage of NADPH by aldose reductase and glutathione reductase. Consequently, this situation can contribute to MG accumulation as a result from a decrease in available of reduced glutathione that is required for glyoxalase system (Cheng and Gonzalez, 1986).

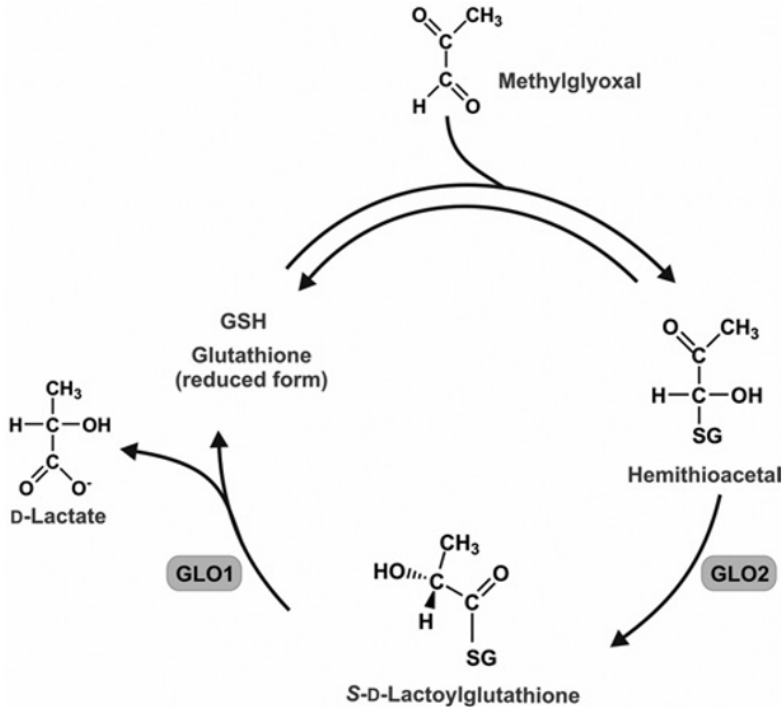

Figure 6 Glyoxalase (GLO) system (Silva et al., 2013)

2.4 Pathological effects of MG

In normal condition, alpha-oxoaldehydes can be mainly degraded through glyoxalase system. Therefore, the accumulation of alpha-oxoaldehyde such as MG comes from the production exceeding the efficacy of degradation system (Beisswenger et al., 2003; Chakraborty et al., 2014). As a highly reactive dicarbonyl compound, it suggests that MG becomes harmful through glycation of protein and free radical generation. For the modification of protein, MG is proposed to be found in a major sources of intracellular and plasma AGEs formation (Kilhovd et al., 2003; Mostafa et al., 2007). MG (1 μM) at physiological level irreversibly formed MG-derived adducts

after a 24-hour incubation in human plasma at 37 ^{o}C (Thornalley, 2005). The MG adducts were slowly degraded over 21 days after the incubation (Thornalley, 2005). Recently published, MG can modify protein and DNA resulting in disfunctionality of those molecules following pathological conditions (Kang, 2003a; Kang, 2003b; Frischmann et al., 2005; Jia et al., 2006; Chang et al., 2011). Excess MG, which is not degraded by glycoxylase system, also non-enzymatically reacts preferably with arginine and lysine residues of proteins and then forms irreversible AGEs (Ahmed et al., 1997). AGEs can cause the modification of protein leading to loss of structure and function of protein related to diabetic complications as earlier mentioned above. Besides, MG-induced protein glycation is a predominant source of ROS and reactive carbonyl species (RCS) generated by both non-oxidative and oxidative pathways (glycoxidation) (Rahbar and Figarola, 2003). MG is a causative factor of oxidative damage of DNA by non-enzymatic crosslinking with lysine contributing to superoxide and hydroxyl radical generation (Lee et al., 1998; Kang, 2003b). Furthermore, MG also increases oxidative stress by reducing antioxidants such as GSH, glutathione peroxidase and glutathione reductase leading to impair the detoxification of MG (Paget et al., 1998; Beard et al., 2003; Park et al., 2003; Nicolay et al., 2006). The damage inflicted by ROS particularly to DNA showed a correlation with life span, genetic mutations, accelerated aging (Barja and Herrero, 2000; Finkel and Holbrook, 2000; Mandavilli et al., 2002). It is also demonstrated that MG has a critical role in pathogenesis of insulin resistant and type II diabetes. MG can directly cause insulin resistance by decreasing tyrosine

phosphorylation of insulin receptor substrate 1 (IRS-1). It supposed to be that MG could non-enzymatically modify amino acid residues especially lysine and arginine that usually found in active sites of insulin signaling protein (Jia and Wu, 2007). The role of MG in inducing oxidative stress is also well validated. ROS generation induced by MG affects to alteration of cellular signaling pathways, leading to the insulin resistance as well (Chang et al., 2005).

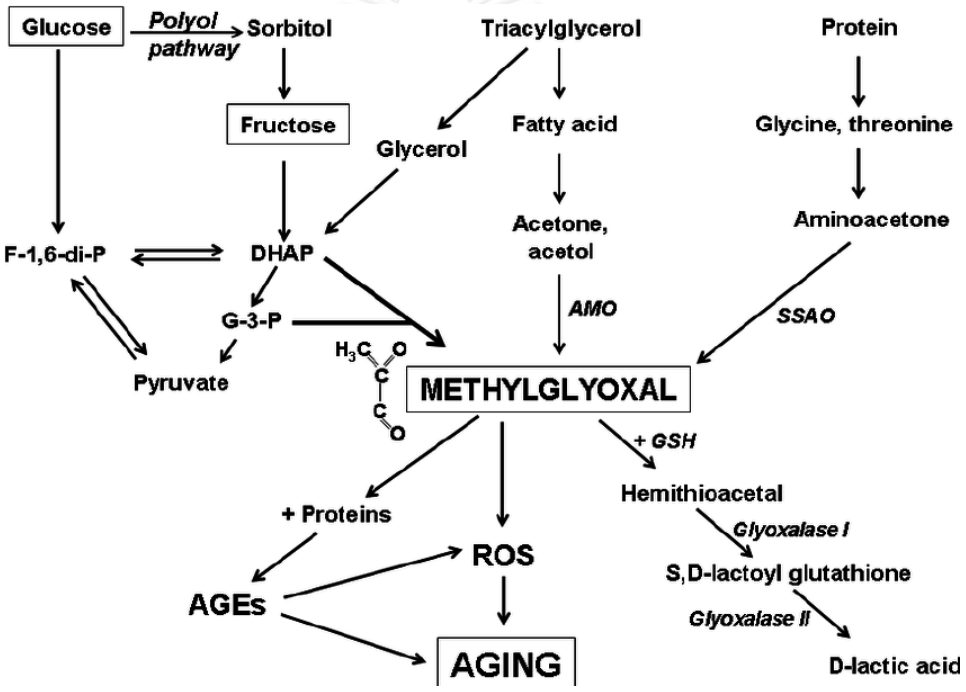

Figure 7 Methylglyoxal: formation, degradation, and cellular effects. DHAP: dihydroxyacetone phosphate; AMO: acetol/acetone monooxygenase, SSAO: semicarbazide-sensitive amine oxidase, F-1,6-di-P: fructose-1,6-diphosphate, G-3-P: glyceraldehyde-3-phosphate (Desai et al., 2010).

2.5 The effect of MG on oxidative DNA damage

Increased MG levels play a major role on development and progression of diabetes and its complications (Vander Jagt, 2008). MG can react with lysine and arginine residues of protein to form advanced glycation end-products (AGEs) by non-enzymatic protein glycation as mention aboved. It has been demonstrated that the glycation reaction between MG and lysine residue of protein also generates reactive oxygen species (ROS) including superoxide and hydroxyl radical generation *in vitro*. Consequently, depletion of thiol-containing protein and an increase in protein carbonyl formation are occurred and indicated as protein oxidation (Guerin-Dubourg et al., 2012). Apart from the protein modification, ROS generation from the reaction between MG and lysine leads to oxidative DNA damage indicating by strand breakage of DNA (Kang, 2003b). Thereby, MG and amino acids system has been used as model to study oxidative DNA damage from ROS production during the glycation. MG-mediated cross-linking of protein contributes to the generation of free radicals including the the enediol radical anion of MG and crosslinked MG dialkylimine radical cation (protonated form) (Suji and Sivakami, 2007). The MG protonated cation form is responsible for the generation of the cross-linked radical cation as a precursor of fluorescent AGEs. Besides, MG-radical anions are capable to donate an electron to oxygen molecule to generate the superoxide radical anion under aerobic conditions (Suji and Sivakami, 2007). Furthermore, the presence of a transition metal ion (such as Cu^{2+}) enhances DNA

damage induced by MG/lysine system due to Fenton reaction producing more highly reactive hydroxyl radicals (Kang, 2003b).

2.6 The effect of MG on obesity

Obesity is one of leading factor in the metabolic syndrome caused by an imbalance between food intake and energy expenditure (Flatt, 2007; Redinger, 2009). Nowadays, obesity is a growing global health problem causing the development of type 2 diabetes, cardiovascular diseases and artherosclerosis (Kahn and Flier, 2000; Greenberg and McDaniel, 2002; Guilherme et al., 2008). Obesity is mainly associated with increased expansion of white adipose tissue through the activation of adipogenesis (Sethi, 2000). The process of adipogenesis involves in the changes of cell morphology from fibroblast-like shape of preadipocyte to mature and increased lipid synthesis and accumulation in adipocytes. Adipogenesis is generally described as a two-step process including cell proliferation and differentiation, resulting in an increase of the number (hyperplasia) and size (hypertrophy) of adipocytes. In early stage, pre-adipocytes are proliferated through activation of Akt and ERK signaling pathway. After the proliferative phase, they undergo to the formation of mature adipocytes from fibroblast-like pre-adipocyte into spherical shape. Accumulation of the triglyceride (TG) in mature adipocyte is activated by expression of the adipogenic transcriptional factors including PPARγ and C/EBPα leading to regulation of fatty acid synthase (FAS) and acetyl CoA carboxylase (ACC) (Niemelä et al., 2008). Moreover, Akt1 and MAPK signaling pathway

plays a pivotal role in regulating adipogenesis from cell proliferation to differentiation (Bost et al., 2005; Feve, 2005; Chuang et al., 2007). Activation of Akt1 promotes cell cycle progression and terminates cell differentiation into mature adipocyte (Jia et al., 2012). It has shown that activation of Akt1 markedly inhibited p21 and p27 (Cdk inhibitors) and subsequently triggered Cdk2 in the cell cycle progression (Jia et al., 2012; Ferguson et al., 2016). As a result, the mature adipocytes expand the size through an increasing in the storage of triglyceride (Jia et al., 2012). In consistency, it has been reported that MG could mediate adipocyte proliferation by increasing phosphorylation of Akt1. Then, activated Akt1 prevents inhibitory effect on Cdk2 by cyclin-dependent-kinase (Cdk) inhibitors (p21 and p27) phosphorylation contributing to proliferation and differentiation of adipocytes (Jia et al., 2012). Besides, it can be hydrolysed by hormone sensitive lipase (HSL) in deprivation status for energy homeostasis responding to catecholamines and insulin (Jaworski et al., 2007). Apart from Akt pathway, ERK signaling pathway also contributes to the commitment effect in adipogenesis by turning proliferative step and increasing differentiation in adipocytes (Sale et al., 1995; Prusty et al., 2002; Tang et al., 2003). As a result, an increase in number and size of adipocytes contributes to adipose tissue inflammation related to accumulation of . Thereafer, Inflammatory cytokines including TNFα and IL-6 were secreted from macrophage involving in pathogenesis of insulin resistance (Qatanani and Lazar, 2007). Therefore, the obesity is preliminary factor for insulin resistance which links to hyperglycemia leading to diabetic complications via glycation reaction.

2.7 Proposed mechanisms of anti-glycation agents

Toxicity of glycation reaction has been repetitively published association with the pathology of several metabolic diseases as mention aboved. The anti-glycating agents have been developed to inhibit AGEs formation, especially natural phytochemical compounds with less side-effects (Wu et al., 2011). The biochemical mechanisms of the natural compounds, shown in the Figure 8 have been proposed as following (Wu et al., 2011):

1) Scavenging of free radicals generated during early stage of glycation

During the early stage, reducing sugar, Schiff's bases and Amadori products are prone to oxidation and generate free radicals and reactive carbonyl groups. In addition, glycated protein can catalyze the production of freeradicals. Therefore, the anti-glycation mechanisms may yield on alleviation of oxidative stress and reactive carbonyl compounds production.

2) Inhibiting the formation of late-stage Amadori products

3) Blocking the reactive carbonyl compounds or carbonyl group in reducing sugars, Schiff's bases or Amadori products

4) Chelating metal ion

AGEs formation is accelerated by the auto-oxidation of reducing sugar, Schiff's bases and Amadori products in the presence of transition metal ions such as copper ion (Cu^{2+}) and ferrous and ferric ion (Fe^{2+} and Fe^{3+}) (Hunt et al., 1988). Therefore, metal ion chelator could be potential to inhibit AGEs formation.

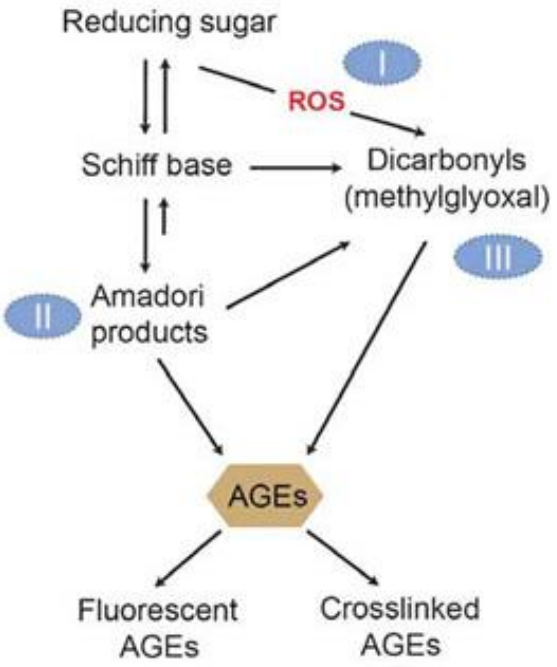

Figure 8 Antiglycation mechanisms of natural compounds. AGE inhibitors have been summarized as indicated by the number. I: Scavenging of free radicals and chelating metal ion. II: Inhibiting the formation of Amadori products, III: Blocking the reactive carbonyl compounds (Wu et al., 2011).

Aspirin was a first anti-glycating agent by acetylating to the free amino group of proteins. Although the competitive binding of the protein with sugar reduced the level of AGEs formation, aspirin must be applied for a long duration with high dose leading to increased side-effects (Rao et al., 1985). Therefore, this anti-glycating drug is unsuitable to use for glycation prevention. Another anti-glycating agent is nucleophilic hydrazine compound called aminoguanidine (AG) (see structure in Figure 9). AG is able to effectively inhibit AGE-induced crosslinking and fluorescent substance production

by trapping reactive carbonyl compound and terminate the Maillard reaction. In animal models, AG can prevent glucose-induced intermolecular collagen crosslinking, AGEs formation, and diabetic complications (Brownlee et al., 1986; Thornalley, 2003b). However, clinical trials of AG that designed to prevent the progression of type I and type II diabetic nephropathy were terminated due to safety concerns. Reported side effects of AG in clinical therapy were gastrointestinal disturbance, abnormalities in liver function tests, flu-like symptoms, and a rare vasculitis (Freedman et al., 1999). Furthermore, kidney tumours were found in AG-treated diabetic rats (Oturai et al., 1996). Other inhibitors of protein glycation include antioxidants, such as vitamin C and vitamin E, and metal ion chelators (desferoxamine and penicillamine) (Elosta et al., 2012). Due to the side effect and safety concerns of several anti-AGE drugs, natural anti-AGEs agents have been developed and investigated to provide a therapeutic approach for delaying and preventing aging and diabetic complications.

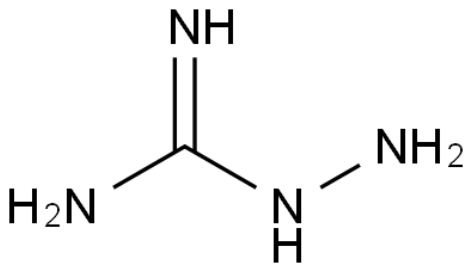

Figure 9 Chemical structure of aminoguanidine (Thornalley, 2003b).

2.8 Beneficial effect of carbonyl trapping ability against glycation.

The increase of reactive carbonyl compounds has associated with the diabetic complication as mentioned above. Non-enzymatic glycation reaction progressively and irreversibly modifies the proteins over time and yield AGEs formation. AGEs are responsible for the development of diabetes mellitus and its complications (Ahmed, 2005). The reaction can be accelerated by reactive oxygen species (ROS) and reactive carbonyl species (RCS), which are produced from glycation, sugar autoxidation (Wu et al., 2011). The accumulation of RCS such as MG derived from carbohydrates or lipids metabolism, are responsible for the formation of advanced glycation end products (AGEs) and the development of various aging-related diseases (Jagt, 2008). Therefore, the carbonyl trapping ability is proposed to be a necessary mechanism to inhibit the formation of AGEs and prevents the development of diabetic complications and age-related diseases. Besides to antioxidant activity to suppress excessive generation RCS, a direct trapping of RCS is the effective strategies to protect from RCS-associated pathogenic conditions (Ho and Wang, 2013). Many evidences have demonstrated that direct trapping ability contributes to inhibiton of MG-derived AGEs formation (Wang et al., 2011; Mesias et al., 2013; Sompong and Adisakwattana, 2015). It has been reported that carbornyl trapping ability of grape skin extract is correlated with total phenolic content (Harsha et al., 2016). Catechin shows the effective MG trapping to form mono-MG-catechin and di-MG-catechin adducts in a time- and dose-dependent manner (Zhu et al., 2014). Proanthocyanidins (Peng et al., 2008a) and genistein (Lv et al., 2011) have

been also shown to inhibit AGEs formation through MG trapping ability. It has been reported that flavonoids exhibit the MG trapping ability (Shao et al., 2014). Quercetin and apigenin exert MG trapping ability at pH 7.4 and 37 °C. The major adducts between MG and quercetin has been revealed as mono- and di-MG adducts. The essential structure to facilitate carbonyl trapping ability have been documented (Shao et al., 2014). The A ring is the active site of flavonoids to enhance the MG-trapping efficacy, and the hydroxyl group at C-5 on the A ring contributes to the trapping efficacy. Base on the trapping mechanism, quercetin showed the best trapping efficacy of MG compared to luteolin, and epicatechin, indicating that the ketone group at the C-4 position of quercetin enhances the trapping efficacy of flavonoids. Consequently, quercetin significantly inhibited MG-mediated AGE formation (Wu and Yen, 2005). Furthermore, an additive effect of MG-trapping ability was found in two flavonoids including phloretin (found in apple) and quercetin (Shao et al., 2014). It is suggested that flavonol and flavone of flavonoids can act as scavengers of reactive dicarbonyl species.

2.9 Beneficial effects of anti-oxidant as anti-glycating agents

Free-radicals are generated during the early stage of glycation. The oxidation of reducing sugar, Schiff's bases and Amadori products could be occurred by themselves to generate free radicals and reactive carbonyl groups in the presence of transition

metal ions and subsequently accelerate the formation of AGEs (Hunt et al., 1988). The reactive oxygen species (ROS) are generated during glycation and glycoxidation that causes the oxidation of side chains of amino acid residues in protein resulting in carbonyl derivatives formation as well as an oxidative defense reduction of protein by decreasing thiol groups (Murphy and Kehrer, 1989; Balu et al., 2005). Therefore, anti-glycation strategies at an early stage involve scavenging hydroxyl radicals and superoxide radicals to alleviate oxidative stress and reducing the generation of reactive carbonyl or dicarbonyl groups. The antioxidant agents can also protect against free-radicals generated during glycation, contributing to reduce the formation of AGEs. Moreover, metal chelators can prevent reducing sugars and Amadori products from self-oxidation, leading to the inhibition of AGE formation (Wu et al., 2011). It has been shown that many antioxidant-containing foods can scavenge free-radicals generated during the glycation process as well as prevent reducing sugars and Amadori products from self-oxidation, resulting in the inhibition of AGE formation (Elosta et al., 2012).

2.10 Phytochemicals with anti-glycation activity

A large number of natural products containing polyphenols, especially edible plants, has been proven relatively safe with less side effects and low toxicity for animals and human. They become more interesting because of their functional properties such as antioxidants and anti-glycation. There has been enormous interest

in the development of alternative medicines for oxidative stress and related disorders. It has been reported that the many phytochemical compounds including flavonoids and anthocyanins show potent free radical scavenging activities as well as metal ion chelating properties (Mira et al., 2002; Kähkönen and Heinonen, 2003). Most of the edible plants have been demonstrated to possess phenolic compounds and flavonoids against AGEs formation in glycation reaction (Cervantes-Laurean et al., 2006; Sang et al., 2007; Urios et al., 2007).

Flavonoids are found in various types of vegetables, tea and red wine. The basic structure of flavonoids is three benzene rings with one or more hydroxyl groups as illustrated in Figure 10. Flavonoids can be divided into different major classes such as flavonols, flavanones, flavones, isoflavones, flavonols and anthocyanidins based on differences in molecular backbone structure (Table 1) (Beecher, 2003). This structure is also the important factor that possess their antioxidant and anti-glycation activity (Matsuda et al., 2003). The inhibitory potency of the flavonoids against AGEs formation was approximately shown in respect to the order of flavone > flavonols > flavanols > flavanone. It is proposed that the hydroxyl group at the C-3 position was found the association with the inhibitory effects on AGEs formation. Similar to flavanols, the presence of the hydroxyl group at the C-5 and C-3 positions in the B ring affects their inhibitory effects against glycoxidation (Matsuda et al., 2003). Furthermore, the correlation of antioxidant activities and anti-glycation ability has also been reported (Wu and Yen, 2005). A number of flavonoids has been reported to exhibit anti-glycation

activity (Chinchansure et al., 2015). For example, the flavonols including kaempferol and quercetin were able to act against glycation reaction through suppress of AGEs in BSA/glucose system in *vitro* (Sasaki et al., 2014). Moreover, short-term feeding (10 days) of kaempferol to old rats was demonstrated the anti-oxidative and anti-inflammatory effects to modulate AGEs accumulation and RAGE expression (Kim et al., 2010b). Quercetin also exhibited a protective effect against glycation and provided in vitro protection against protein damage (Kim et al., 2011).

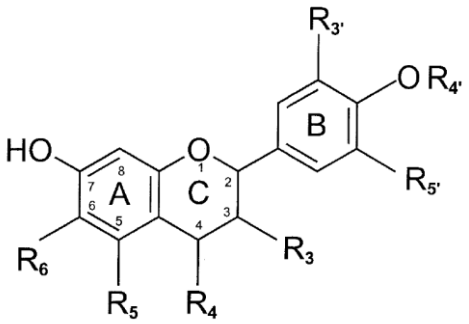

Figure 10 The basic structure of Flavonoids (Beecher, 2003).

Flavonoid subclass	B-ring connection to C ring (position on C ring)	C-ring unsaturation	C-ring functional groups	Prominent food flavonoids[2]	Typical rich food sources[3]
Flavanol	2	None	3-Hydroxy	(+)-Catechin (C) (+)-Gallocatechin (GC) (−)-Epicatechin (EC) (−)-Epigallocatechin (EGC)	Teas, red grapes and red wines
			3-O-gallate	(−)-Epicatechin-3-gallate (ECG) (−)-Epigallocatechin-3-gallate (EGCG)	
Flavanones	2	None	4-Oxo	Eriodictyol Hesperetin Naringenin	Citrus foods
Flavones	2	2-3 Double bond	4-Oxo	Apigenin Luteolin	Green leafy spices, e.g., Parsley
Isoflavones	3	2-3 Double bond	4-Oxo	Daidzein Genistein Glycitein Biochanin A Formononentin	Soybeans, soy foods and legumes
Flavonols	2	2-3 Double bond	3-Hydroxy, 4-Oxo	Isorhamnetin Kaempferol Myricetin Quercetin	Nearly ubiquitous in foods, e.g., Quercetin
Anthocyanidins	2	1-2, 3-4 Double bonds	3-Hydroxy	Cyanidin Delphinidin Malvidin Pelargonidin Petunidin Peonidin	Red, purple and blue berries

Table 1 Flavonoid subclasses, their chemical characteristics, names of prominent food flavonoids and typical food sources (Beecher, 2003).

2.9 Anthocyanins

Anthocyanidins are members of the flavonoid family of polyphenol phytochemicals found in various plant foods. Anthocyanidins are the most important water-soluble components of the red, blue and purple pigments of the majority of flower petals, fruits and vegetables (Tsao, 2010). Anthocyanidins in edible plants is primarily found in glycosidic forms, commonly called as anthocyanins. It has been revealed that most of anthocyanins are based on cyanidin, delphinidin and pelargonidin and their methylated derivatives as illustrated in Figure 11. A total of more than 500 anthocyanins are classified depending on the hydroxylation, methoxylation patterns on the B ring, and glycosylation with different sugar units (Tsao, 2010).

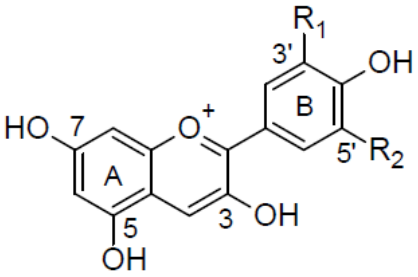

Anthocyanidin	R_1	R_2	Colour
Pelargonidin	H	H	Orange
Cyanidin	OH	H	Orange-red
Delphinidin	OH	OH	Bluish-red
Peonodin	OCH_3	H	Orange-red
Petunidin	OCH_3	OH	Bluish-red
Malvidin	OCH_3	OCH_3	Bluish-red

Figure 11 The basic structure of major anthocyanidins (Miguel, 2011).

Apart from nutritional value in the food, anthocyanins in some food, and edible plants and fruits has shown to play an important role in the prevention of many diseases such as cardiovascular diseases involving mechanisms of antioxidant activity, anti-inflammatory activity by inhibition of digestive enzymes including α-glucosidase, α-amylase,and lipase which are the clinical therapeutic targets for management type II diabetes and obesity, as well as in the retardation of the aging diseases such as Alzheimer's disease (Ames et al., 1993; Miguel, 2011; Guo et al., 2016; Wallace et al., 2016). Anthocyanins have also been reported to exhibit anti-diabetic properties (Ghosh and Konishi, 2007). The antioxidant capacity of anthocyanins in various fruits has been proved with a various antioxidant assay such as a hydrogen transfer-based assay including oxygen radical absorbance capacity (ORAC), electron transfer-based assays

including ferric reducing antioxidant potential (FRAP), trolox equivalent antioxidant capacity (TEAC), and 2,2-diphenyl-1-picrylhydrazyl (DPPH) free radical scavenging activity, scavenging activity including superoxide and peroxynitrite ($ONOO^-$) scavenging activities, ability to bind heavy metals including iron, zinc and copper chelating activities (Havsteen, 1983), and induction of antioxidant enzymes including glutathione-*S*-transferase (GST), glutathione reductase (GR), glutathione peroxidase (GPx) and superoxide dismutase (Miguel, 2011). It was also demonstrated *in vivo study* that anthocyanins showed potent antioxidants and prevent the oxidative damage (Tsuda, 2012). Antioxidant activities can be explained to play an important role for some other beneficial effects of anthocyanins especially anti-glycation effects (Khangholi et al., 2016). For instance, cyanidin-3-rutinoside exerts anti-glycation effects on monosaccharides or MG/BSA system through antioxidant and carbonyl scavenging activities (Thilavech et al., 2015; Thilavech et al., 2016). Therefore, anthocyanin existing in edible fruits and plans could be approach as antioxidant and anti-glycation.

2.9 *Clitoria ternatea* (Butterfly pea, Anchan)

Clitoria ternatea (CT), commonly called butterfly-pea or blue pea, is a well-known traditional plant that has been used as the Ayurvedic medicine for centuries. In Southeast Asia, the blue flower pigment is traditionally used as natural food colorant and herbal drink. The phytochemical analysis of petal of CT reveals the presence of six major delphinidin-derivative ternatins including ternatins A1-A3, B1-B4, C1-C5 and

D1-D3 as the major bioactive constituents in CT (Figure 14) (Mukherjee et al., 2008). Derivative of kaempferol, quercetin and myricetin are also been reported in CT flower such as kaempferol, kaempferol 3-2”-rhamnosylrutinoside, kaempferol 3-neohesperidoside, kaempferol 3-rutinoside, kaempferol 3-glucoside, quercetin, quercetin 3-2”-rhamnosylrutinoside, quercetin 3-neohesperidoside, quercetin 3-rutinoside, quercetin 3-glucoside, myricetin 3-neohesperidoside, myricetin 3-rutinoside and myricetin 3-glucoside, respectively (Kazuma et al., 2003a).

Figure 12 *Clitoria ternatea* or butterfly pea flower

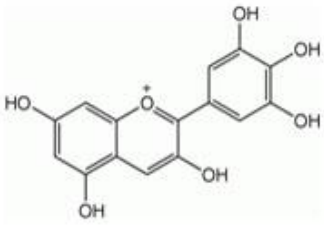

Delphinidin

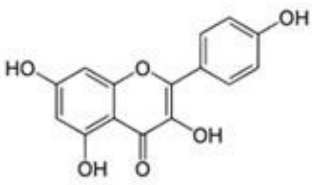

Kaempferol

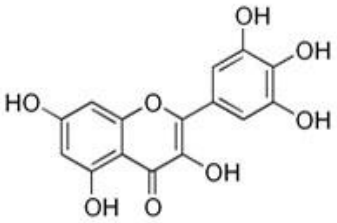

Myricetin

Figure 13 Chemical structures of delphinidin, kaempferol and myricetin (Mukherjee et al., 2008)

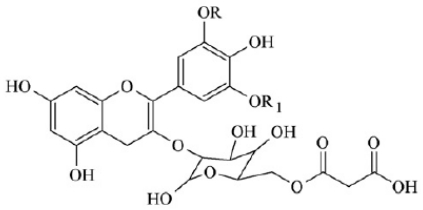

Delphinidin 3 - malonyl glucoside (9) (G is D-glucose and C is p-coumaric acid)

Ternatin	R	R^1
Ternatin A1 (10)	GCGCG	GCGCG
Ternatin A2 (11)	GCGCG	GCG
Ternatin A3 (12)	GCG	GCG
Ternatin B1 (13)	GCGCG	GCGC
Ternatin B2 (14)	GCGC	GCG
Ternatin B3 (15)	GCGCG	GC
Ternatin B4 (16)	GCG	GC
Ternatin C1 (17)	GCGC	G
Ternatin C2 (18)	GCGCG	G
Ternatin C3 (19)	GC	G
Ternatin C4 (20)	GCG	G
Ternatin C5 (21)	G	G
Ternatin D1 (22)	GCGC	GCGC
Ternatin D2 (23)	GCGC	GC
Ternatin D3 (24)	GC	GC

Figure 14 Chemical structures of ternatins A1-A3, B1-B4, C1-C5 and D1-D3 (Mukherjee et al., 2008)

2.10 Pharmacological activities of CT flower

2.10.1 Antioxidant activity

CT has been extensively documented for its various pharmacological activities. CT is deserved as potential sources of antioxidant compounds due to its flavonoids and anthocyanins contents. It was reported that CT showed the antioxidant activity measured by 1,1-diphenyl 2-picrylhydrazyl (DPPH) scavenging activity in both leaves and flowers (Rabeta and An Nabil, 2013). Methanol extracts of CT also showed the radical scavenging activity ability such as hydroxyl radical scavenging activity (Patil and Patil, 2011). The potential antioxidant activity of CT extracts and an extract containing eye gel formulation was investigated (Kamkaen and Wilkinson, 2009). DPPH scavenging activity of aqueous extracts was shown to have stronger antioxidant activity than ethanol extracts represented by IC_{50} at 1 mg/ml and 4 mg/ml, respectively. An eye gel formulation containing aqueous extracts of CT was also shown to maintain this activity. In addition, water extraction of CT showed antioxidant activity as measured by DPPH radical scavenging assay and oxygen radical absorbance capacity (ORAC). The antioxidant properties of CT flower were shown to protect erythrocytes against AAPH-induced hemolysis by suppressing membrane lipid peroxidation, protein carbonyl group formation and preventing the reduction of glutathione concentration (Phrueksanan et al., 2014).

2.10.2 Antidiabetic acitivitiy

Antidiabetic effect of CT was demonstrated by inhibiton of intestinal glucosidase enzymes (IC_{50} of 3.15±0.19 mg/mL), intestinal sucrase (IC_{50} of 4.41±0.15 mg/mL), and pancreatic α-amylase (IC_{50} 4.05±0.32 mg/mL) (Adisakwattana et al., 2012a). Chronic administration of aqueous extracts of CT (100mg/kg) for 14 days decreased the hyperglycemia of the alloxan-induced diabetic rats as compared to diabetic control group (Gunjan et al., 2010). The blood glucose level was significantly decreased at day 7 and 14 after the diabetes induction representing antidiabetic effect. The effect was comparable to glibenclamide which is a standard antidiabetic drug. Antihyperglycemic and antioxidative activity of ethanol extract of *CT* (EECT) (200 and 400 mg/kg) was investigated in normal and streptozotocin-induced diabetic rats. It is suggested that EECT has potential therapeutic effects on hyperglycemia and oxidative stress in diabetic rats (Talpate et al., 2013). The evidence supported that the antidiabetic effect of CT was demonstrated by investigating the aqueous extract of CT leaves and flowers (400 mg/kg body weight) on serum glucose of alloxan-induced diabetic rats. It was reported that CT leaves and flowers were able to reduce serum glucose, glycosylated hemoglobin and the activities of gluconeogenic enzyme, wheresas increased serum insulin, liver and skeletal muscle glycogen and the activity of the glycolytic enzyme. This study clarified that the leaf and flower extract of CT exerted antihyperglycaemic effect on alloxan-induced diabetic rats (Daisy and Rajathi, 2009; Daisy et al., 2009). Furthermore, antihyperlipidemic of CT was examined in diet-

induced hyperlipidemic rats. It was found that CT (500 mg/kg) reduced serum total cholesterol, triglycerides, very low-density lipoprotein cholesterol, and low-density lipoprotein cholesterol levels indicating antihyperlipidemic effect against experimentally-induced hyperlipidemia (Solanki and Jain, 2010).

2.10.3 Anti-inflammatory activity

Anti-inflammatory, analgesic and antipyretic activities of CT have been reported (Mukherjee et al., 2008; Nair et al., 2015). The evidence has proved that twelve phenolic compounds including nine ternatin anthocyanins and three glycosylated quercetins identified from the blue flowers of CT exert anti-inflammatory effect by suppressing the excessive production of pro-inflammatory mediators from macrophage cells (Nair et al., 2015). CT showed anti-inflammatory properties to suppress lipopolysaccharide (LPS)-induced inflammation in RAW 264.7 macrophage cells. Flavonols fraction of CT showed strong potency on inhibition of COX-2 activity and partial ROS suppression. Moreover, the ternatin anthocyanins fraction of CT exerted inhibitory effect on nuclear NF-κB translocation, iNOS protein expression, and nitric oxide production through a non-ROS suppression mechanism**.** The petroleum ether (60-80°C) extract of CT flower extract possessed significant anti-inflammatory and analgesic properties in rat (Mukherjee et al., 2008). Besides, the methanol extract of CT root significantly reduced the normal body temperature and yeast induced pyrexia of rats in a dose-dependent manner and maintained up to 5 hours after administration.

The anti-pyretic effect of the extract was comparable to that effect of oral administration of paracetamol at concentration 150 mg/kg (Parimaladevi et al., 2004).

2.10.4 Central nervous system effect

CT has shown a beneficial effect on central nervous system such as nootropic, anxiolytic, antidepressant, anticonvulsant (Jain et al., 2003). The nootropic effect (facilitation of intellectual performance, learning and memory) of the methanol extract of CT was represented by decrease of the time required for rats to occupy the central platform in the elevated plus maze (EPM) and and increase of the discrimination index in object recognition tests. The duration of immobility in tail suspension test (indicating antidepressant activity), stress-induced ulcers and the convulsing action of pentylenetetrazol (PTZ) and maximum electroshock (MES) were reduced by the methanol extract of CT in this study. Oral administration of the aqueous root extract (100 mg/kg) in rat for 30 days contributed to improved learning and memory by raising the level of acetylcholine in the hippocampus (Rai et al., 2002).

2.10.5 Anti-hemolysis

It has been reported that CTE (400µg/ml) is capable to protect AAPH-induced hemolysis in canine erythrocytes. Additionally, CTE decreases membrane lipid peroxidation and protein carbonyl group formation and prevented the reduction of glutathione concentration in AAPH-induced oxidation of erythrocytes. It is indicated

that CTE may have the potential to prevent free radical-induced hemolysis, protein oxidation and lipid peroxidation due to its antioxidant activity in canine erythrocytes (Phrueksanan et al., 2014).

2.11 Digestion of CTE

Recent study showed that simulated gastrointestinal digestion affected to the degradation, antioxidant and biological activities of CTE. However, microencapsulation of CTE improve the thermal stability with 188 °C. After simulated gastrointestinal digestion, the microencapsulation of CTE using alginate could also reduce degradation of polyphenol and increase biological activity without chemical interaction between CTE and alginate. Moreover, remained higher amount of polyphenols and improved antioxidant activities, pancreatic α-amylase inhibitory activity, and bile acid binding were found in microencapsulation of CTE (Pasukamonset et al., 2016).

2.12 Toxicity and safety of *Clitoria ternatea*

LD_{50} of ethanol extract of CT root was more than 1,300 mg/kg in mice (Kelemu et al., 2004). Acute oral toxicity study was performed by administrating the ethanolic extract of aerial and root parts of CT up to 3,000 mg/kg bodyweight. The result showed that there was no lethality in mice but the animals showed signs of central nervous system depression at dose from 1,500 mg/kg (Taranalli and Cheeramkuzhy, 2000). In

consistent with previous study, the oral administration of methanol extract of CT root extract was claimed to be safe even at dose 3.2 g/kg body weight in rats (Parimaladevi et al., 2004).

CHAPTER III

MATERIALS AND METHODS

3.1 Materials

3.1.1 Plant material

The dried flower of *Clitoria ternatea* was purchased from the local herbal shop in Bangkok, Thailand. The plant has been authenticated at the Princess Sirindhorn Plant Herbarium, Plant Varieties Protection Division, Department of Agriculture, Thailand, Voucher specimen: BKU066793.

3.1.2 Chemicals

1-deoxy-1-morpholinofructose (DMF)	Sigma-Aldrich (USA)
2,2- azinobis3- ethylbenzothiazoline- 6- sulfonic acid (Trolox)	Sigma-Aldrich (USA)
2,2-diphenyl-1-picrylhydrazyl (DPPH)	Sigma-Aldrich (USA)
2,4-dinitrophenylhydrazine (DNPH)	Sigma-Aldrich (USA)
2,4,6- tripyridyl-S-triazine (TPTZ)	Sigma-Aldrich (USA)
5-methylquinoxaline (5-MQ)	Sigma-Aldrich (USA)
5,5′-dithiobisnitro benzoic acid (DTNB)	Sigma-Aldrich (USA)

Aminoguanidine (AG)	Sigma-Aldrich (USA)
Bovine serum albumin (BSA)	Sigma-Aldrich (USA)
BSA fraction V	Sigma-Aldrich (USA)
Dexamethasone	Sigma-Aldrich (USA)
DMEM (Dulbecco' s modification of Eagle' s medium)	Corning (USA)
EDTA	Sigma-Aldrich (USA)
Iron (III) chloride ($FeCl_3$)	Sigma-Aldrich (USA)
Fetal bovine serum (FBS)	Gibco (USA)
Fructose	Fluka (USA)
Folin–Ciocalteu's phenol reagent	Fluka (USA)
Gallic acid	Fluka (USA)
Insulin	Sigma-Aldrich (USA)
Isobutylethylxanthine (IBMX)	Sigma-Aldrich (USA)
Isopropanol	Fisher scientific (Canada)
Iron sulfate ($FeSO_4$)	Sigma-Aldrich (USA)
L-cysteine	Sigma-Aldrich (USA)
Methanol	Fisher scientific (USA)
Methylglyoxal (MG)	Sigma-Aldrich (USA)
Nitroblue tetrazolium (NBT)	Sigma-Aldrich (USA)

O-phenylenediamine (*O*-PD)	Sigma-Aldrich (USA)
Oil red O	Sigma-Aldrich (USA)
Penicillin-Streptomycin solution	Mediatech Inc. (USA)
Potassium persulfate ($K_2S_2O_4$)	Merck (Germany)
Propidium iodide	Sigma-Aldrich (USA)
Rnase A	Sigma-Aldrich (USA)
TEMED	Fisher scientific (USA)
Thiazolyl blue tetrazolium bromide	Biosynth (USA)
Thiobarbituric acid (TBA)	Sigma-Aldrich (USA)
Thioflavin T reagent	Sigma-Aldrich (USA)
Trichloroacetic acid (TCA)	Sigma-Aldrich (USA)
Tris-HCl	Merck (Germany)
Trypan blue	Lonza (USA)
Trypsin EDTA	Mediatech Inc. (USA)
Xanthine	Sigma-Aldrich (USA)
Xanthine oxidase	Sigma-Aldrich (USA)

3.1.3 Reagent

Adipogenesis colorimetric/fluorometric assay kit	Biovision (USA)
Acetyl coA carboxylase (ACC) primary antibody	Cell Signaling Technology (USA)
BCA protein assay kit	Thermo scientific (USA)

CEBPα primary antibody	Cell Signaling Technology (USA)
Fatty acid synthase (FAS) primary antibody	Cell Signaling Technology (USA)
GAPDH primary antibody	Cell Signaling Technology (USA)
iScript™ cDNA synthesis kit	Bio Rad (USA)
Lipolysis colorimetric assay kit	Biovision (USA)
Phosphorylated Akt (T308) primary antibody	Cell Signaling Technology (USA)
Phosphorylated MAPK (T202/ Y204) primary antibody	Cell Signaling Technology (USA)
PPARγ primary antibody	Cell Signaling Technology (USA)
Primer for PCR	Thermo scientific (USA)
RNeasy plus mini kit	Qiagen (USA)
N^{ε}-(carboxymethyl) lysine (CML) test kit	Cell Biolabs Inc. (USA)
SsoAdvanced™ Universal Probes Supermix	Bio Rad (USA)
Total Akt (T308) primary antibody	Cell Signaling Technology (USA)
Total p44/42 (T202/Y204) primary antibody	Cell Signaling Technology (USA)
West pico chemiluminescence substrate	Thermo scientific (USA)

3.1.4 Laboratory equipment company

Analytical balance	Sartorius (Germany)
Autopipetts	Gilson (France)

Autoclave	Hirayama (Japan)
C1000 Touch thermal cycler	Bio Rad (USA)
Centrifuge	Heraeus, Biofuge (Germany)
Freezer -20°C	Sanyo (Japan)
Gel Doc imager	Syngene (UK)
Gel electrophoresis and power supply	Bio Rad (USA)
High–performance liquid chromatography (HPLC)	Shimadzu Corporation (Japan)
Light microscope	Olympus (Japan)
Nanodrop-1000 spectrophotometer	Thermo Scientific (USA)
pH meter	Thermo Scientific (USA)
Pipette	Thermo Scientific (USA)
PX1™ PCR plate sealer	Bio Rad (USA)
Spectrofluorometer	Perkin Elmer (USA)
Spectrophotometer	Molecular devices (USA)
Spray dry machine	Eyela world (Japan)
TC 20™ automated cell counter	Biorad (USA)
Vortex	Thermo Scientific, USA
Water bath	Memmert (Michigan)

3.1.5 Lab devices

Cell counting slide	Bio Rad (USA)
Glass plate	Bio Rad (USA)
Glassware	Corning (USA)
Nylon filter (0.22 µL)	Corning (USA)
Plasticware	Thermo Scientific (USA)
Plasticware (for cell culture)	Corning (USA)
QIAprep spin column	Qiagen (USA)

3.2 Methods

3.2.1 Phytochemical analysis

3.2.1.1 Preparation of *Cliteria ternatea* extract (CTE)

The extraction of dried CT flower was modified according to a previously published method (Adisakwattana et al., 2012a). Briefly, the dried plant (300 g) was extracted with distilled water (1 L) at 95 °C for 2 h. The sample was filtered through Whatman 70 mm filter paper. The aqueous solution was dried using a spray dryer SD-100 (Eyela world, Tokyo Rikakikai Co., LTD, Japan). The spray drying condition was inlet temperature (178°C), outlet temperature (80°C), blower (0.9 m^3/min) and atomizing (90 kPa).

3.2.1.2 Total phenolic content

An aliquot sample (10 µL) was added Folin-Ciocalteu reagent (90 µL) followed by 10% (w/v) Na_2CO_3 (100 µL) and kept for 2 h at room temperature. The mixture was measured at the wavelength 750 nm with a spectrophotometer. Gallic acid (0-1,000 µg/mL) was used as a standard for the calibration curve. Total phenolic content was expressed as mg gallic acid equivalents/g dry weight of extract (Adisakwattana et al., 2012a).

3.2.1.3 Quantification of flavonoid constituents

Quantification of flavonoid constituents was performed according to a previously published method. The sample solution (100 µL) was added to 30 µL of $AlCl_3$ solution (10%w/ v), 30 µL of $NaNO_2$ (15% w/v), 400 µL of 4% NaOH, and 440 µL of distilled water. After incubation at room temperature for 10min, the absorbance was measured immediately at 510 nm. Catechin (0-1,000 µg/mL) was used as a standard (Adisakwattana et al., 2012a).

3.2.1.4 Anthocyanin content

Total anthocyanin content (TAC) in the extract was determined by using pH differential method. The extract (10 µL) was added to two buffer systems including 0.025 M potassium chloride (490 µL) at pH 1.0, and 0.4 M sodium acetate (490 µL) at

pH 4.5, respectively. The calculated absorption was determined using the equation of monomeric anthocyanin pigment (mg/L) = (A × MW × DF × 1000)/(ε × 1) where A = (A_{510} - A_{700}) pH1.0 - (A_{510} - A_{700}) pH 4.5; MW is the molecular weight of cyanidin-3-glucoside (449.2), ε is the molar absorptivity (26,900), and DF is the dilution factor. The TAC in the testing solution was calculated as cyanidin-3-glucoside equivalents (Jariyapamornkoon et al., 2013).

3.2.2 LC-MS/MS analysis

3.2.2.1 Sample preparation for LC-MS/MS

Anthocyanin fractions were obtained using an activated Oasis HLB cartridge (Waters Corp., Milford, MA), according to the modified procedure of previous study with minor modification (Wongs-Aree et al., 2006). Briefly, the dried CTE was resolubilized in distilled water and applied to an activated Oasis HLB cartridge. The cartridge was washed with 0.01% hydrochloric acid in water, followed by ethyl acetate and then 0.01% hydrochloric acid in methanol to elute the anthocyanins. The anthocyanins were dried with nitrogen gas and used for LC-MS/MS analysis. The purified CTE was resolubilized with 0.5% formic acid solution to give a final concentration of 1 mg/mL and filtered through a 0.45 μm pore size poly-(tetrafluoroethylene) (PTFE) membrane syringe filter (Corning, New York, USA) prior to injection into the LCMS/MS for identification and quantification of anthocyanins.

3.2.2.2 Characterization of CTE

The phytochemicals in the enriched extract were directly analyzed by liquid chromatography and tandem mass spectrometry (LC-MS/MS) according to the conditions previously described by previous study (Nair et al., 2015). LC/MS/MS was performed using a Quadrupole/Time-Of-Flight Mass Spectrometer (QTOF LC-MS/MS; Model-6540 UHD Agilent Technologies, USA) using a Dual ESI ion source equipped with an Agilent 1260 series liquid chromatograph. A 150 × 4.6 mm, particle size 5 µm C18 reversed phase column (VertiSep™ AQS - Vertical Chromatography CO., LTD.) was used at a flow rate of 0.5 mL/min and 40 min of the total run time. The HPLC gradients were consisted of eluent A; 0.1% formic acid in water and eluent B 0.1% formic acid in acetonitrile. The system was run with the following gradient program: 0 min: 95% of linear gradient until 5% of A in 40 min and post run for 5 min. The mass spectral data were acquired with the following ESI inlet conditions: the scanning mass-to-charge (m/z) ranging from 100 to 1700 with a scan rate of 4.00 spectra s^{-1}, the capillary voltage of 3500 V (positive mode) and the fragmentor of 100 V. The pressure of the nebulizer was set at 30 psi, the drying gas temperature at 350°C, and the continuous gas flow to 10 L/min.

3.2.3 Protective effect of CTE against glycation of BSA induced by fructose and MG *in vitro*

3.2.3.1 Antiglycation activity

The glycated BSA formation was performed according to previous study with minor modification (Adisakwattana et al., 2012b). In brief, 500 µL of BSA (10 mg/mL) was incubated with 0.5 M fructose (460 µL) or 1.0 mM MG (460 µL) in a 0.1 M phosphate buffered saline (PBS), pH 7.4 containing 0.02% sodium azide in the dark at 37 °c for 7, 14, 21, and 28 days or 7 days, respectively. Before incubation, 40 µL of CTE (250-1,000 µg/mL) and 40 µL aminoguanidine (AG, 1,000 µg/mL) were added to the mixtures. The fluorescent AGEs formation of glycated BSA in mixtures (50 µL) was assayed by using spectrofluorometer at excitation and emission wavelength of 355 nm and 460 nm, respectively. Aminoguanidine (AG) was used as a positive control in this study. The results were expressed as a percentage inhibition of the corresponding control value.

3.2.3.2 Determination of Fructosamine

After incubation for 7, 14, 21, and 28 days, the concentration of fructosamine, which is represented as the Amadori product, was determined using a nitroblue tetrazolium (NBT) assay according to a previous study (Adisakwattana et al., 2012b). In brief, the glycated BSA (10 µL) was incubated with 0.5 mM NBT (90 µL) in 2 M sodium carbonate buffer (pH 10.4) at 37 °c for 10 and 15 min time points. The absorbance was measured at the wavelength of 590 nm. The concentration of fructosamine (mmol/mL)

was calculated from standard curve using 1-deoxy-1-morpholino-fructose (1-DMF, 0-10 mmol/L) as the standard.

3.2.3.3 Determination of protein carbonyl content

After incubation for 7, 14, 21, and 28 days, protein carbonyl group was determined by 2,4-dinitrophenylhydrazine (DNPH) according to a previous study (Adisakwattana et al., 2012b). Briefly, the glycated BSA (200 µL) was incubated with 10 mM DNPH in 2.5 M HCl (800 µL) in dark room for 1 h. Protein precipitation was done by 20% w/v trichloroacetic acid (TCA, 1 mL) on ice for 5 min and centrifuged at 10,000 rpm 4°c for 10 min. The protein pellet was washed with 0.5 mL of ethanol/ethyl acetate mixture (1:1 v/v) three times and then dissolved in 6 M of guanidine hydrochloride (pH 2.3, 500 µL). The absorbance was measured at wavelength of 370 nm. The carbonyl content was calculated from the extinction coefficient for DNPH (ε = 22,000 $M^{-1} \cdot cm^{-1}$). The results were expressed as nmol carbonyls/mg protein.

3.2.3.4 Determination of protein thiol group

After incubation for 7, 14, 21, and 28 days, the free thiol concentration of glycated BSA was measured using Ellman's assay (Adisakwattana et al., 2012b). Briefly, glycated samples (70 µL) were incubated with 2.5 mM DTNB solutions (130 µL) for 15 min and then the absorbance was read at wavelength of 410 nm. The free thiol

concentration of samples was calculated based on the standard curve prepared by using various concentration of L-cysteine (0-100 nmol).

3.2.3.5 Carbonyl trapping activities

The CTE (125-1,000 µg/mL) was incubated with 1 mM MG at 37°c. After 1 day of incubation, the quantification of MG was detected base on level of 2-MQ production. 2-MQ was analyzed by high-performance liquid chromatography (HPLC) with 5-MQ as internal standard according to previous study (Peng et al., 2008b). 20 mM *o*-phenylenediamine (*o*-PD) containing 100 µL of 5 mM 5-MQ was added and kept at room temperature for 30 min. HPLC equipped with a LC-10AD pump, SPD-10A UV-Vis detector and LC-Solution software. A C18 (Inertsil ODS 3V) column (250 × 4.6 mm i.d.; 5 µm particle size) was selected to detect the remaining MG in samples represented as 2-MQ. The mobile phase of HPLC system was composed of HPLC grade water and methanol (50:50, v/v). The flow rate and injection volume were 1.2 mL/min and 10 µL, respectively, with 15-min total running time. The absorbance was recorded at the wavelength of 315 nm. The percentage of MG reduction was calculated using the equation below:

$$\%\text{Inhibition} = \frac{(\text{Level of MG in control} - \text{Level of MG in sample})}{\text{Level of MG in control}} \times 100$$

3.2.4 Antioxidant properties of CTE

3.2.4.1 DPPH radical scavenging activity

DPPH (1,1-diphenyl 2-picrylhydrazyl) radical scavenging activity was measured according to the previous method (Makynen et al., 2013). Briefly, the extract (0-1 mg/mL, 50 µL) was added with 0.2 mM DPPH (50 µL) as the free radical source and incubated for 30 min at room temperature. The decrease in the solution absorbance was measured at 515 nm. The IC_{50} values were calculated from plots of log concentration of inhibitor concentration versus percentage inhibition curves. Ascorbic acid (0-12.5 µg/mL) was used as a positive control for this study.

3.2.4.2 Trolox equivalent antioxidant capacity assay (TEAC)

Assessment of ABTS radical-scavenging activity was done according to a previously published method (Makynen et al., 2013). The radical anion ($ABTS^{\bullet+}$) was produced by adding 2.45 mM potassium persulfate ($K_2S_2O_4$) and 7 mM ABTS (1:1 ratio). The mixture was incubated at room temperature for at least 16 hours in the dark. The $ABTS^{\bullet+}$ solution was diluted in 0.1 M PBS, pH 7.4 to absorbance at 0.700±0.02 nm. The extract (0-60 mg/mL, 10 µL) was added to $ABTS^{\bullet+}$ solution (90 µL) for hydrogen atom transfer (HAT). The decrease in the solution absorbance was measured at 734 nm. The TEAC value was calculated from the standard curve prepared by using a Trolox (0-1 mg/ml).

3.2.4.3 Ferric reducing antioxidant power (FRAP)

The reducing power was measured according to a previous method (Makynen et al., 2013). The freshly prepared FRAP reagent contained 25 mL of 0.3 M sodium acetate buffer solution (pH 3.6), 2.5 mL of 10 mM 2,4,6- tripyridyl-S-triazine (TPTZ) in 40 mM HCl and 2.5 mL of 20 mM $FeCl_3$. The extract (0-2 mg/mL, 10 µL) was added to FRAP solution (90 µL) as oxidizing reagent and incubated for 30 min at 37°C. The increase in the solution absorbance was measured at 595 nm using a spectrophotometer. FRAP value was calculated from a standard curve using $FeSO_4$ (0-1 mM). FRAP value was expressed as mmol $FeSO_4$/mg dried extract.

3.2.4.4 Hydroxyl radical scavenging activity (HRSA)

Hydroxyl radical scavenging activity was measured according a previous method (Makynen et al., 2013). Briefly, hydroxyl radical was generated from Fenton reaction mixture including 0.3 mM $FeCl_3$, 0.6 mM ascorbic acid, 34 mM H_2O_2 solution, 17 mM Deoxyribose, 1.2 mM EDTA in ratio 2:2:1:1:1 with incubation for 1 h at 37 °C. 300 µL of 2.8% (W/V) TCA and 150 µL of 1% (W/V) TBA were then added into the mixture and incubated at 100 °C 10 min. After the solution cooled down, the thiobarbituric acid reactive substance (TBARS) was measured at wavelength of 532 nm. The IC_{50} value was calculated from plots of log concentration of inhibitor concentration versus percentage inhibition curves. A trolox (0-60 mg/mL) was used as a positive control for this study.

3.2.4.5 Superoxide radical scavenging activity (SRSA)

Superoxide radical scavenging activity was measured according a previous method (Makynen et al., 2013). Briefly, superoxide radical was produced by activity of enzyme xanthine oxidase (50 µL) that modify xanthine in the reaction mixture containing 0.3 mM xanthine (500 µl), 0.15 mM NBT (250 µl) and 0.6 mM EDTA (250 µl). 50 µl of the extract (0-1.5 mg/mL) or standard trolox (0-2 mg/mL) was added and followed by incubation at 37 °c for 40 min. The absorbance was measured at 560 nm. The IC_{50} value was calculated from plots of log concentration of inhibitor concentration versus percentage inhibition curves. A trolox was used as a positive control for this study.

3.2.4.6 Ferrous ion chelating power

The metal chelating power was measured according to a previously published method (Jariyapamornkoon et al., 2013). Briefly, 0.1% 2,2′-bipyridyl (500 µL), 0.1 M Tris-HCl buffer (pH 7.4, 500 µL) and 1 mM $FeSO_4$ (125 µL) were added for induce redox reaction of Fe^{2+} to form 2,2′-bipyridyl-Fe^{2+} complex in red solution. The extract (0-55 mg/mL, 125 µL) was added for competitive with 2,2′-bipyridyl in reducing reaction. The decrease in the solution absorbance was measured at 522 nm. The IC_{50} value was calculated from plots of log concentration of inhibitor concentration versus percentage inhibition curves. EDTA (0-2 mg/mL) was used as a positive control for this study.

3.2.5 Effect of CTE on oxidative DNA damage induced by AAPH or MG/lysine system, *in vitro*

3.2.5.1 Analysis of DNA strand break

The pUC19 plasmid was extracted and purified from *Escherichia coli* by using QIAprep spin miniprep kit according to manufacturer's instruction and DNA concentration was quantified by using the Nanodrop-1000 spectrophotometer (Thermo Scientific, USA). DNA strand break was performed according to previous study (Meeprom et al., 2015). Briefly, purified plasmid pUC19 DNA (0.25 µg) was added together with AAPH (final concentration: 12.5 mM) or 2 µL of 250 MG (final concentration: 50 mM), 2 µL of 250 mM lysine (final concentration: 50 mM) and 2 µL of CTE at various 5X concentrations (final concentrations: 125-1000 µg/mL) with or without 1 µL of 3 mM $CuSO_4$ (final concentration: 300 µM) into reaction mixture (total volume: 10 µL). The reaction mixture was incubated for 3 h at 37 °C and then stopped the reaction by freezing at -20 °C for 90 min. As a consequence, the sample was assessed by electrophoresis in 0.8% agarose gel in Tris-borate-EDTA (TBE) buffer. The band of DNA was visualized by staining Ethidium bromide and photographed by Gel Doc imager (Syngene, UK) under UV light. The intensity of each band was quantified using GeneTools software (Syngene, UK). The results were shown as percentage of open circular form of plasmid DNA by following formulation.

$$\%\text{Open circular form} = \frac{\text{Intensity of open circular form}}{\text{Intensity of open circular and supercoil forms}} \times 100$$

3.2.4.2 Measurement of superoxide anion

Superoxide was determined by cytochrome *c* reduction assay as earlier described (Thilavech et al., 2016). Briefly, the reaction mixture (total volume: 200 µL) contained 50 µL of 200 mM MG (final concentration: 50 mM) and 50 µL of 200 mM lysine (final concentration: 50 mM) with or without 50 µL of CTE (final concentration: 0.125-1 mg/mL). 50 µL of 40 µM cytochrome *c* (final concentration: 10 µM) was then added into the reaction mixture. The reduction rate was measured as increased absorbance at 550 nm every 10 min until 60 min. The results were expressed as nmol/mL by using molar extinction coefficient (27,700 $M^{-1}cm^{-1}$).

3.2.4.3 Measurement of hydroxyl radical

Detection of hydroxyl radical was represented by measuring of thiobarbituric acid reactive 2-deoxy-D-ribose oxidation products as previously published (Thilavech et al., 2016). The assay mixture (total volume: 200 µL) including 50 µL of 200 mM MG (final concentration: 50 µM) and 50 µL of 200 mM lysine (final concentration: 50 µM) was incubated with 50 µL of 80 mM 2-deoxy-D-ribose (final concentration: 20 µM) for 120 and 180 min in the absence or presence of 50 µL of CTE (final concentration: 0.125-1.000 mg/mL). Consequently, 2.8% (W/V) TCA (200 µL) and 1% (W/V) TBA (200 µL) were respectively added to the assay mixture following by heating 100°C for 10 min. After the mixture was cooled down at the room temperature, the by-product of

2-deoxy-D-ribose was measured at 532 nm. The concentration of TBARS was represented as nmol/mL of MDA calculated from MDA standard curve (0-20 µM).

3.2.5 Inhibitory effect of CT extract on MG-inuced adipogenesis *in vitro*

3.2.5.1 Culture and differentiation of 3T3-L1 cells

3T3-L1 cells were cultured and differentiated as described by ATCC's instruction (Galvis et al., 2011). Briefly, the cells ($2x10^4$) were grown in DMEM containing 10% fetal bovine serum, 2 mM L-glutamine, 100 I.U/mL penicillin and 100 µg/mL streptomycin. After the cells reached 100% confluence, they were grown in the DMEM supplemented with 10 µg/mL insulin, 0.5 mM IBMX and 1 µM dexamethasone (differentiation medium). At day 5 until day 9, the cells were then grown in DMEM supplemented with 10 µg/mL insulin (post-differentiation media).

3.2.5.2 Cell viability assay

Cell viability was determined by MTT [3-(4,5-Dimethylthiazol-2-yl)-2,5-Diphenyltetrazolium Bromide] as previously described (Galvis et al., 2011). After the 3T3-L1 cells ($1x10^4$ cells/mL) were treated by 10 µL of CTE (125-2000 µg/mL) for 1 h, MTT reagent (10 µL) was added and incubated at 37 °c for 2 h. The resulting intracellular purple formazan crystal was then solubilized by 10% SDS (100 µL). The absorbance was measure at 570 nm.

The 3T3-L1 cells viability was analyzes by Trypan blue assay as previous study with minor modification (Drira et al., 2011). The 3T3-L1 cells ($1x10^4$ cells/mL) were

incubated with 10 µL of CTE (125-2000 µg/mL) for 1 h. The 50 µL of trypsinized cell suspension were immediately stained with 50 µL of 0.4% trypan blue for 3 min. The viable cells were counted by automated cell counter (Biorad, USA). The viability was expressed as viable cell number.

3.2.5.3 MTT proliferation assay

The MTT proliferation assay was performed according to previously published method (Jia et al., 2012). In brief, 3T3-L1 cells were seeded in to 96-well plate at concentration of $1x10^4$ cells/mL. After the cells adhered to the plate, the cells were starved in serum-free media with 5 mg/mL of BSA for 24 h. The cells were incubated with various concentrations of CTE (500-1,000 µg/mL) in the presence or absence 10 µM MG for 2 h, and the cells were then incubated with 10 µL of MTT in the dark for 2 h. 10% SDS (100 µL) was subsequently added to dissolve the insoluble formazan crystal for 2 h. The absorbance was measured at 570 nm.

3.2.5.4 Cell cycle by Flow cytometry

Cell cycle analysis was performed following a previously published report with slight modification (Jang et al., 2015). After the 3T3L1 cells ($1x10^4$ cells/mL) were incubated with CTE (125-500 µg/mL) with/without 10 µM MG for 24 h, the cells were trypsinized and fixed with 50% ethanol at 4 °C for 2 h. The cells were then washed and re-suspended in 10 mM PBS containing RNase A and 50 µg/mL propidium iodide

for 30 min at room temperature. DNA content was measured by flow cytometer and analyzed using Flowjo software. The cells at least 1×10^4 counts were made for each sample.

3.2.5.5 Oil red O assay

Oil red O assay was performed according to previously described study with slight modification (Galvis et al., 2011). In brief, 3T3-L1 pre-adipocytes cells ($2x10^4$ cells/mL) were incubated with CTE (500-1,000 µg/mL) in the presence or absence 10 µM MG until day 9 and differentiated mature adipocytes were then fixed by 10% formaldehyde. After the cells were stained with 60% oil red O solution for 10 min, cells were washed by PBS twice. Finally, the cells were incubated with 100% isopropanol at 37 °C for 10 min. The absorbance was measured at 540 nm.

3.2.5.6 Western blot analysis

Western blot analysis was performed following a previously described method (Yang et al., 2013). The cells were lysed with ice-cold RIPA buffer (50 mM Tris–HCl pH 8.0, 150 mM NaCl, 1% NP40, 0.1% SDS and 0.5% sodium deoxycholate) containing protease inhibitor (2 mM PMSF) and phosphatase inhibitor (100 mM NaF, 1 mM Na_3VO_4). After centrifugation, the protein content was quantitated by using pierce® BCA protein assay kit (Thermo Scientific, USA). The lysate was resolved by SDS-PAGE and transferred

to nitrocellulose membrane. The membrane was then blocked and probed for specific markers by specific primary antibody. After incubation with horseradish peroxidase-conjugated secondary antibody, membrane-bound target protein was developed and detected using chemiluminescent system (Thermo scientific, USA). The intensity of each band was quantified by using software image J. Relative expression levels of Akt1 and ERK1/2 were depicted as a ratio of P (Phospho)-Akt1 (T308) to T (Total)-Akt1 and P (Phospho)-ERK1/2 (T202/Y204) to T (Total)-ERK1/2, respectively. Relative expression levels of PPARγ, CEBPα, FAS and ACC proteins were shown in ratio of PPARγ, CEBPα, FAS and ACC to GAPDH, respectively.

3.2.5.7 Triglyceride accumulation

Triglyceride content was measured by employing adipogenesis colorimetric/fluorometric assay kit (Biovision, USA) according to manufacturer's instruction. Briefly, 3T3L1 cells ($2x10^4$) were seeded into 96-well plate with differentiation process together with CTE (500-1,000 µg/mL) in the presence or absence 10 µM MG until they became mature adipocytes. After that, lipid droplets (100 µL) were extracted by lipid extraction buffer and 5 µL of the solution containing triglyceride was then converted to glycerol and fatty acid by lipase enzyme. The released glycerol was measured at wavelength of 570 nm as a representative of triglyceride.

3.2.5.8 Lipolysis assay

Lipolysis assay was performed following manufacturer's instruction of lipolysis colorimetric assay kit (Biovision, USA). Briefly, 3T3L1 cells ($2x10^4$ cells/mL) were seeded into 96-well plate with differentiation process until they turned into mature adipocytes. After differentiation, the cells were treated by the addition of CTE (500-1,000 µg/mL) with/without 10 µM MG for 1 h. Lipolysis was then induced by incubation with 1.5 µl of 10 µM isoproterenol (synthetic catecholamine) for 3 h which activates β-adrenergic receptor and catalyzes the alteration of ATP to cAMP as a second messenger. The activation of hormone-sensitive lipase hydrolyzed triglyceride to glycerol and fatty acids. Glycerol released from 3T3-L1 cells was measured at wavelength of 570 nm. The result was shown as nmol glycerol/mg protein/h.

3.2.5.9 Real-time PCR

After treatment of 3T3-L1 cells with CTE, RNA was extracted from 3T3-L1 cells by using RNeasy Plus Mini Kit (QIAGEN, USA) and cDNA library was synthesized by using iScript cDNA synthesis kit (BIO-RAD, USA) according to manufacturer's suggestion. Reverse transcription was performed with 200 ng of total RNA sample, 1X iScript reaction mix and 1XiScript reverse transcriptase. Quantitative analysis of cDNA was performed using CFX96 Touch™ real time PCR detection system (BIO-RAD, USA) and SsoAdvanced™ universal probes supermix (BIO-RAD, USA) according to manufacturer's instruction. Briefly, amplification of the target cDNA was carried out with each 10 µL

PCR mixtures containing 1 µL cDNA, 5 µL SSO probes, 0.5 µL primers and 3.5 µL nuclease free water. Target cDNA was amplified by using verified commercially available primer pairs (Mm01205647_g1 for Beta-actin, Mm01331626_m1 for Akt1, Mm00440940_m1 for PPARγ and Mm00514283_s1 for CEBPα, Thermo Fisher Scientific, USA). PCR reaction condition was set as follows: it was begun by denaturation cycle at 95°C for 30 minutes, followed by 95 °C 10 minutes and 60°C for 25 minutes, respectively. The mRNA expression was normalized with beta-actin following by using $2^{-\Delta\Delta CT}$ method. Relative gene expression was shown as fold change in mRNA expression level compared with control.

3.3 Statistical analysis

All experiments were done at least in triplicate (n=3). The statistical significance was determined by one-way analysis of variance (ANOVA) and Duncan's post hoc analysis. The values are shown as mean ± standard error of mean (SEM). $P < 0.05$ was considered as statistical significance. The graphs were made by Sigma Plot (version 10; Systat Software Inc., San Jose, CA, USA). The data were analyzed by statistical software, SPSS version 16 for windows (SPSS Inc., Chicago, IL, USA).

CHAPTER IV

RESULTS

4.1 Phytochemical analysis

The content of total phenolic compounds in CTE was 53.00±0.34 mg gallic acid equivalents/ g dried extract. The content of flavonoid in CTE was 11. 20±0. 33 mg catechin equivalents/ g dried extract. Moreover, the content of total anthocyanin in CTE was 1.46±0.04 mg cyanidin-3-glucoside equivalents/g dried extract.

4.2 Characterization and identification of phenolic compounds in CTE by LC-MS/MS

From the chromatogram obtained by LC/MS/MS (Figure 15), 14 compounds were identified based on retention times, high-resolution mass spectrum data (MS and MS/MS) of the fragment ions, and comparisons with previously published literatures (Nair et al., 2015; Shen et al., 2016). As reported in Table 2, the compounds were identified: preternatin A3, ternatin B2, ternatin D2, quercetin-3-rutinoside, ternatin D1, kaemferol-3-*O*-(2-rhamnosyl) rutinoside, delphinidin-3-glucoside, kaemferol-3-*O*-rutinoside, delphinidin-3-*O*-(6-O-*p*-coumaryl)glucoside-pyruvic acid, apigenin 7-*O*-neohesperidoside, (+)-catechin 7-*O*-β-glucoside, syringetin-3-*O*-glucoside, quercetin

triglycoside, and delphinidin derivatives.

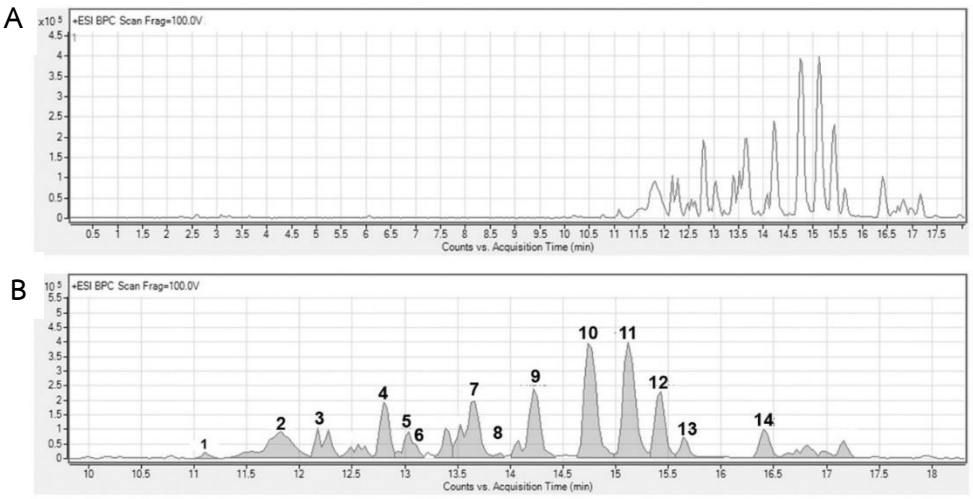

Figure 15 Chromatogram of the *Clitoria ternatea* extract.

Table 2 Chromatographic MS and MS/MS data of compounds identified in *Clitoria ternatea* extract (CTE).

No.	R_t(min)	Compound	Product ion
1	11.098	Preternatin A3	1405 $[M+H]^+$, MS/MS: 1329, 1183, 1021, 876, 739, 627, 493, 471
2	11.826	Delphinidin derivatives	788 $[M+H]^+$, MS/MS: 801 $[M+Na]^+$, 788 [Quercetin 3-glucoside+dihexose]
3	12.277	Ternatin B2	1638 $[M+H]^+$, MS/MS: 1389, 1243, 1081, 949, 757, 611, 465, 303
4	12.797	Ternatin D2	1475 $[M+H]^+$, MS/MS: 741, 595, 449, 287
5	13.040	Quercetin-3-rutinoside (Rutin)	611 [M+H]+, MS/MS: 465, 303
6	13.109	Ternatin D1	1783 $[M+H]^+$, 1697 $[M\text{-Malonyl}]^+$, MS/MS: 1535, 1227, 1081, 919, 465, 303
7	13.664	Kaemferol-3-*O*-(2-rhamnosyl)rutinoside	741 $[M+H]^+$, MS/MS: 595, 449, 287
8	14.080	Delphinidin-3-glucoside (Myrtillin)	465 $[M+H]^+$, MS/MS: 487 $[M+Na]^+$, 303
9	14.218	Kaemferol-3-*O*-rutinoside	595 $[M+H]^+$, MS/MS: 588, 566, 449, 287
10	14.738	Delphinidin-3-*O*-(6-*O*-p-coumaryl)glucoside-pyruvic acid	679 $[M+H]^+$, MS/MS: 701 $[M+Na]^+$, 679, 595, 470, 340
11	15.119	Apigenin7-*O*-neohesperidoside (Rhoifolin)	792 $[M+H]^+$, MS/MS: 814 $[M+Na]^+$, 792, 396
12	15.4311	(+)-Catechin 7-*O*-β-glucoside	453 $[M+H]^+$, MS/MS: 927 $[2M+Na]^+$, 905 $[2M+H]^+$, 814, 453
13	15.639	Syringetin-3-*O*-glucoside	509 $[M+H]^+$, MS/MS: 509
14	16.402	Quercetin triglycoside	759 $[M+H]^+$, MS/MS: 781 $[M+Na]^+$

4.3 Protective effect of CTE against glycation of BSA induced by fructose and MG *in vitro*

4.3.1 Antiglycation activity of CTE

Figure 16A showed the effects of CTE (250-1,000 µg/mL) on the formation of fluorescent AGEs at 7, 14, 21, and 28 days of incubation in BSA/fructose systems. Compared with BSA, the fluorescent intensity of fructose-induced glycated BSA was 1.6-fold, 1.7-fold, 3.5-fold, and 6.8-fold higher than non-glycated BSA after days 7, 14, 21, and 28 respectively. When CTE was added to the solution, the formation of AGEs was suppressed in a concentration-dependent manner during 14–28 days of incubation. At day 28, the percentage inhibition of CTE at concentration of 250, 500, and 1,000 µg/mL was 18.35%, 26.40%, and 49.40%, respectively. In the meantime, AG (1,000 µg/mL) inhibited AGE formation by 93.45 ± 0.45%. Likewise, the 4.51-fold increase of fluorescent intensity of glycated BSA was induced by MG at day 7 as shown in Figure 16B. The addition of CTE at concentration of 250, 500, and 1,000 µg/mL and AG (1,000 µg/mL) contributed to the inhibition of formation of AGEs at 20.68%, 28.89%, 45.72%, and 85.10%, respectively.

A

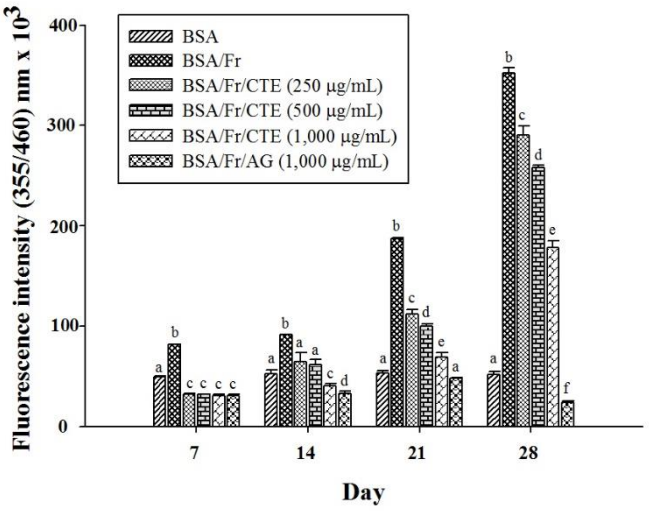

B

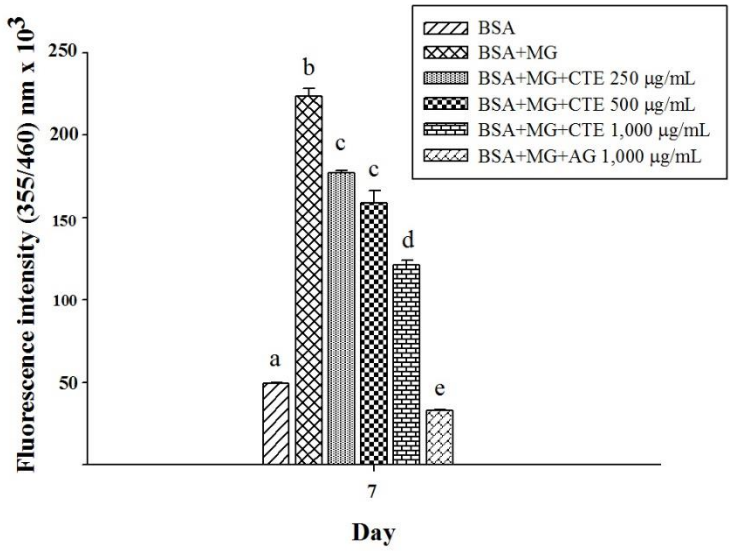

Figure 16 The effects of *Clitoria ternatea* extract (CTE, 250-1,000 µg/mL) and aminoguanidine (AG, 1,000 µg/mL) on fluorescent AGE formation in BSA/fructose (A) and BSA/MG (B) system. Each value represents the mean ± SEM (n=5). Significance is shown in groups that do not share a common letter ($p < 0.05$).

4.3.2 The effect of CTE on the level of fructosamine

The level of fructosamine in glycated BSA was gradually increased 2.0-fold to 3.6-fold during 28 days of incubation (Figure 17). CTE showed a significant reduction in fructosamine level in glycated BSA throughout the incubation period. At day 28, the percentage reduction of fructosamine level by CTE (250-1,000 µg/mL) was in the range of 14.47% to 35.66% while AG at a concentration of 1,000 µg/ml had the percentage reduction of 25.96%.

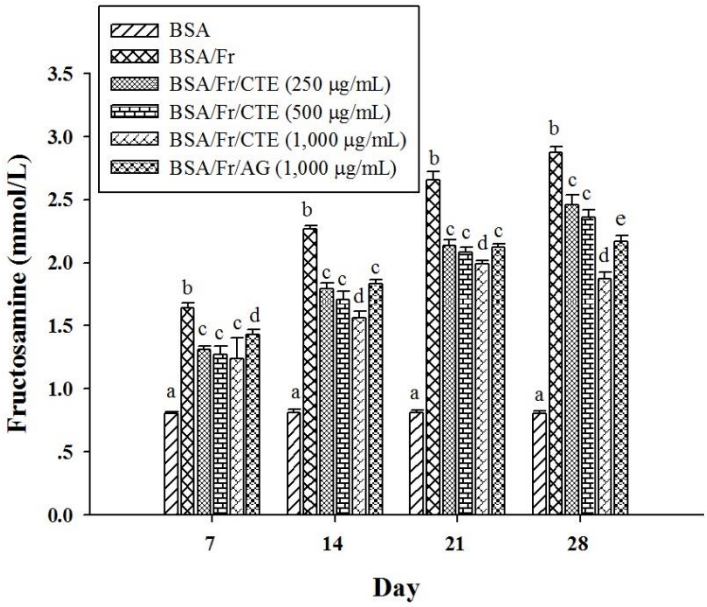

Figure 17 The effects of *Clitoria ternatea* extract (CTE, 250-1,000 µg/mL) and aminoguanidine (AG, 1,000 µg/mL) on the level of fructosamine in BSA/fructose system. Each value represents the mean ± SEM (n=5). Significance is shown in groups that do not share a common letter ($p < 0.05$).

4.3.3 The effect of CTE on protein carbonyl content

Figure 18A-18B showed the effect of CTE on protein carbonyl content represented as an oxidative modification of BSA. The carbonyl content of glycated BSA was significantly increased during the experimental period (3.0-fold to 9.4-fold increase in BSA/fructose and 3.1-fold increase in BSA/MG systems) whereas BSA/fructose or BSA/MG together with CTE (250–1,000 μg/mL) significantly attenuated an increase in the protein carbonyl content of BSA. Compared to non-glycated BSA at day 28 of incubation, the carbonyl content was reduced by CTE at concentrations of 250-1,000 μg/mL with the range of 8.23% to 11.34%, whereas that by AG showed a percentage of 17.71%. Similarly, carbonyl content of glycated BSA in BSA/MG system was reduced at 16.56%-21.97% inhibition by CTE (250-1,000 μg/mL) while AG showed 69.02% inhibition.

A

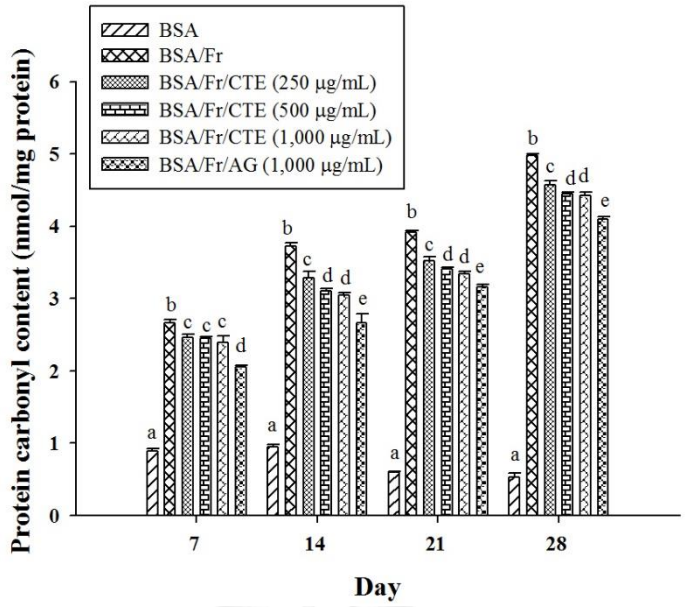

B

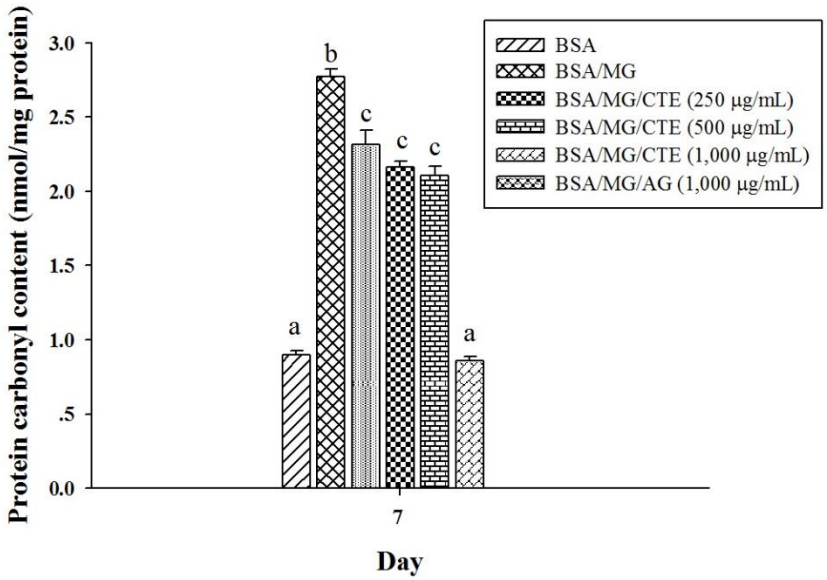

Figure 18 The effects of *Clitoria ternatea* extract (CTE, 250-1,000 µg/mL) and aminoguanidine (AG, 1,000 µg/mL) on the level of protein carbonyl in BSA/fructose (A) and BSA/MG (B) system. Each value represents the mean ± SEM (n=5). Significance is shown in groups that do not share a common letter ($p < 0.05$).

4.3.4 The effect of CTE on protein thiol group

The structural alteration in BSA mediated by protein glycation is commonly detected by depleting the thiol group. When BSA was incubated with fructose or MG, the level of thiol groups continuously decreased throughout the experimental period. From day 7 to 28, the percentage of depleting thiol group was in the range of 50.3%-91.6% in BSA/fructose and 55.5% in BSA/MG systems, respectively (Figure 19A-19B). The results demonstrated that CTE at the concentration of 250–1,000 µg/mL significantly attenuated the depleting protein thiol group of glycated BSA during the study. At day 28, the percentage prevention of depleting thiol groups by CTE was observed in the BSA/fructose (23.47% to 45.6%) and BSA/MG (15.18%-22.52%) systems whereas AG significantly prevented the depletion of protein thiol groups by 79.57% and 43.71%, respectively.

A

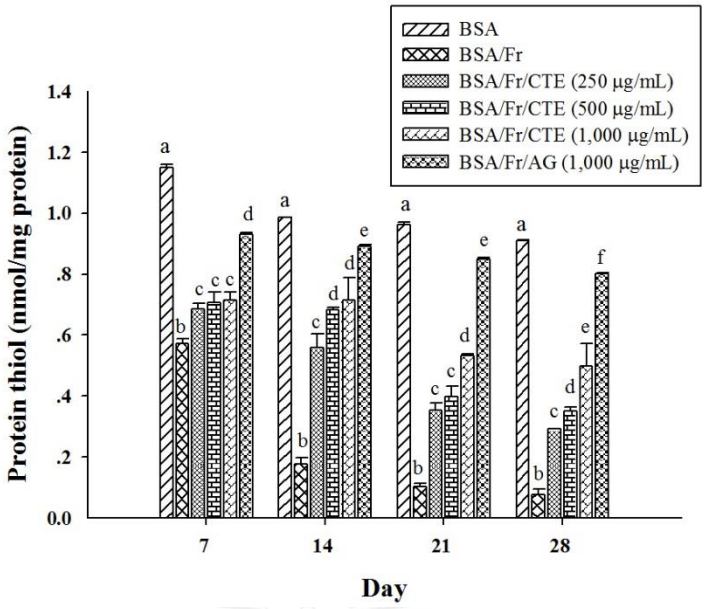

B

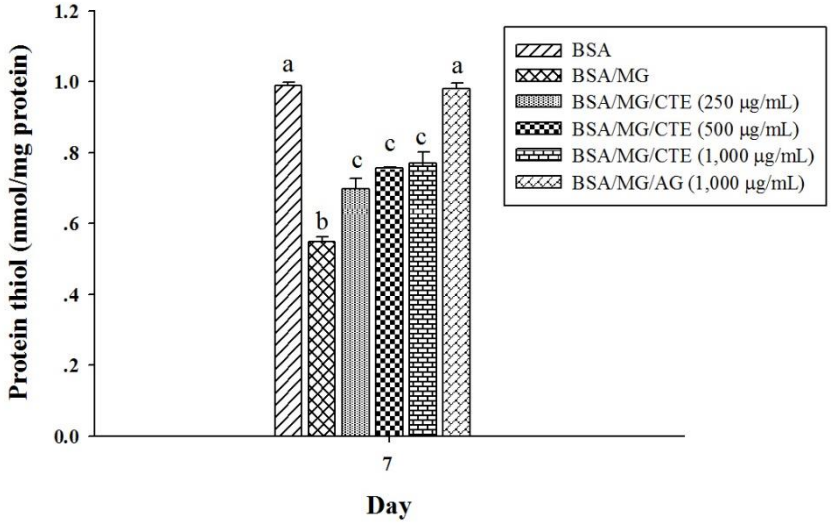

Figure 19 The effects of *Clitoria ternatea* extract (CTE, 250-1,000 µg/mL) and aminoguanidine (AG, 1,000 µg/mL) on the level of protein thiol group in BSA/fructose (A) and BSA/MG (B) system. Each value represents the mean ± SEM (n=5). Significance is shown in groups that do not share a common letter ($p < 0.05$).

4.3.5 The effect of CTE on amyloid cross-β structure

The thioflavin T is used to determine the quantification of amyloid cross β structure which represented protein aggregation in glycated BSA. As shown in Figure 20A-20B, the glycated BSA induced by fructose and MG exhibited an elevation of amyloid cross β conformation over non-glycated BSA at day 28 and 7 of incubation up to 3.8-fold and 2.1-fold, respectively. CTE at concentrations of 250–1,000 μg/mL suppressed the level of amyloid cross β structure in a concentration-dependent manner for both BSA/fructose (12.12%, 15.35%, and 26.04%) and BSA/MG (5.99%, 10.39%, and 14.17%) systems. Likewise, a significant decrease in the level of amyloid cross β structure (36.73% in BSA/fructose and 42.14% in BSA/MG) was observed in the presence of AG at same period of incubation.

A

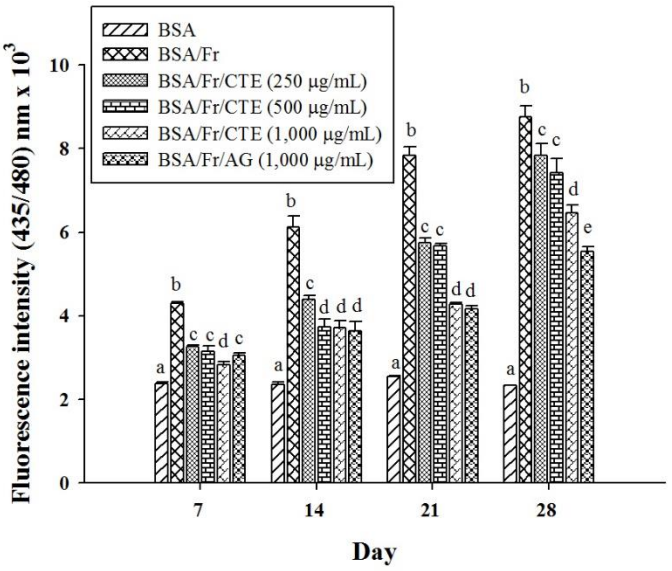

B

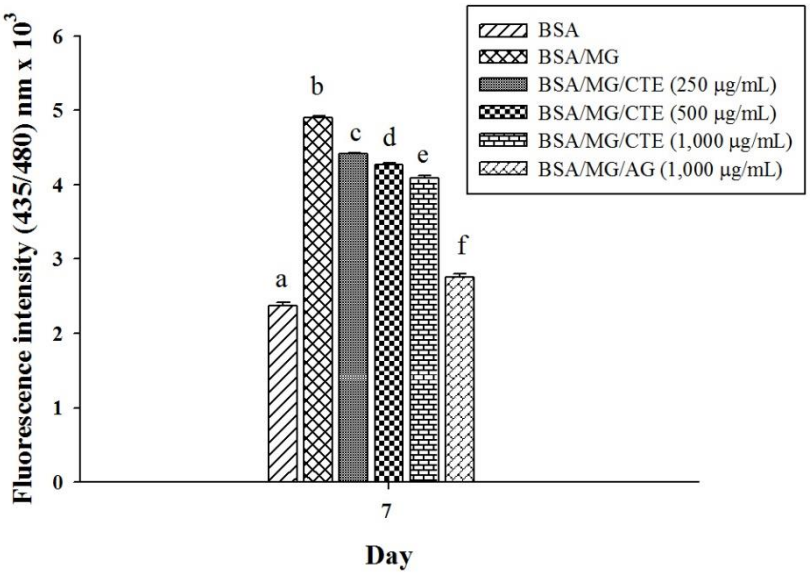

Figure 20 The effects of *Clitoria ternatea* extract (CTE, 250-1,000 µg/mL) and aminoguanidine (AG, 1,000 µg/mL) on the level of the amyloid cross β-structure in BSA/fructose (A) and BSA/MG (B) system. Each value represents the mean ± SEM (n=5). Significance is shown in groups that do not share a common letter ($p < 0.05$).

4.3.6 Determination of N^{ε}-CML

The formation of N^{ε}-CML, a non-fluorescent AGE, was illustrated in Figure 21A-21B. After 7 days of incubation, glycated BSA induced by fructose presented a 10.5-fold increase in N^{ε}-CML formation, whereas there was 4.5-fold increase in MG-induced glycated BSA when compared to non-glycated BSA. CTE at a concentration of 250, 500, and 1,000 µg/mL significantly inhibited N^{ε}-CML formation in range from 54.30% to 84.51% in BSA/fructose system and 13.89% to 54.83% in BSA/MG system. Similarly, AG significantly reduced the formation of N^{ε}-CML by 91.55% and 57.75% for BSA/fructose and BSA/MG systems, respectively.

A

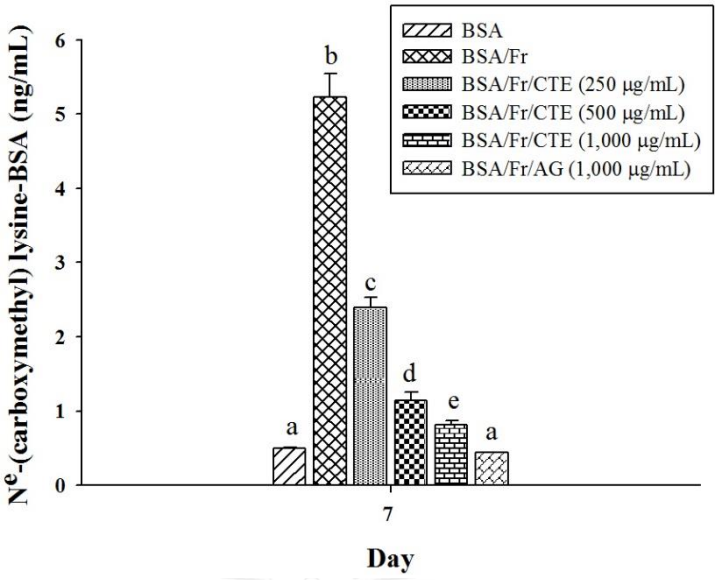

B

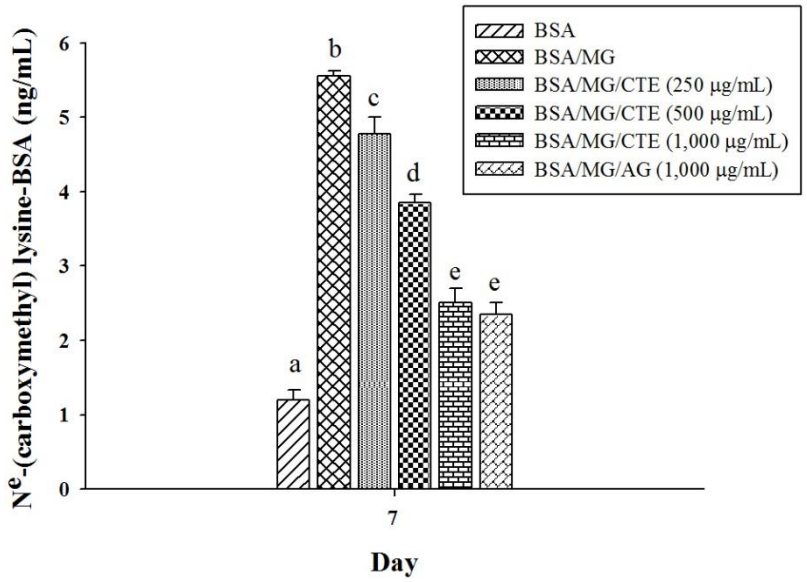

Figure 21 The effects of *Clitoria ternatea* extract (CTE, 250-1,000 µg/mL) and aminoguanidine (AG, 1,000 µg/mL) on CML formation in BSA/fructose (A) and BSA/MG (B) system. Each value represents the mean ± SEM (n=5). Significance is shown in groups that do not share a common letter ($p < 0.05$).

4.3.7 Methylglyoxal trapping ability

The results showed that the direct MG-trapping capacity of CTE (250-1,000 µg/mL) and AG (1,000 µg/mL) was investigated after 24 h of incubation. The level of 2-MQ, a product from the reaction of MG and *o*-PD, represented free MG remaining from the trapping reaction. In Figure 22A-22E, the chromatogram results showed that CTE (250-1,000 µg/mL) exhibited MG-trapping ability with the values of 15.04±0.28% to 43.17±0.23% at 24 h. Taken together, AG (1,000 µg/mL) showed MG-trapping ability in %inhibition of 100±0.23% at 24 h of incubation.

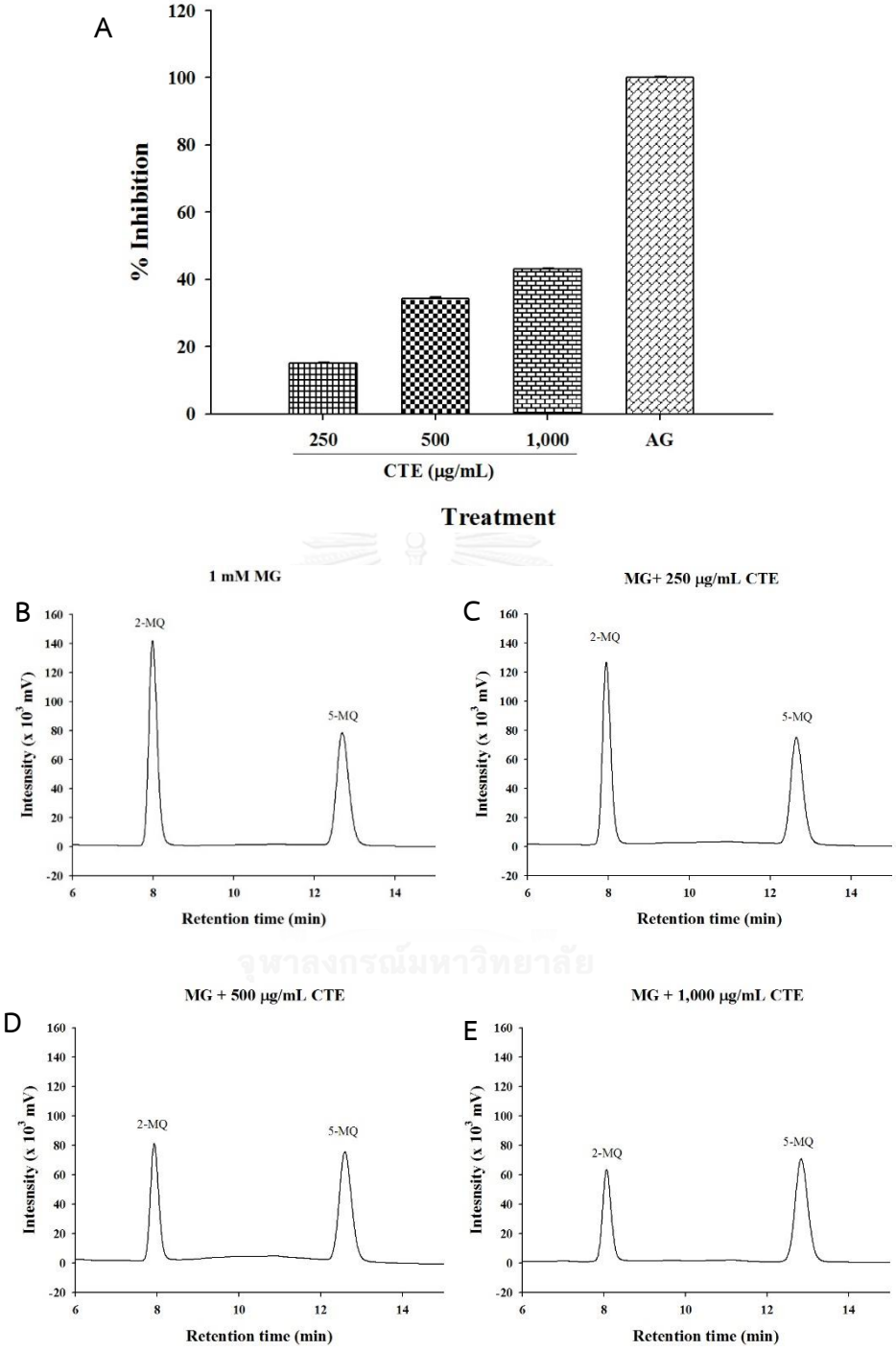
A
% Inhibition
120
100
80
60
40
20
0
250
500
1,000
AG
CTE (µg/mL)
Treatment
B
1 mM MG
C
MG+ 250 µg/mL CTE
D
MG + 500 µg/mL CTE
E
MG + 1,000 µg/mL CTE
2-MQ
5-MQ
Intesnsity (x 10³ mV)
Retention time (min)

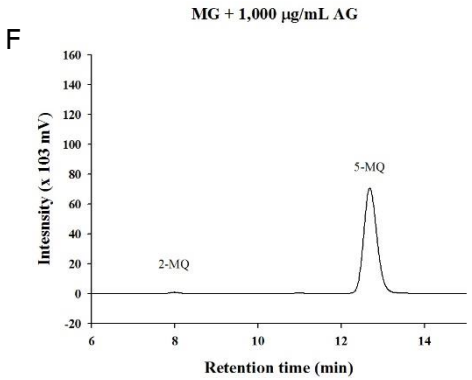

Figure 22 The effects of *Clitoria ternatea* extract (CTE) on direct MG-trapping capacity (A). The HPLC chromatogram of 1 mM methylglyoxal (MG) (B) after reacting with CTE (250-1,000 µg/mL) (C-E) or aminoguanidine (AG; 1,000 µg/mL) (F) at the incubation time of 24 h. MG was detected as 2-methylquinoxaline (2-MQ) after derivatization using o-phenylenediamine (*o*-PD) at 315 nm. 5-methylquinoxaline (5-MQ) was used as the internal standard.

4.4 Antioxidant properties of CTE

In DPPH assay, CTE had significant radical scavenging activity with the IC_{50} value of 0.47±0.01 mg/mL (Table 3). The results indicated that CTE had 235-times less potency than that observed for ascorbic acid (0.002±0.001 mg/mL). According to the results from TEAC and FRAP, CTE had the ability of 0.17±0.01 mg trolox equivalents/mg dried extract and 0.38±0.01 mmol $FeSO_4$ equivalents/mg dried extract, respectively. In the SRSA assay, the IC_{50} value of CTE was found to be 26.31±4.22 mg/mL. However, CTE had 45-times less potency than trolox (0.58±0.04 mg/mL). The results showed that CTE exhibited less potent antioxidant activity with FICP and HRSA.

Table 3 Antioxidant activities of *Clitoria ternatea* extract (CTE) including DPPH radical scavenging activity, TEAC, FRAP, HRSA, SRSA, and FICP

	Antioxidant activities					
	DPPH	TEAC	FRAP	HRSA	SRSA	FICP
CTE	0.467 ± 0.005	0.168 ± 0.001	0.379 ± 0.009	19.18 ± 3.40	26.31 ± 4.22	$>10^3$
Ascorbic acid	0.002 ± 0.001	-	-	-	-	-
Trolox	-	-	-	2.03 ± 0.04	0.574 ± 0.04	-
EDTA	-	-	-	-	-	8.88 ± 1.60

Data are expressed as mean ± S.E.M, n = 3. DPPH radical scavenging activity, hydroxyl radical scavenging activity (HRSA), and superoxide radical scavenging activity (SRSA) are expressed as the IC_{50} value (mg/mL). Trolox equivalent antioxidant capacity (TEAC), ferric reducing antioxidant power (FRAP), and ferrous ion chelating power (FICP) are expressed as mg trolox/mg dried extract, mmol $FeSO_4$/mg dried extract, and mg EDTA/mg dried extract, respectively.

4.5 Effect of CTE on oxidative DNA damage induced by MG/lysine and AAPH system, *in vitro*

4.5.1 DNA strand breakage

The band intensity of DNA fragments on agarose gel indicating the strand breakage of plasmid DNA after incubating with or without lysine or MG or $CuSO_4$ or CTE (250 and 1,000 µg/mL) is illustrated in Figure 23. The DNA was detected as major bands of supercoiled form (SC) and opened circular form (OC), respectively. The results from control experiments showed that there was no OC band when DNA was incubated with lysine or MG or $CuSO_4$ or CTE. Moreover, there was no difference in the band intensity of both SC and OC was observed between the treatments. The incubation of DNA with lysine/MG system markedly induced DNA stand breakage with 2.7-fold increase in the intensity of OC band when compared to untreated DNA. The effect of CTE on preventing DNA strand breakage in the absence of Cu^{2+} is demonstrated in Figure 24A-24B. CTE significantly attenuated DNA damage at 250 (38.61%), 500 (49.29%) and 1,000 µg/mL (56.62%). In addition, after pUC19 (0.25 µg) was incubated with 50 mM lysine and 50 mM MG in the presence of Cu^{2+} with or without various CTE concentrations (125-1,000 µg/mL). Figure 25A, untreated plasmid DNA was detected as major band of supercoiled form (SC) (lane 1 on gel). The addition of MG/lysine/Cu^{2+} system to plasmid DNA caused DNA strand break of plasmid DNA represented by increasing the intensity of open circular band (OC) (lane 2 on gel). In MG/lysine/Cu^{2+}

system-induced DNA damage was inhibited by CTE (125-1,000 µg/mL) with the percentage inhibition of 7.93±0.21% to 53.40±1.31% as illustrated in Figure 25B.

In similar pattern, 12.5 mM AAPH increasing the intensity of OC band (lane 2 on gel) shown in Figure 26A-26B. In the presence of CTE (125-1,000 µg/mL), the intensity of OC band was significantly reduced by 15.88±0.13% to 88.33±0.80%, respectively.

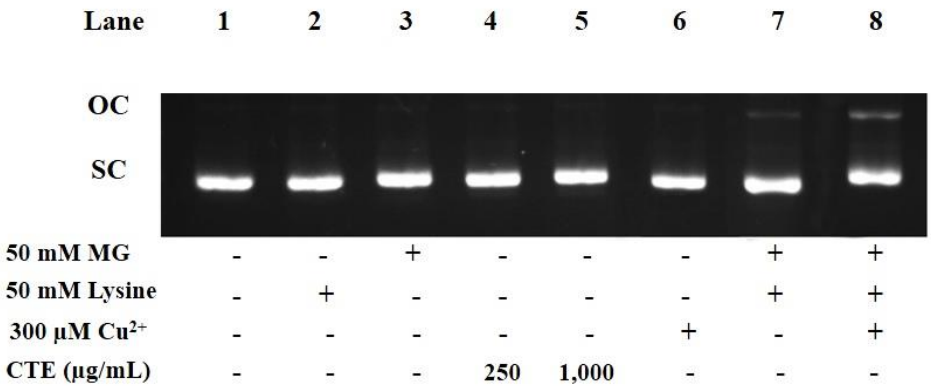

Figure 23 The band intensity of open circular form (OC) and supercoiled form (SC) of plasmid DNA after pUC19 (0.25 µg) is incubated with the following treatments (lane 1-8): no treatment, 50 mM lysine, 50 mM methylglyoxal (MG), 250 and 1,000 µg/mL *Clitoria ternatea* extract (CTE), 300 µM $CuSO_4$, 50 mM lysine and 50 mM MG, and 50 mM lysine, 50 mM MG and 300 µM $CuSO_4$ respectively.

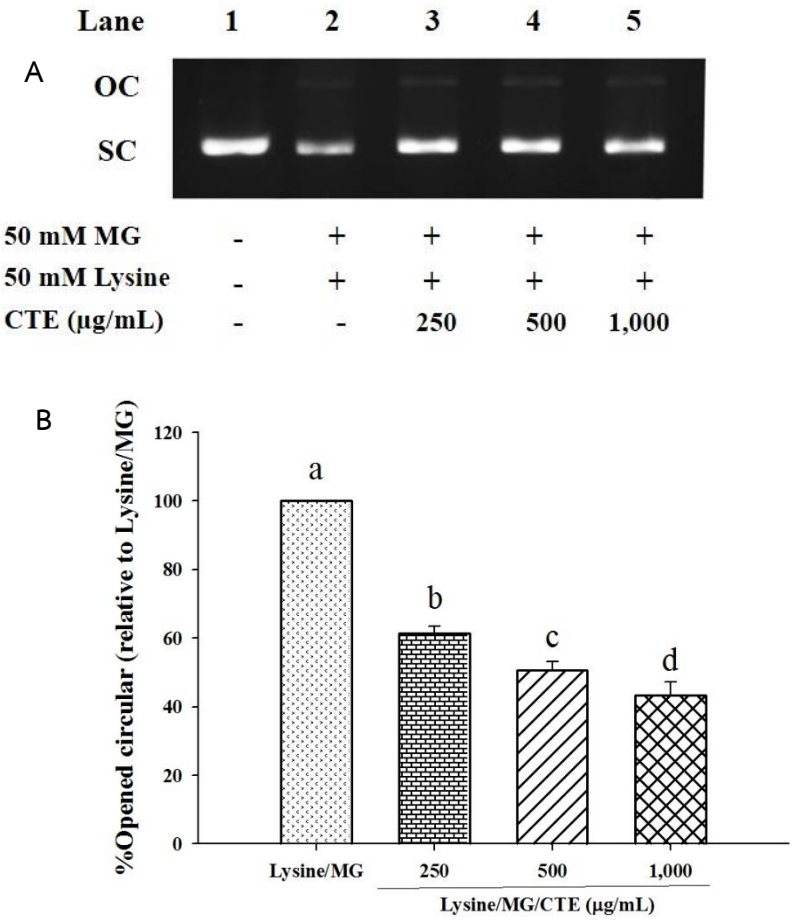

Figure 24 The effects of *Clitoria ternatea* extract (CTE) on Lysine/methylglyoxal (MG)-induced DNA strand breakage. The band intensity of open circular form (OC) and supercoiled form (SC) of plasmid DNA after pUC19 (0.25 µg) is incubated with the following treatments (lane 1-5): no treatment, 50 mM lysine and 50 mM methylglyoxal (MG), 50 mM lysine, 50 mM MG and 250-1,000 µg/mL *Clitoria ternatea* extract (CTE), respectively (A). The percentage of OC is represented in % of control relative to Lysine/MG system treated DNA (B). Results are presented as mean ± SEM (n=3). Significance is shown in groups that do not share a common letter ($p < 0.05$).

A

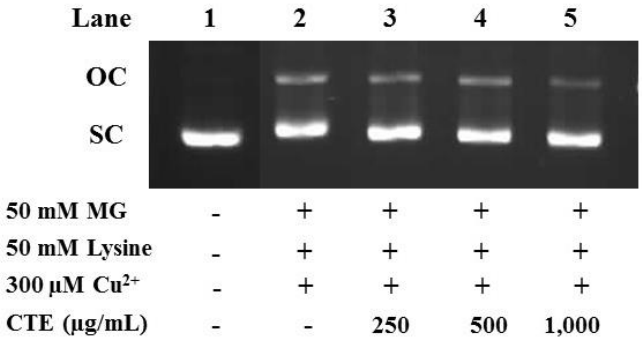

B

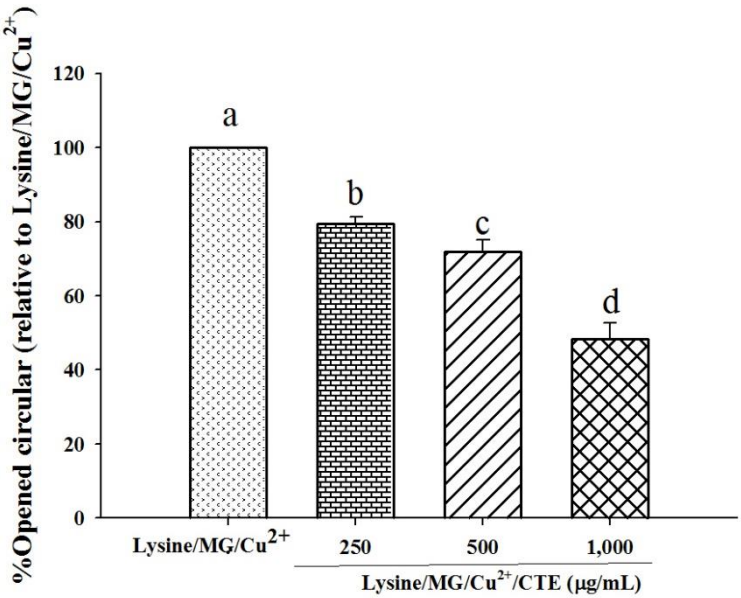

Figure 25 The effects of *Clitoria ternatea* extract (CTE) on Lysine/methylglyoxal (MG)/Cu^{2+}-induced DNA strand breakage. The band intensity of open circular form (OC) and supercoiled form (SC) of plasmid DNA after pUC19 (0.25 µg) is incubated with the following treatments (lane 1-6): no treatment, 50 mM lysine, 50 mM methylglyoxal (MG), 300 µM $CuSO_4$ and 250-1,000 µg/mL *Clitoria ternatea* extract (CTE), respectively (A). The percentage of OC is represented in % of control relative to Lysine/MG/Cu^{2+} system treated DNA (B). Results are presented as mean ± SEM (n=3). Significance is shown in groups that do not share a common letter ($p < 0.05$).

A

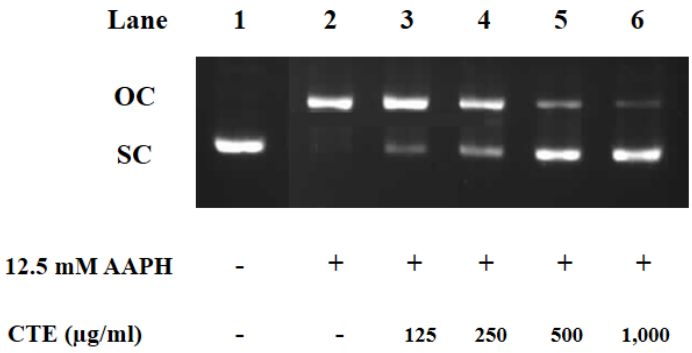

B

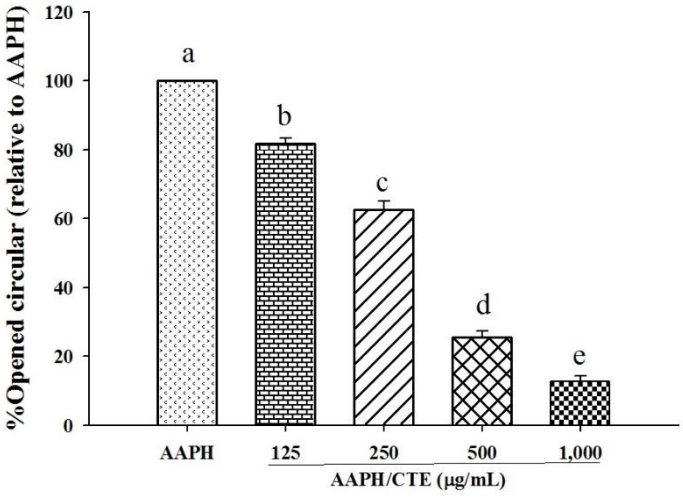

Figure 26 The effects of *Clitoria ternatea* extract (CTE) on 2,2'-azobis(2-amidinopropane) dihydrochloride (AAPH)-induced DNA strand breakage. The band intensity of open circular form (OC) and supercoiled form (SC) of plasmid DNA after pUC19 (0.25 µg) is incubated with the following treatments (lane 1-6): no treatment, 12.5 mM AAPH and, 12.5 mM AAPH and 125-1,000 µg/mL *Clitoria ternatea* extract (CTE), 300 µM $CuSO_4$, respectively (A). The percentage of OC is represented in % of control relative to AAPH induced-DNA damage (B). Results are presented as mean ± SEM (n=3). Significance is shown in groups that do not share a common letter ($p < 0.05$).

4.5.2 Superoxide anion production

As illustrated in Figure 27, the results showed that the reduced form of cytochrome *c* was increased during 60 min of incubation taken together with an increase of superoxide anion. Superoxide anion was generated from the reaction of 50 mM MG and 50mM lysine to 5.42±0.15 nmol/mL at 180 min. The production of superoxide anion was reduced by CTE (125-1,000 µg/mL) after 10 min of incubation. At 60 min of incubation, CTE (125-1,000 µg/mL) inhibited MG/lysine system-induced superoxide anion production at 21.67±1.38%, 41.91±1.02%, 70.95±2.34% and 100±2.21%, respectively.

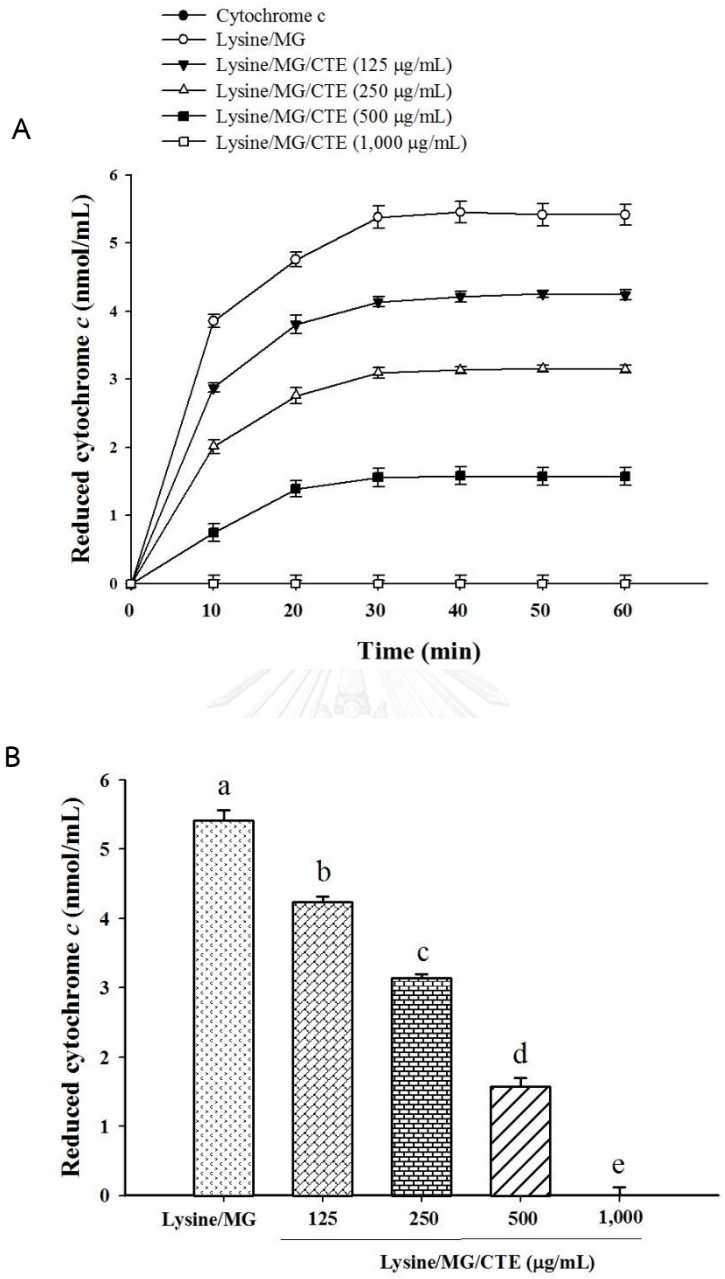

Figure 27 The effects of *Clitoria ternatea* extract (CTE) on the production of superoxide anion in lysine/methylglyoxal (MG) glycation within 60 mins (A) and at the incubation time of 60 min (B). Results are presented as mean ± SEM (n=5). Significance is shown in groups that do not share a common letter ($p < 0.05$).

4.5.3 Hydroxyl radical production

Figure 28A-28B showed that the increase of TBARS mediated by MG/lysine system referring to the production of hydroxyl radicals at 120 and 180 min respectively. In similarly to superoxide anion formation, CTE (125-1,000 µg/mL) was able to suppress the generation of hydroxyl radical. The percentage inhibition of hydroxyl radical generation by CTE (125-1,000 µg/mL) was 37.60±3.41% to 83.26±0.99% at 120 min and 14.05±0.26% to 70.86±2.82% at 180 min.

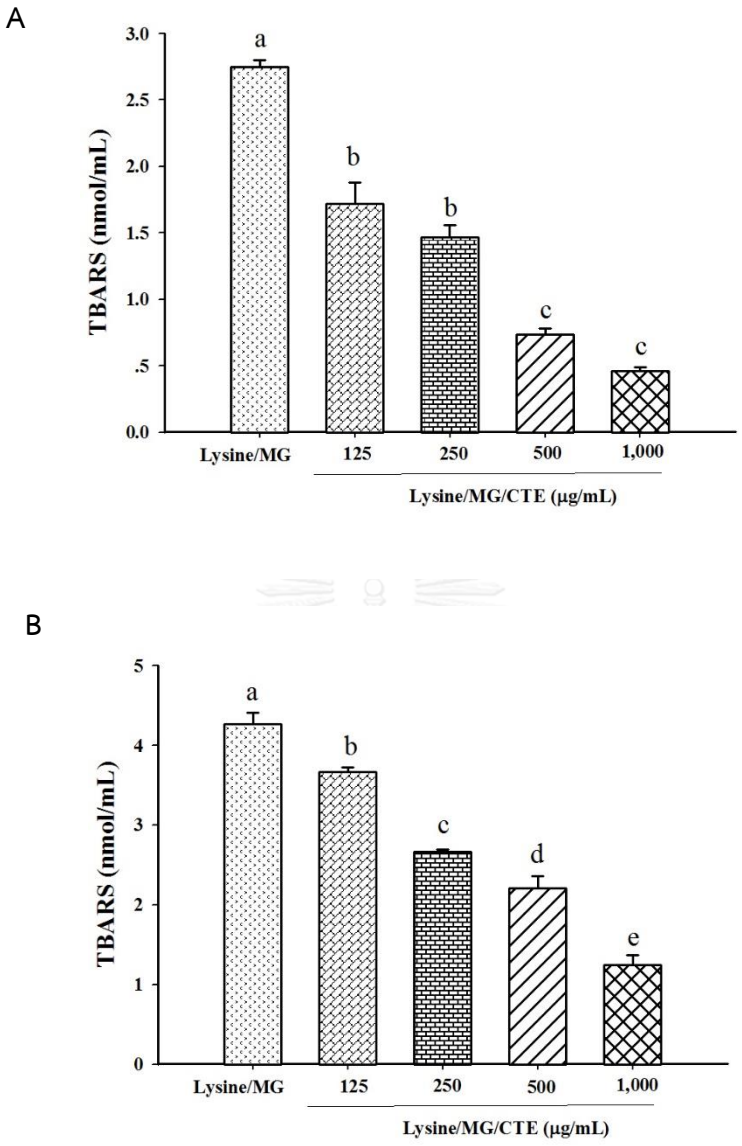

Figure 28 The effects of *Clitoria ternatea* extract (CTE) on the production of hydroxyl radical in lysine/methylglyoxal (MG) glycation at 120 (A) and 180 min (B). Results are presented as mean ± SEM (n=3). Significance is shown in groups that do not share a common letter ($p < 0.05$).

4.6 Inhibitory effect of CTE on MG-induced adipogenesis *in vitro*

4.6.1 The effects of CTE on cell viability and cell proliferation of 3T3-L1 preadipocyte cells

To determine whether CTE has cytotoxicity to 3T3-L1 cells, various concentrations of CTE (500-2,000 µg/mL) were incubated with 3T3-L1 cells during adipogenesis process. There was no toxicity of CTE to 3T3-L1 cells at the concentration up to 2,000 µg/mL as determined by Trypan blue and MTT viability assay (Figure 29A-29B). Figure 30A demonstrated that maximum effect of MG on cell proliferation was shown at the concentration of 10 µM. In contrast, CTE (500-1,000 µg/mL) significantly inhibited proliferation of 3T3-L1 mediated by MG at 12.77±2.76% to 34.75±3.74%, as shown in Figure 30B. CTE also inhibited proliferation of 3T3-L1 without induction of MG at 13.07±1.08% to 58.39±1.66% (Figure 31).

A

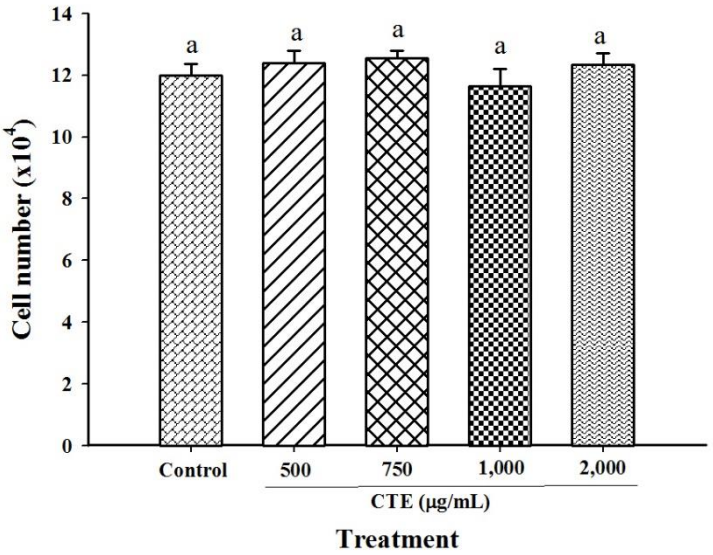

B

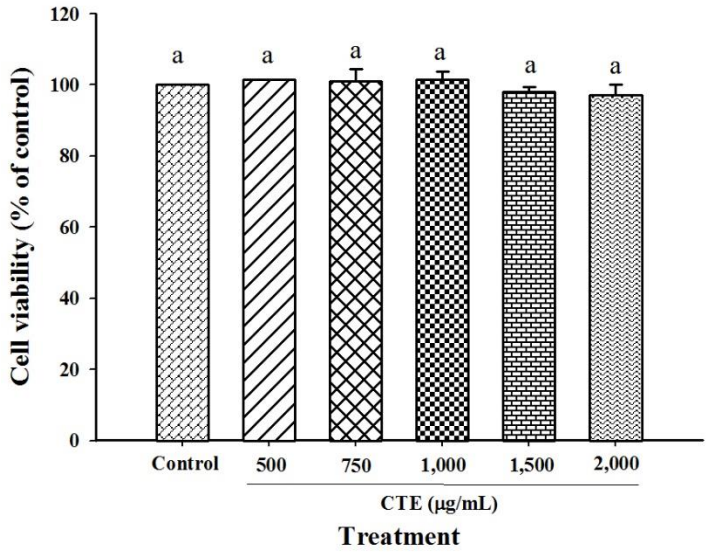

Figure 29 Effects of *Clitoria ternatea* extract (CTE, 500–2,000 µg/mL) on the cell viability of 3T3-L1 cells by trypan blue assay (A) and MTT assay (B) after 2 h of incubation. Each value represents the mean ± SEM (n=3). Significance is shown in groups that do not share a common letter ($p < 0.05$).

A

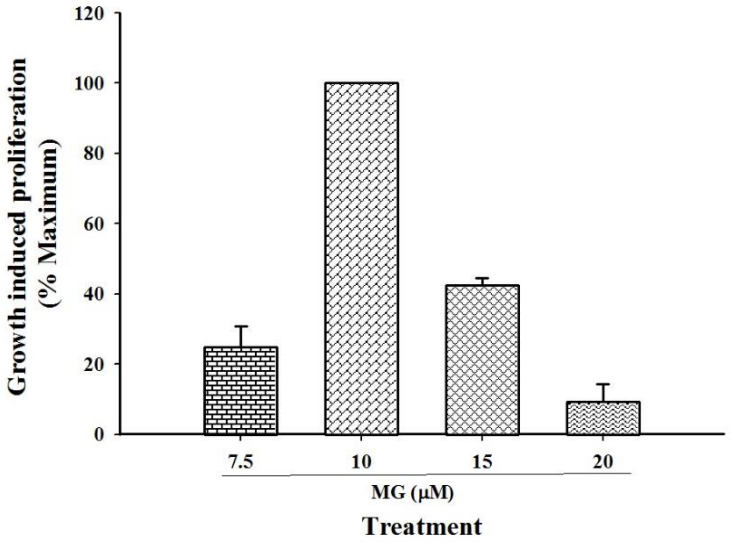

B

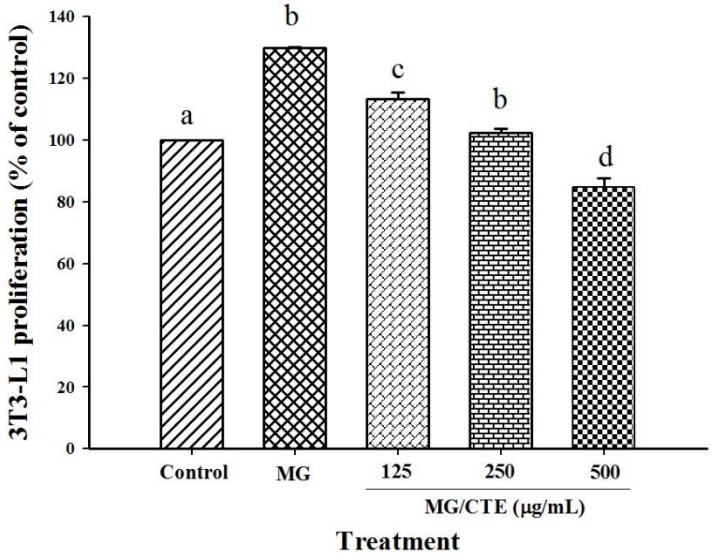

Figure 30 Effects of 10 µM methylglyoxal (MG) (A) and MG with 125–500 µg/mL *Clitoria ternatea* extract (CTE) (B) on cell proliferation of 3T3-L1 cells after 24 h of incubation. Each value represents the mean ± SEM (n=3). Significance is shown in groups that do not share a common letter ($p < 0.05$).

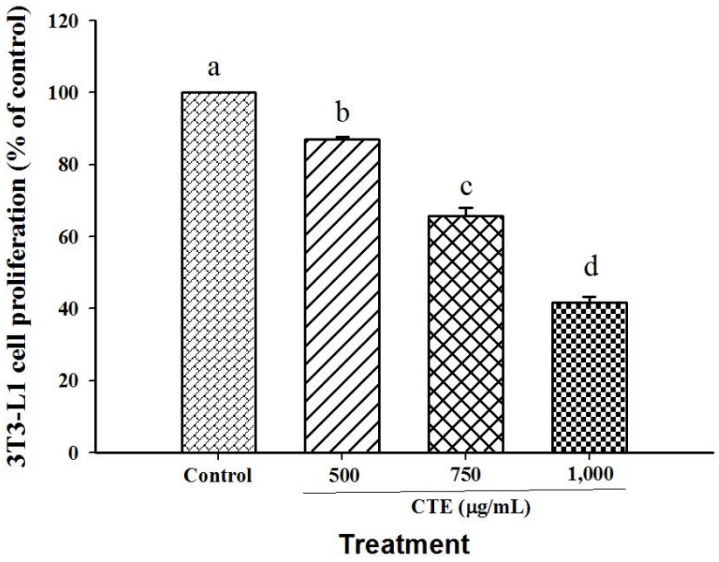

Figure 31 Effects of *Clitoria ternatea* extract (CTE, 500-1,000 µg/mL) on cell proliferation of 3T3-L1 cells after 24 h of incubation. Each value represents the mean ± SEM (n=3). Significance is shown in groups that do not share a common letter ($p < 0.05$).

4.6.2 The effects of CTE on the cell cycle of 3T3-L1 cells

As shown in Figure32A-32E, the results showed that 10 μM MG significantly increased cell distribution in G2/M from control at 46.26±5.29% to 56.12±1.58%, whereas it decreased G0/G1 from 34.3±2.01% to 23.34±1.42%. In contrast, CTE (250-750 μg/mL) significantly delayed MG-induced cell cycle progression by increased cell distribution to 33.56±1.18%-44.01±0.85% in G0/G1 phase and it decreased the cell distribution to 48.13±1.99%-44.52±0.32%. In similarity to Figure 33A-33D, CTE (250-750 μg/mL) alone delayed cell cycle by increased cell distribution in G0/G1 phase from control at 34.23±2.01% to 44.88±1.07%-52.26±2.62%. In addition, it concentration-dependently decreased G2/M phase from control at 46.26±5.29 to 43.07±0.64-38.83±0.46%.

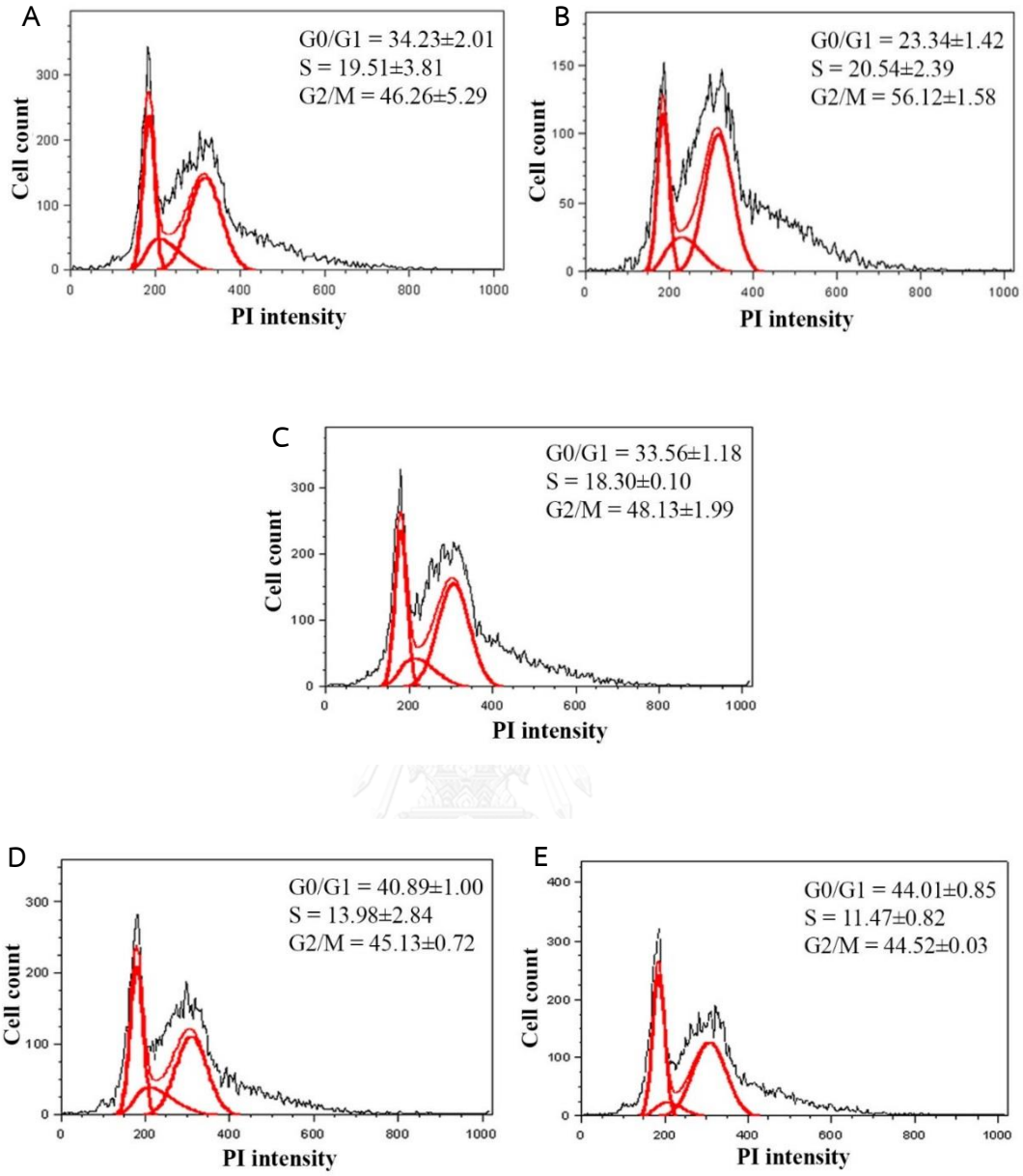
A
G0/G1 = 34.23±2.01
S = 19.51±3.81
G2/M = 46.26±5.29
Cell count
PI intensity
B
G0/G1 = 23.34±1.42
S = 20.54±2.39
G2/M = 56.12±1.58
Cell count
PI intensity
C
G0/G1 = 33.56±1.18
S = 18.30±0.10
G2/M = 48.13±1.99
Cell count
PI intensity
D
G0/G1 = 40.89±1.00
S = 13.98±2.84
G2/M = 45.13±0.72
Cell count
PI intensity
E
G0/G1 = 44.01±0.85
S = 11.47±0.82
G2/M = 44.52±0.03
Cell count
PI intensity

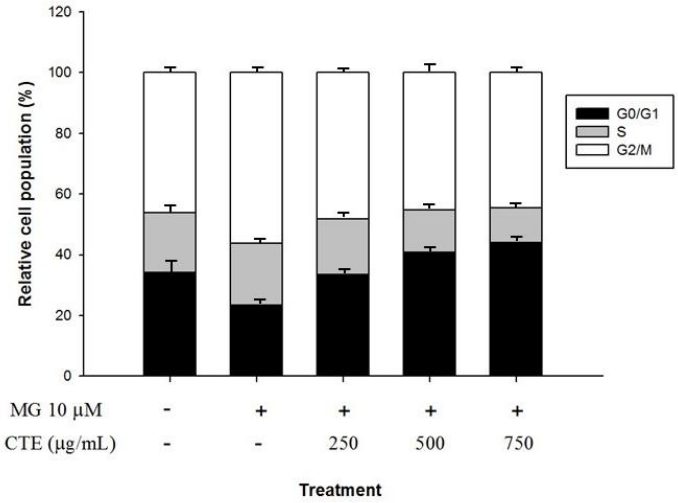

Figure 32 Effects of *Clitoria ternatea* extract (CTE; 250-750 µg/mL) on cell cycle of 3T3-L1 cells mediated by 10 µM methylglyoxal (MG). The histograms are shown as control (A), 10 µM MG (B), 10 µM MG and CTE at 250 (C), 500 (D), and 750 (E) µg/mL. Each value represents the mean ± SEM (n=3). Significance is shown in groups that do not share a common letter ($p < 0.05$).

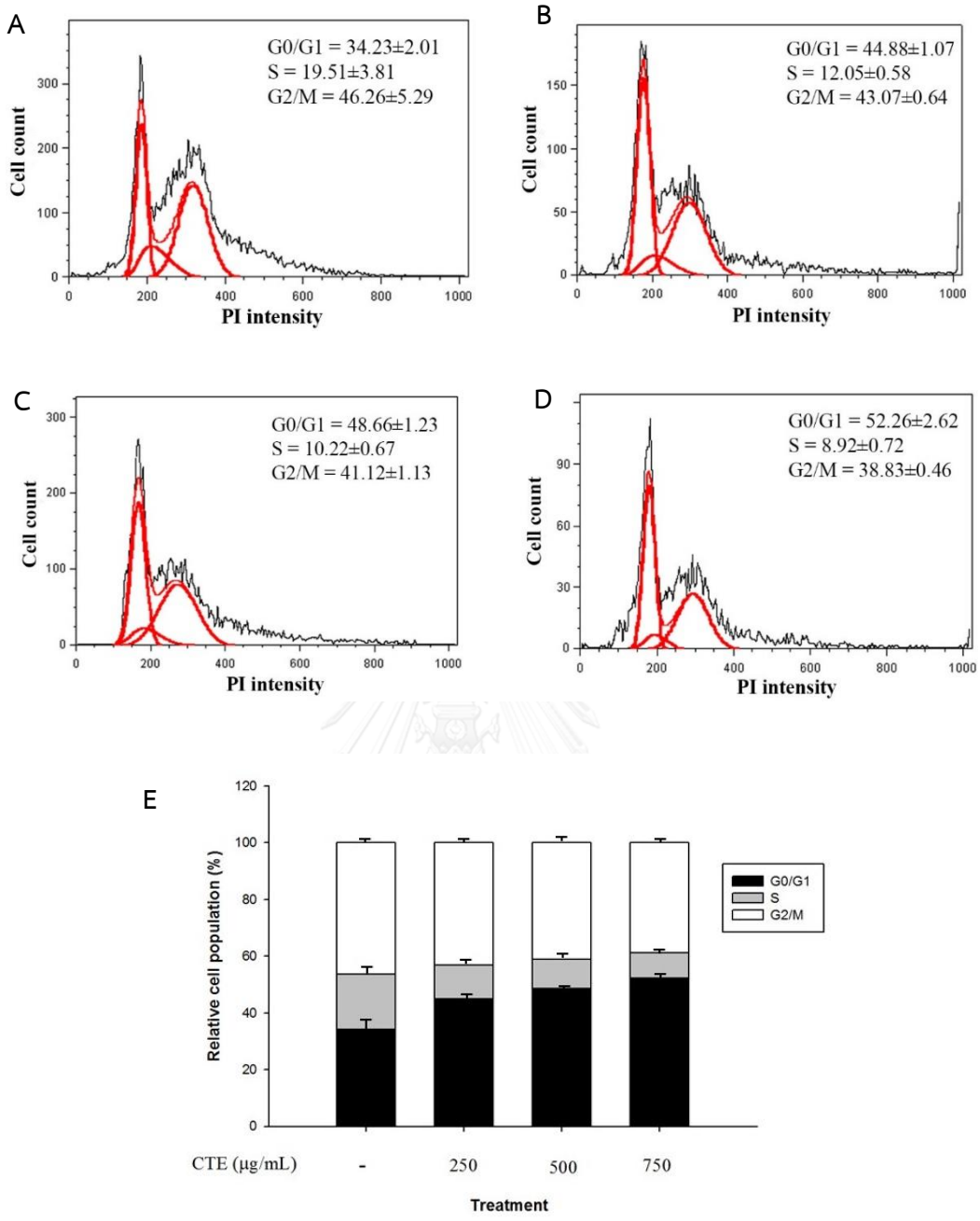

Figure 33 Effects of *Clitoria ternatea* extract (CTE; 250-750 µg/mL) on cell cycle of 3T3-L1 cells. The histograms are shown as control (A), CTE at 250 (B), 500 (C), and 750 (D) µg/mL. Each value represents the mean ± SEM (n=3). Significance is shown in groups that do not share a common letter ($p < 0.05$).

4.6.3 The effects of CTE on Akt1 and ERK1/2 signaling pathways in 3T3-L1 cells

The results demonstrated that 10 μM MG significantly increased the phosphorylation levels of Akt (T308) to 172.09±5.06% compared to the control, as shown in Figure 34. However, CTE at concentration of 500, 750 and 1,000 μg/mL significantly reduced the expression of *p*-Akt by 38.99±3.83%, 49.59±3.75% and 91.43±5.55% when compared to MG, respectively. CTE (500-1,000 μg/mL) alone suppressed the *p*-Akt expression with ranging from 45.16±1.37% to 91.95±0.31%, as compared to the control (Figure 35). Furthermore, CTE at concentration of 750 and 1,000 μg/mL also significantly suppressed the phosphorylation of ERK1/2 (T202/Y204) about 62.15% and 94.04%, respectively (Figure 36). However, CTE (500 μg/mL) did not significantly alter the phosphorylation level of ERK1/2.

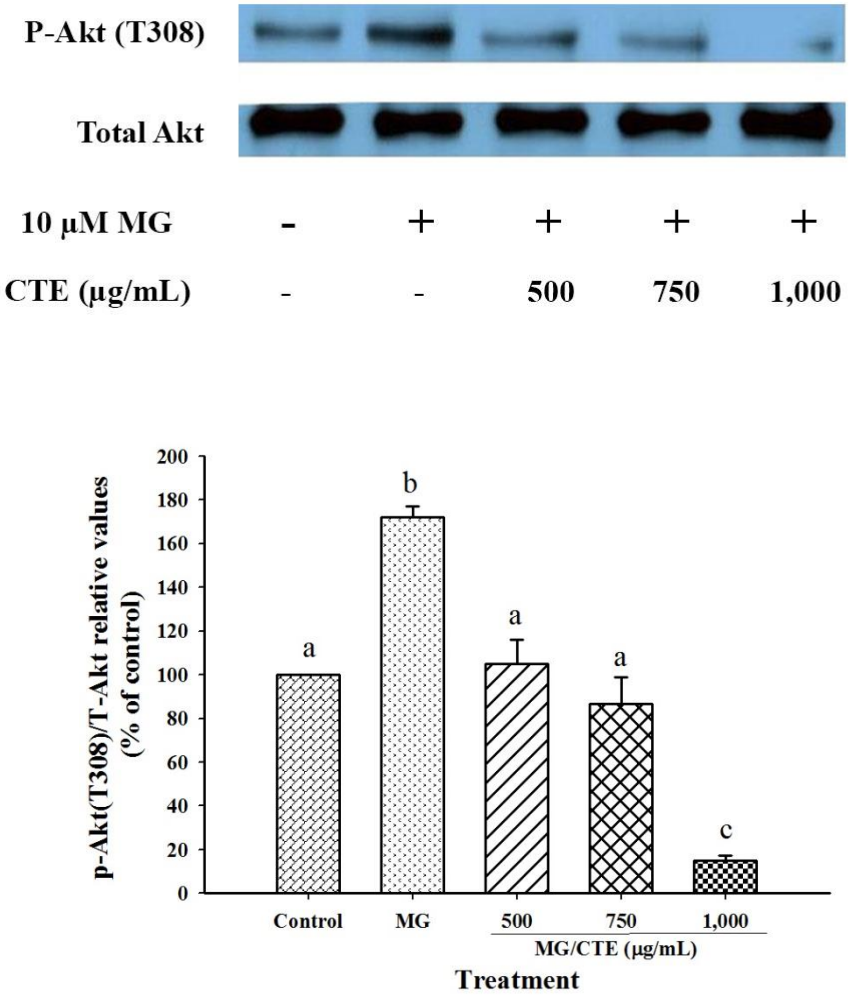

Figure 34 Effects of *Clitoria ternatea* extract (CTE, 500-1,000 μg/mL) on Akt pathway of 3T3-L1 cells mediated by 10 μM methylglyoxal (MG). The relative values of *p*-Akt1 (T308) to T-Akt1 are shown in the percentage of control. Each value represents the mean ± SEM (n=3). Significance is shown in groups that do not share a common letter ($p < 0.05$).

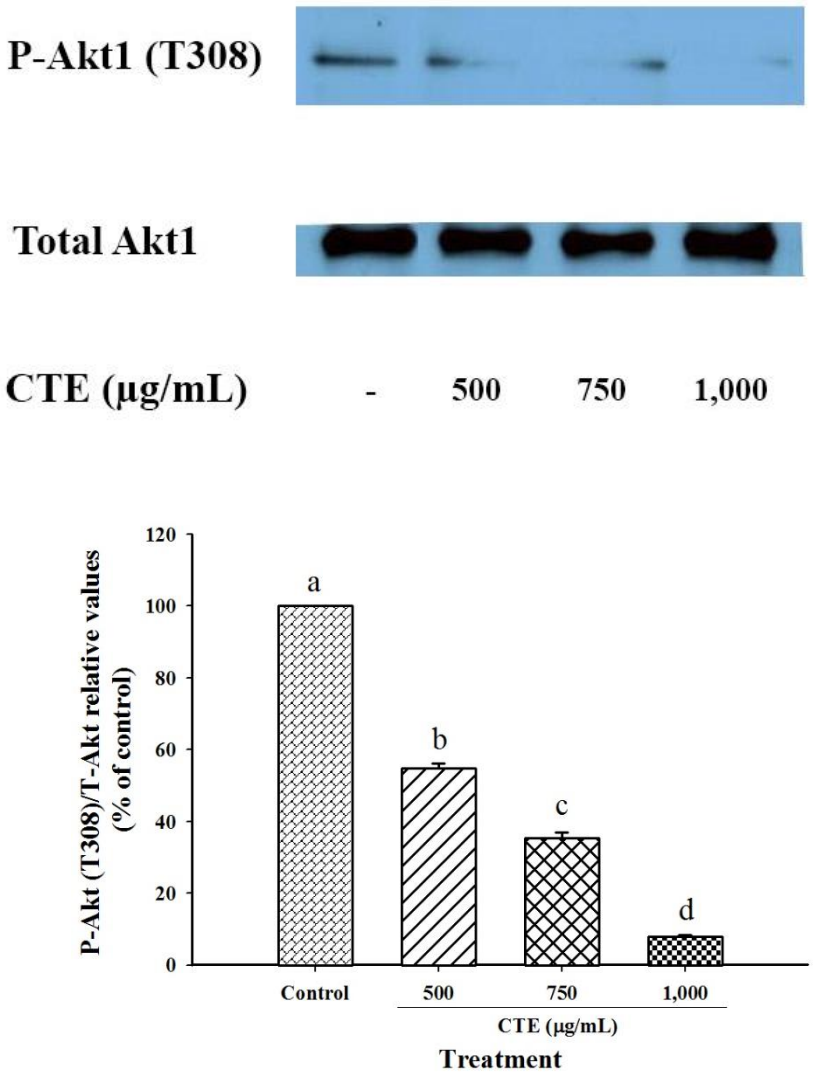

Figure 35 Effects of *Clitoria ternatea* extract (CTE, 500-1,000 µg/mL) on Akt pathway of 3T3-L1 cells. The relative values of *p*-Akt1 (T308) to T-Akt1 are shown in the percentage of control. Each value represents the mean ± SEM (n=3). Significance is shown in groups that do not share a common letter ($p < 0.05$).

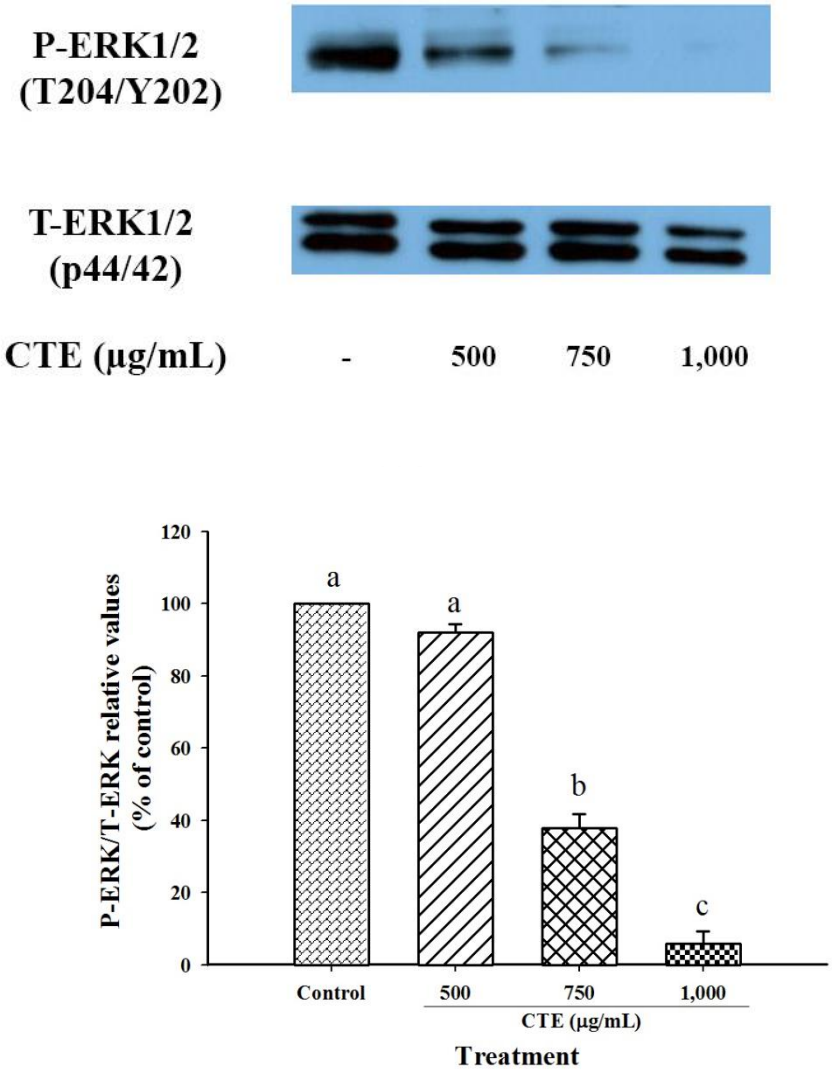

Figure 36 Effects of *Clitoria ternatea* extract (CTE, 500-1,000 µg/mL) on ERK pathway of 3T3-L1 cells. The relative values of *p*-ERK (T204/Y202) to T-ERK are shown in the percentage of control. Each value represents the mean ± SEM (n= 3). Significance is shown in groups that do not share a common letter ($p < 0.05$).

4.6.4 The effects of CTE on lipid accumulation in 3T3-L1 cells

After the cells were exposed to the inducer including dexamethasone, insulin, and IBMX, 3T3-L1 cells were differentiated to mature adipocytes, as characterized by triglyceride-rich lipid droplet structure histologically. The result demonstrated that 10 μM MG significantly increased Oil-red O staining lipid droplet approximately 31.78±1.52% compared to the control. On the contrary, CTE (500-1,000 μg/mL) significantly inhibited lipid droplet at 21.51±1.75%, 31.90±1.54% and 50.18±2.21% compared to MG as shown in Figure 37A-37E. In the absence of MG, CTE (500-1,000 μg/mL) also significantly decreased Oil-red O staining lipid droplet (26.40±2.14%, 52.86±2.33% and 68.25±2.78%) when compared to control (Figure 38).

Furthermore, the accumulation of TG was significantly increased to 154.38±2.61% when the cells were incubated with MG (10 μM) (Figure 39A). On the contrary, the MG-induced accumulation of TG was significantly inhibited by CTE (500-1000 μg/ml) at 23.86±2.60 - 47.72±3.21% as compared to MG. In meanwhile, the accumulation of TG was lowered when the cells was incubated with CTE alone at the concentration of 500, 750 and 1000 μg/mL (59.05 - 74.30%), as shown in Figure 39B.

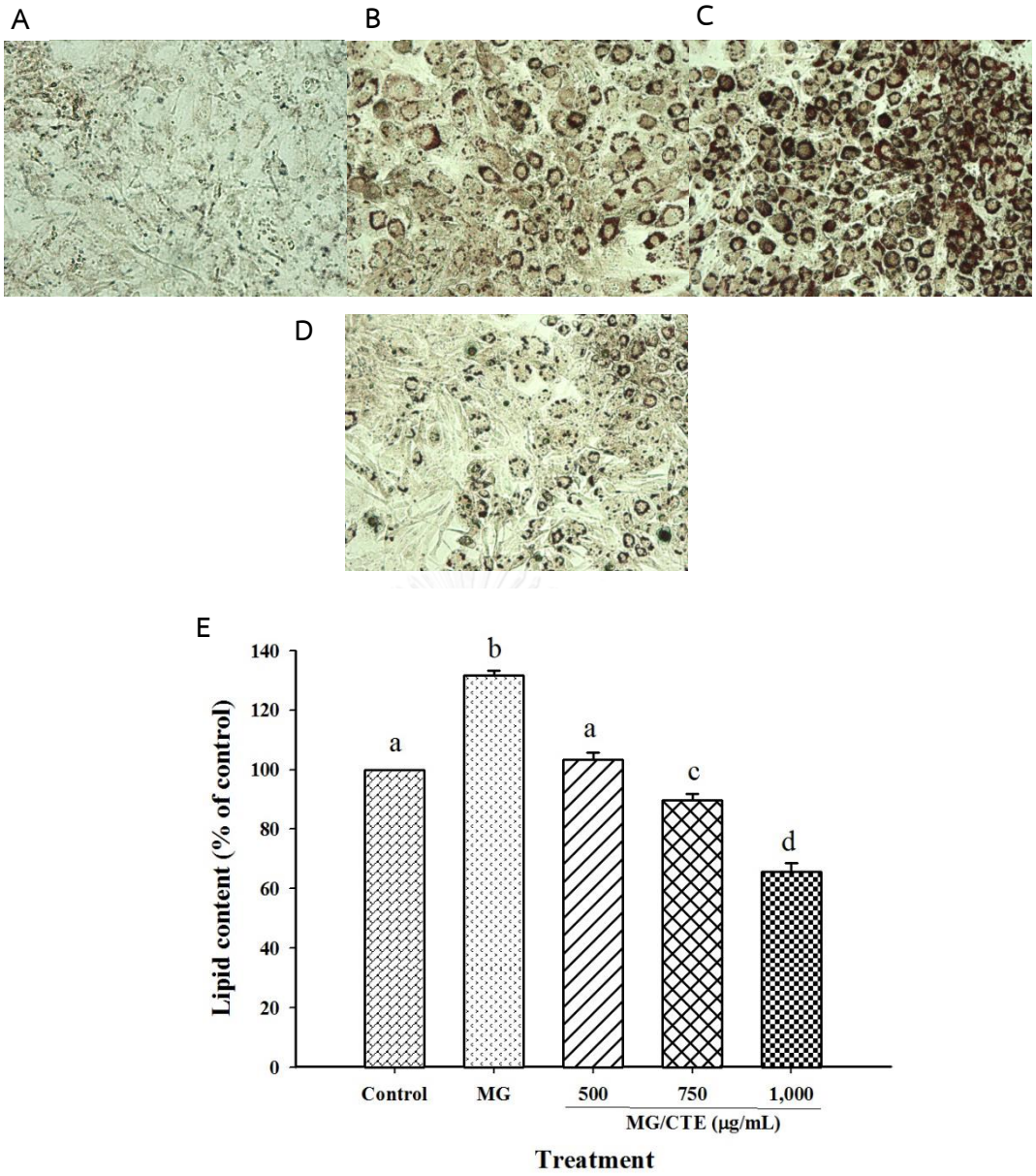

Figure 37 Effects of *Clitoria ternatea* extract (CTE, 500-1,000 µg/mL) on lipid accumulation of 3T3-L1 cells mediated by 10 µM methylglyoxal (MG). Undifferentiated cells (A), Differentiated cells (B), 10 µM MG (C), and 10 µM MG plus 1,000 µg/mL CTE (D) are stained by Oil red O (40X magnification). The quantification of lipid content is shown in % of control (E). Each value represents the mean ± SEM (n=3). Significance is shown in groups that do not share a common letter ($p < 0.05$).

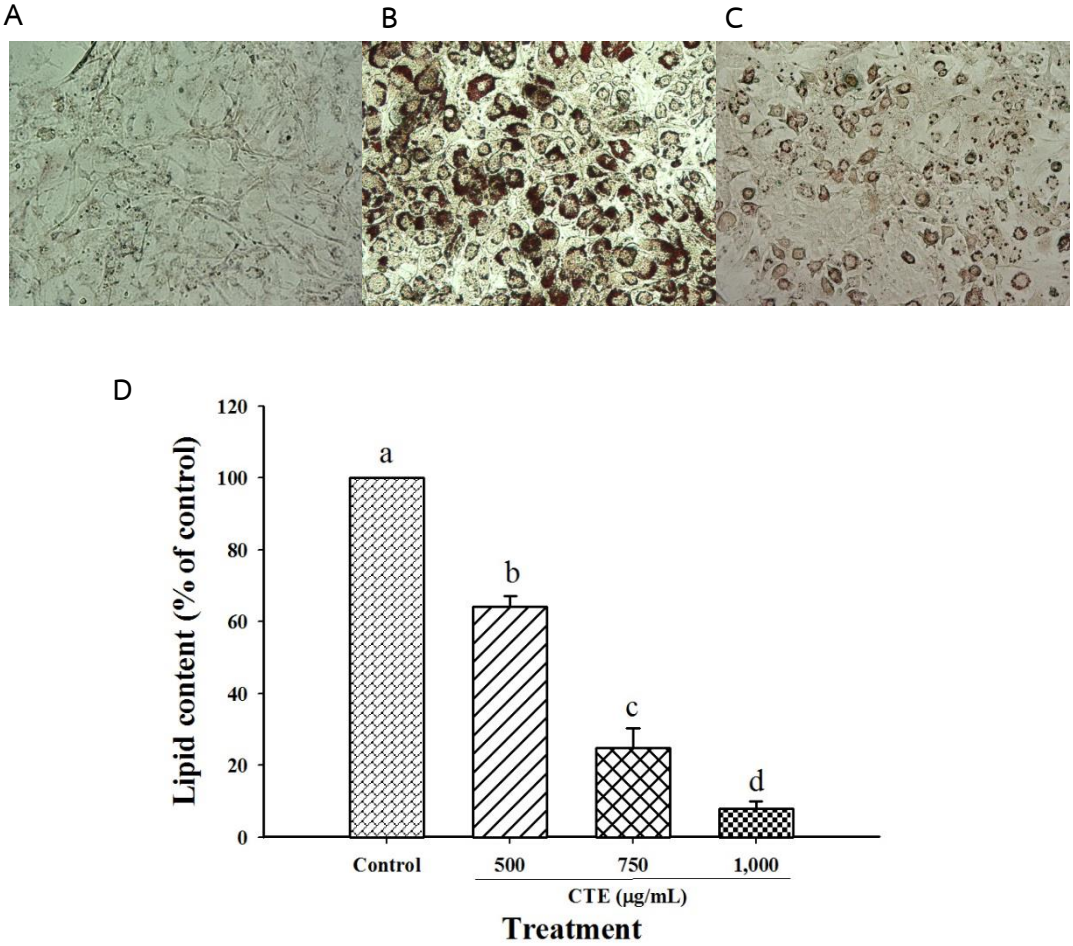

Figure 38 Effects of *Clitoria ternatea* extract (CTE, 500-1,000 µg/mL) on lipid accumulation of 3T3-L1 cells. Undifferentiated cells (A), Control (B) and CTE 1,000 µg/mL (C) are stained by Oil red O (40X magnification). The quantification of lipid content is shown in % of control (D). Each value represents the mean ± SEM (n=3). Significance is shown in groups that do not share a common letter ($p < 0.05$).

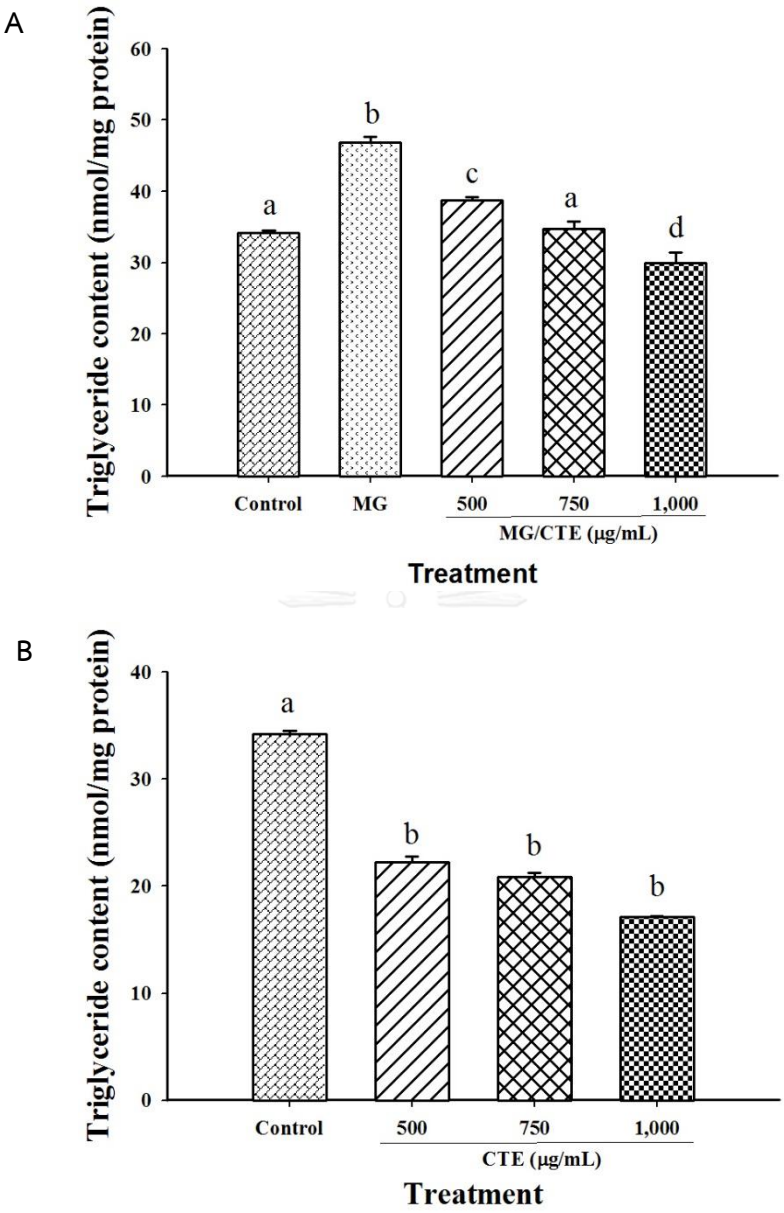

Figure 39 Effects of *Clitoria ternatea* extract (CTE, 500-1,000 µg/mL) on triglyceride accumulation of 3T3-L1 cells in the presence (A) or absence of 10 µM methylglyoxal (MG) (B). Triglyceride content is shown in nmol/mg protein. Each value represents the mean ± SEM (n=3). Significance is shown in groups that do not share a common letter ($p < 0.05$).

4.6.5 The effects of CTE on lipolysis in 3T3-L1 cells

After the 3T3-L1 cells were turned into mature adipocytes. They were exposed to the 10 μM MG with or without various concentrations of CTE (500-1,000 μg/ml) for 1 h. As illustrated in Figure 40A, MG significantly decreased the lipolysis activity about 23.41% when compared to control. However, CTE (500-1,000 μg/mL) significantly increased MG-induced lipolysis in a dose-dependent manner which ranged from 35.54 to 75.14% when compared to MG. Figure 40B shows that CTE (500-1,000 μg/mL) also significantly increased lipolysis without induction of MG in a concentration-dependent manner (27.90-57.88%).

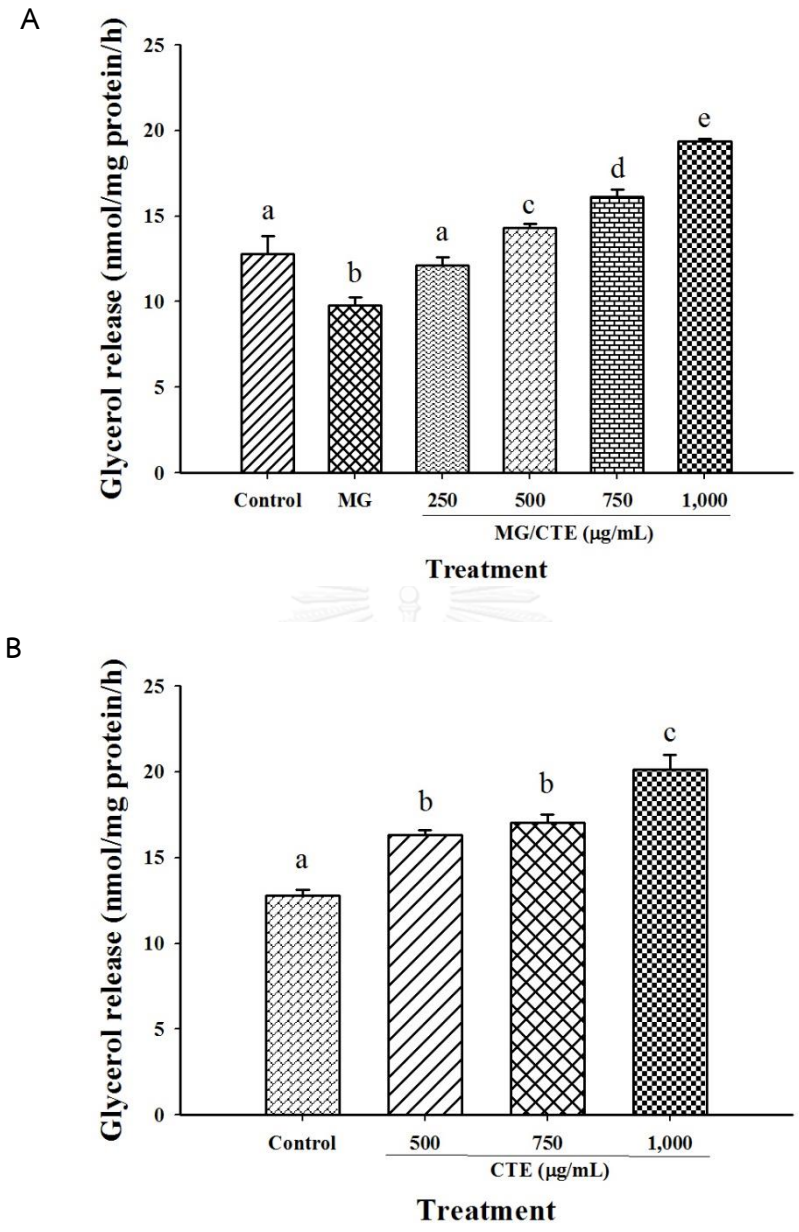

Figure 40 Effects of *Clitoria ternatea* extract (CTE, 500-1,000 µg/mL) on lipolysis of 3T3-L1 cells in the presence (A) or absence of 10 µM methylglyoxal (MG) (B). Lipolysis is shown as glycerol release in nmol/mg protein/h. Each value represents the mean ± SEM (n=3). Significance is shown in groups that do not share a common letter ($p < 0.05$).

4.6.6 Inhibitory effects of CTE on adipogenic transcription factors and lipogenic enzymes

In respect to Figure 41A and 41B, mRNA expression of PPARγ and C/EBPα were increased at 31.54% and 34.05%, respectively, after incubation with 10 μM MG. In contrast, CTE (500-1,000 μg/mL) significantly inhibited expression of PPARγ and C/EBPα in gene levels at 42.45±2.10%-78.50±4.29% and 44.00±4.67%-70.20±2.34%, respectively. In addition, CTE (500-1,000 μg/mL) significantly suppressed mRNA expression of PPARγ (38.33±3.96%-59.83±2.50%) and C/EBPα (21.49±2.22%-58.94±1.74%) in the absence of MG (Figure 42A-42B).

Furthermore, protein expression of PPARγ, C/EBPα, ACC and FAS was increased by 22.62%, 31.53%, 24.44% and 41.32%, respectively, when the 3T-L1 cells were incubated with 10 μM MG as illustrated in Figure 43A-43D. Conversely, 500-1,000 μg/mL of CTE significantly inhibited protein expression of PPARγ (2.43±0.32%-81.45±7.13%), C/EBPα (21.03±3.55%-81.46±4.55%), ACC (64.64±6.94%-98.21±9.50%) and FAS (44.97±1.59%-94.42±8.77%). However, 500 μg/mL of CTE was not significant for PPARγ reduction. Consistently, the same concentrations of CTE without MG also reduced the protein levels of PPARγ (53.50±5.71%- 99.99±0.01%) and C/EBPα (34.36±1.78%-62.16±1.43%), as shown in Figure 44A-44B. As illustrated on figure 44C to 44D, CTE (500-1,000 μg/mL) significantly decreased protein levels of FAS (2.17±1.14%-

38.30±1.27%) and ACC (52.60±0.92% to 82.85±3.98%). However, 500 μg/mL of CTE was not significant for FAS reduction.

A

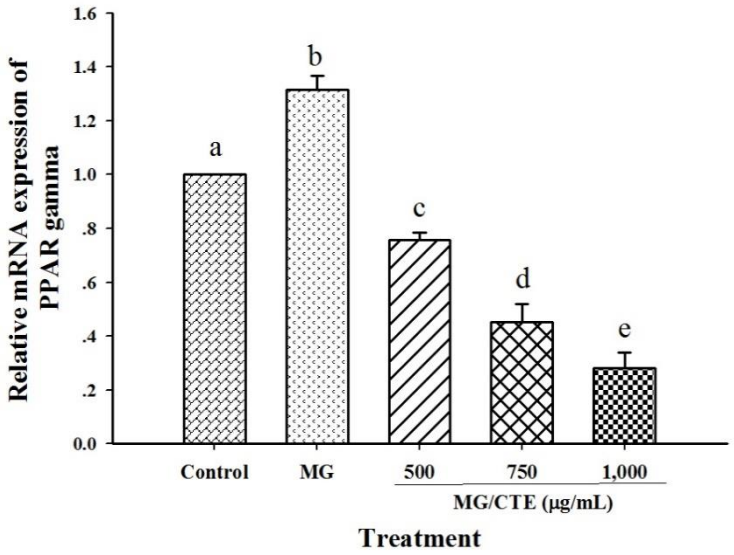

B

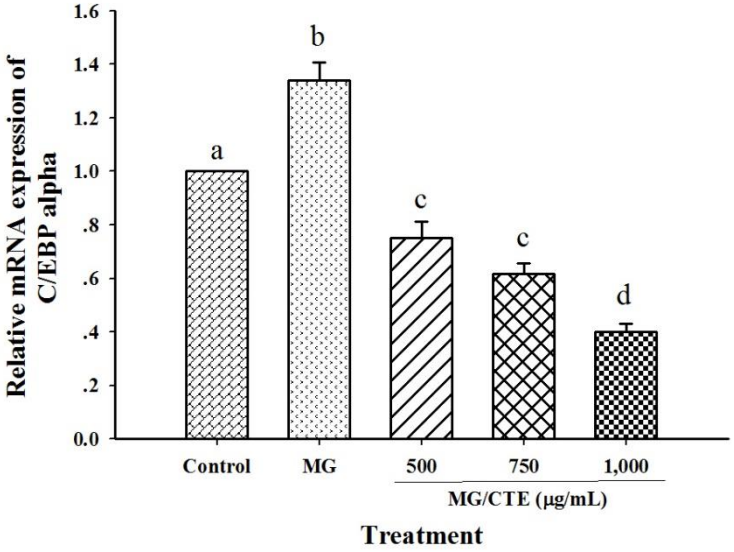

Figure 41 Effects of *Clitoria ternatea* extract (CTE, 500-1,000 µg/mL) on mRNA expression of PPARγ and C/EBPα of 3T3-L1 cells induced by 10 µM methylglyoxal (MG). mRNA expression of PPARγ (A) and C/EBPα (B) are shown in relative values to beta-actin. Each value represents the mean ± SEM (n=3). Significance is shown in groups that do not share a common letter ($p < 0.05$).

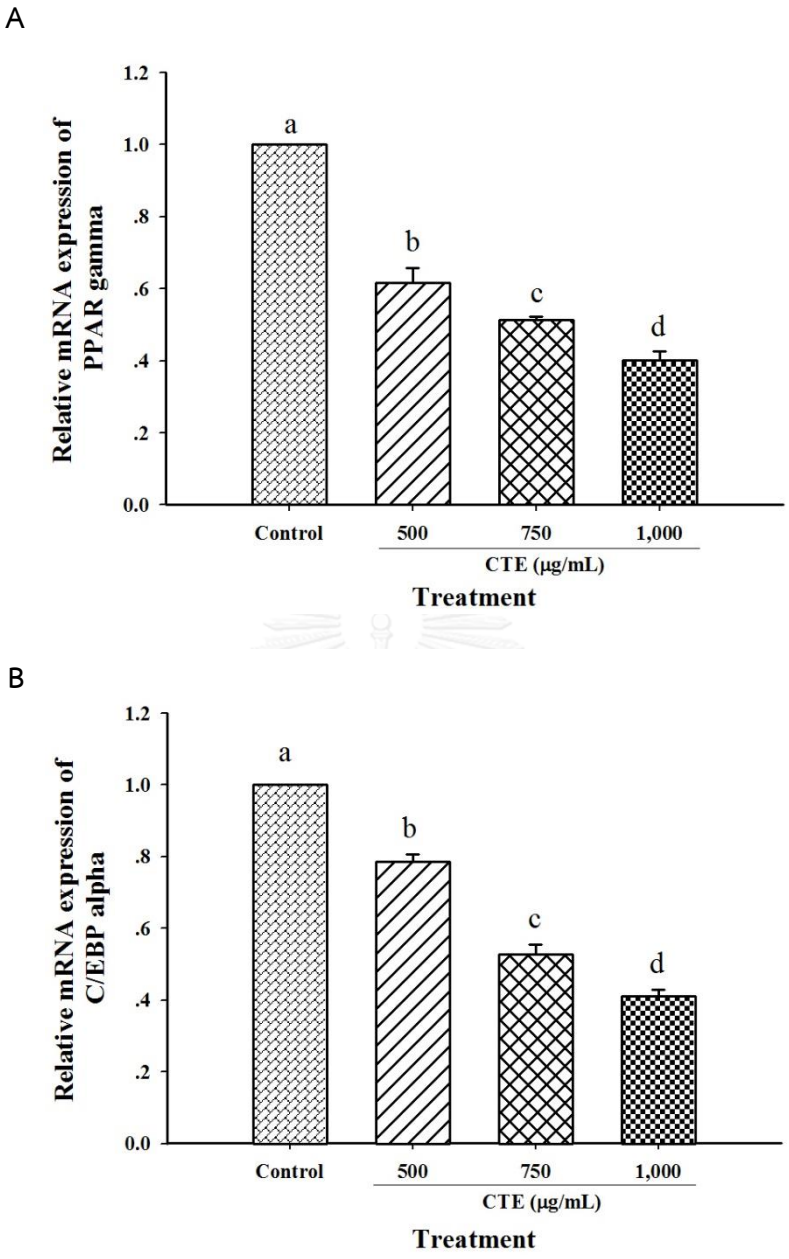

Figure 42 Effects of *Clitoria ternatea* extract (CTE, 500-1,000 µg/mL) on mRNA expression of PPARγ and C/EBPα of 3T3-L1 cells. mRNA expression of PPARγ (A) and C/EBPα (B) are shown in relative values to beta-actin. Each value represents the mean ± SEM (n=3). Significance is shown in groups that do not share a common letter ($p < 0.05$).

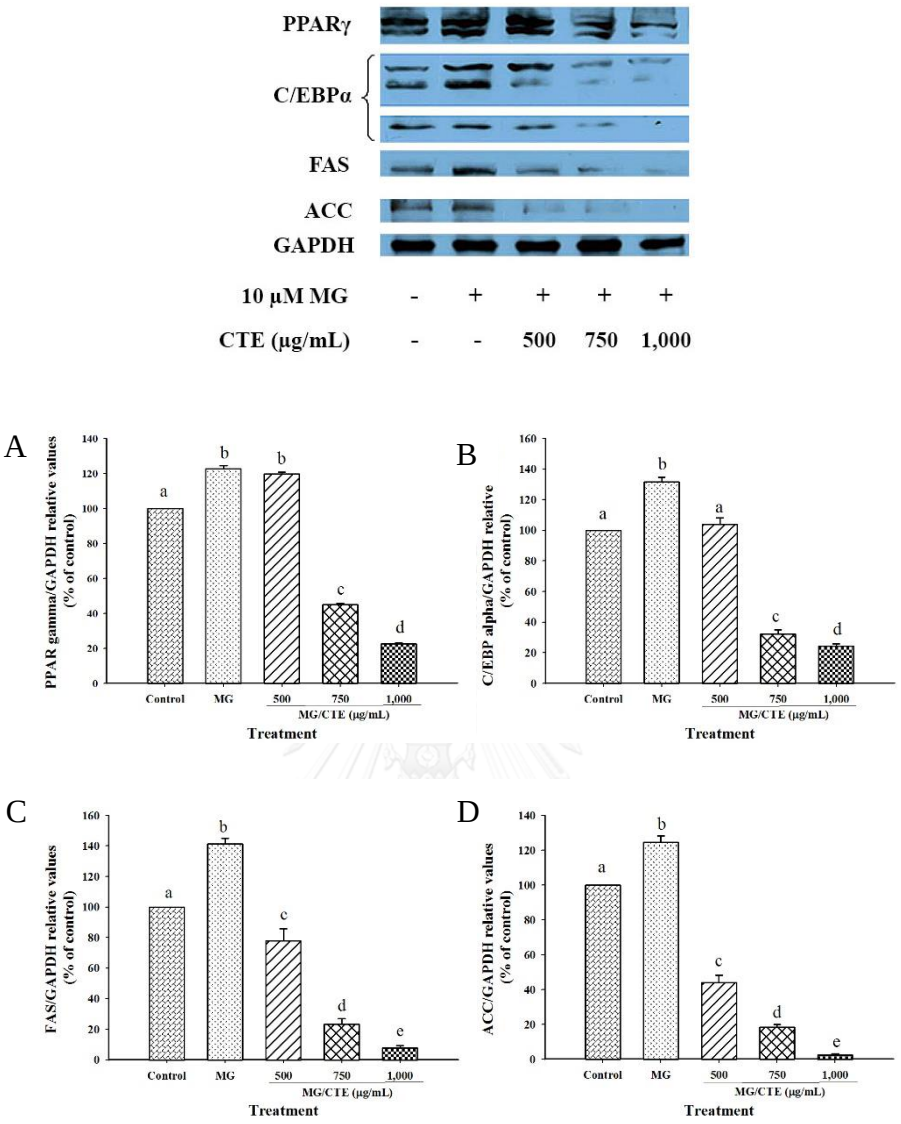

Figure 43 Effects of *Clitoria ternatea* extract (CTE, 500-1,000 μg/mL) on protein levels of adipogenic transcription factors of 3T3-L1 cells mediated by 10 μM methylglyoxal (MG). The relative values of PPARγ (A), C/EBPα (B), FAS (C), and ACC (D) to GAPDH are shown in % of control. Each value represents the mean ± SEM (n=3). Significance is shown in groups that do not share a common letter ($p < 0.05$).

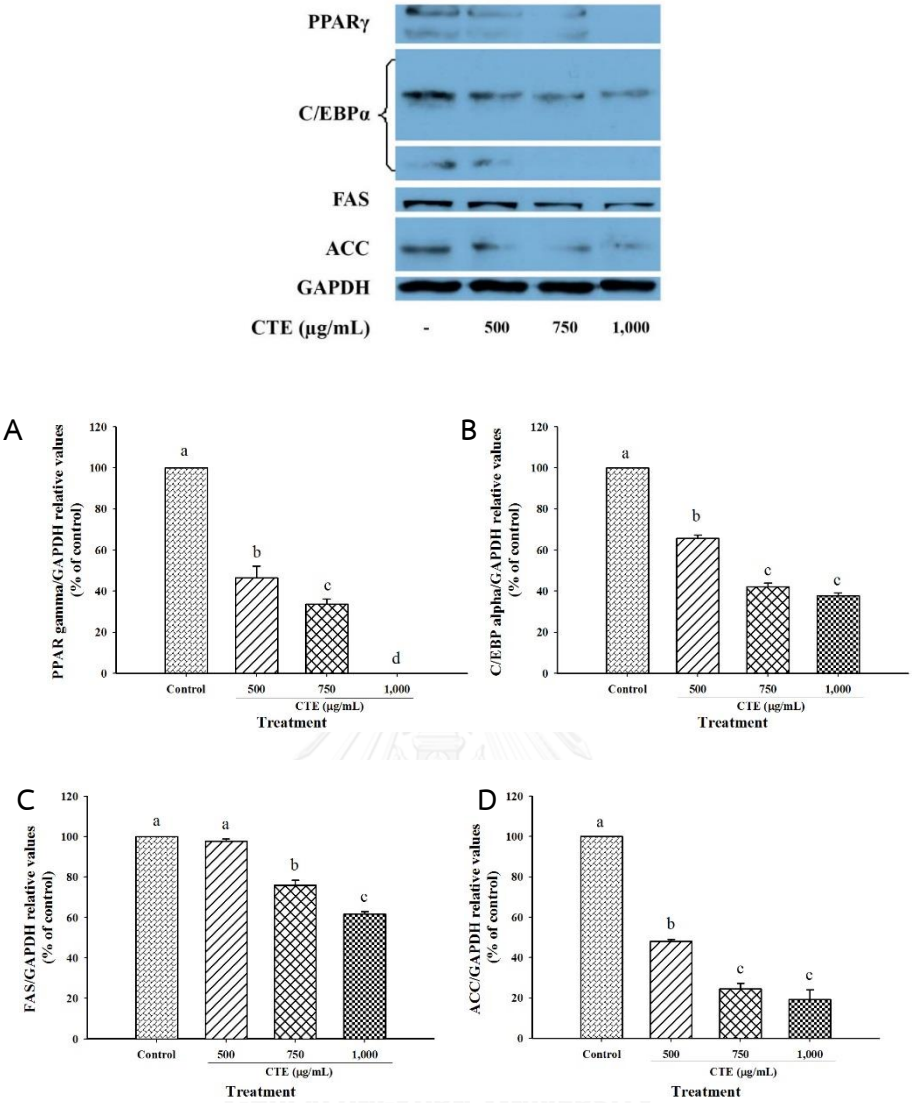

Figure 44 Effects of *Clitoria ternatea* extract (CTE, 500-1,000 μg/mL) on protein levels of adipogenic transcription factors of 3T3-L1 cells. The relative values of PPARγ (A), C/EBPα (B), FAS (C), and ACC (D) to GAPDH are shown in % of control. Each value represents the mean ± SEM (n=3). Significance is shown in groups that do not share a common letter ($p < 0.05$).

CHAPTER V

DISCUSSION

5.1 Phytochemical compounds in CTE

It has been reported that the phytochemical components isolated from *Clitoria ternatea* flower extract (CTE) are the six polyacylated derivatives of delphinidin 3,3',5'-triglucoside, named ternatin A1, A2, B1, B2, D1 and D2 (Terahara et al., 1990). Delphinidin-based ternatins, a group of polyacylated delphinidin derivatives, are the unique phytochemicals in CTE. New ternatins including ternatins A1-A3, B1-B4, C1-C5 and D1-D3 consist of delphinidin 3,3',5'-triglucoside attached with malonic acid, glucose, *p*-coumaric acid have also been reported (Terahara et al., 1996; Terahara et al., 1998). Flavonol glycosides were also isolated from CTE such as kaempferol 3-*O*-(2"-*O*-α-rhamnosyl-6"-*O*-malonyl)- β-glucoside, quercetin 3-*O*-(2"-*O*-α-rhamnosyl-6"-*O*-malonyl)-β-glucoside, and myricetin 3-*O*-(2",6"-di-*O*-α-rhamnosyl)- β-glucoside (Kazuma et al., 2003b). Furthermore, CTE contains delphinidin-3,5-glucoside, delphinidin-3β-glucoside, rutin and derivatives of delphinidin, kaempferol and quercetin (Kazuma et al., 2003b; Nair et al., 2015; Shen et al., 2016). In the similar pattern, the major bioactive compounds in CTE are on the basis of flavanol glycosides and delphinidin derivative ternatins in this study including preternatin A3, ternatin B2,

ternatin D2, quercetin-3-rutinoside (rutin), ternatin D1, kaemferol-3-*O*-(2-rhamnosyl) rutinoside, delphinidin-3-glucoside (myrtillin), kaemferol-3-*O*-rutinoside, delphinidin-3-*O*-(6-*O*-*p*-coumaryl) glucoside-pyruvic acid, apigenin 7-*O*-neohesperidoside (Rhoifolin), (+)-catechin 7-*O*-β-glucoside, syringetin-3-*O*-glucoside, quercetin triglycoside, and delphinidin derivatives.

5.2 Protective effect of CTE against glycation of BSA induced by fructose *in vitro*

Albumin is a target protein for the glycation reaction due to its abundance in serum (Wautier and Guillausseau, 2001). Protein glycation occurs by the covalent binding of aldehyde or ketone groups of reducing sugars to the free amino groups of proteins, leading to the formation of fluorescent AGEs that can be identified by increasing fluorescent intensity (Jariyapamornkoon et al., 2013). The level of the Amadori products can be determined by colorimetric assay. Our results in this experiment showed that CTE effectively inhibited fructose induced fluorescent AGEs formation in a concentration dependent manner. In addition, the inhibitory effect of CTE consequently suppressed the formation of fructosamine (Amadori adducts) and AGEs. Previous studies have shown the ability of phenolic-enriched plant extracts against fructose-induced protein glycation (Dearlove et al., 2008; Dorsey and Greenspan, 2014). For example, pomelo extract (0.25–1.00 mg/mL) inhibited the overall formation of AGEs approximately 50-86% (Caengprasath et al., 2013). At concentrations of 1.00 mg/mL, Beijing grass, pennywort, gingko, Cat's Whiskers and

grape seed containing phenolic compounds and flavonoids had the percentage inhibition of protein glycation ranging 17-41% at week 4 of experiments (Adisakwattana et al., 2010). *Mesona chinensis* Benth (Chinese Mesona), most widely consumed as an herbal beverage and a gelatin-type dessert, also showed the percentage inhibition of 39.60-59.42% with concentration of 0.25-1.00 mg/mL at week 4 of incubation (Adisakwattana et al., 2014). Our findings suggest that CTE is a moderate antiglycating agent in comparison with other phenolic-enriched extracts.

Abundant evidences exist that an excessive production of reactive oxygen species (ROS) and reactive nitrogen species are generated during glycation and glycoxidation (Singh et al., 2001; Ahmed, 2005; Wu et al., 2011). The production of ROS causes the oxidation of amino acid residues of protein to form a carbonyl derivative, which diminishes the oxidative defence of protein by eliminating the thiol groups (Chesne et al., 2006; Roche et al., 2008). In the present study, the protein oxidation was observed by increasing protein carbonyl content and depleting protein thiol group of BSA. Conversely, the reduction of protein carbonyl content and oxidation of thiol group of BSA/fructose system was affected by CTE. Evidence supports that the formation of AGEs could generate free radicals and highly reactive intermediates in the early stages of glycation (Smith and Thornalley, 1992). Moreover, the Amadori products are subsequently degraded into α-dicarbonyl compounds such as methylglyoxal, glyoxal, and deoxyglucosones. These compounds are more reactive than the reducing sugars with respect to their ability to react with amino groups of proteins and

consequently generate the cross-linked methylglyoxal dialkylimine radical cation and the enediol radical anion of methylglyoxal, which leads to the formation of AGEs (Kang, 2003b). In addition, the methylglyoxal anions directly react with molecular oxygen to generate the superoxide anion radicals whereas hydroxyl radicals can be generated during the reaction of methylglyoxal with lysine in the presence of metal ions (Fe^{3+} and Cu^{2+}) (Kang, 2003b). When ROS is increased from protein glycation reaction, antioxidant enzymes (superoxidae dismutase, catalase, and glutathione reductase) primarily account for intracellular defense while non-enzyme antioxidants (vitamin C and E) help protect various components against oxidative damage in plasma (Szaleczky et al., 1999). Interestingly, it has been shown that free radical scavengers from natural products can act as non-enzyme antioxidants to prevent against reducing sugar-induced glycation and oxidative modification to protein (Wu et al., 2011). Therefore, various antioxidant activity methods have been used to investigate the free radical scavenging ability of CTE. The findings indicate that CTE exhibits the ability to scavenge different forms of free radicals, thus suggesting that its potential might be used for preventing formation of AGEs and oxidative modification to protein.

Phytochemical compounds including polyphenolics, flavonoids and anthocyanins, present in plant-based foods, provide beneficial effects on free radical scavenging properties (Rice-Evans et al., 1997; Pietta, 2000; Einbond et al., 2004). The phytochemical analysis of *Clitoria ternatea* flower petal extract revealed the presence of bioactive compounds such as delphinidin-3,5-glucoside, delphinidin-3β-glucoside,

malvidin-3β-glucoside, kaemphferol, p-coumaric acid and six major ternatins (ternatins A1, A2, B1, B2, D1 and D2) (Terahara et al., 1996). The previous findings demonstrated in the phytochemical compounds possibly contributing to anti-glycation and antioxidant activity, the amount of phenolics and flavonoids in plant-based foods is highly related to their activity (Kusirisin et al., 2009; Ho et al., 2010; Ramkissoon et al., 2013). In the view of the above-mentioned, the possible mechanisms by which CTE exerts antiglycation and antioxidant activity may be in association with the phytochemical compounds in the extract. Other mechanisms of antiglycation, in particular for inhibiting the formation of late-stage Amadori products, breaking the cross-linking structures in the intracellular formed AGEs, and blocking the receptor for advanced glycation end products (RAGEs) have been proposed (Wu et al., 2011). Further comprehensive studies of CTE are required to clarify the antiglycation mechanisms described above.

5.3 Protective effect of CTE against glycation of BSA induced by methylglyoxal (MG) *in vitro*

The progression of macrovascular and micorvascular diabetic complications are associated with advanced glycation end products (AGEs) formation (Nowotny et al., 2015). Methylglyoxal (MG) is highly reactive dicarbonyl compound which irreversibly reacts with protein to form AGEs (Vander Jagt, 2008). In this study, MG markedly increased the formation of fluorescent AGEs at day 7. Previous study demonstrated

that MG was more reactive inducer than fructose to form fluorescent AGEs (Li et al., 2008). Additionally, the formation of non-fluorescent AGEs (N^{ε}-CML) and oxidation indicator (carbonyl content and free thiol group) were increased by induction of MG. However, this study showed that the CTE exhibited inhibitory effects on fluorescent and non-fluorescent AGEs formation at advanced stage of glycation process. In intermediate stage of glycation reaction, oxidation of reducing sugars including glucose, fructose and Amadori's product contributes to formation of dicarbonyl compound and protein oxidation indicating by increase of carbonyl content and loss of free thiol groups (Murphy and Kehrer, 1989). In this study, MG-induced glycation resulted in the increase of carbonyl content and reduction of free thiol groups which were consistent with previous studies (Meeprom et al., 2015; Thilavech et al., 2016) The results indicate that CTE also suppressed MG-induced protein oxidation by reducing the carbonyl content and preventing loss of free thiol groups. Extensively, Blackcurrant, *Nigella sativa* (Black seed) and *Vigna radiata* (Mung bean) extract exert inhibitory effects on MG-mediated AGEs formation (Chen et al., 2014). The present study showed that MG-induced formation of AGEs was attenuated by CTE throughout the glycation process. However, MG/BSA system did not effect to the Amadori products because MG is able to mediate AGEs formation without this pathway (data not shown). These findings suggest that CTE effectively attenuates initiation and intermediate stages of protein glycation and consequently inhibits the AGE formation in the late stage.

5.4 Effect of CTE on oxidative DNA damage induced by AAPH or MG/lysine system, *in vitro*

Apart from glycation damage to protein, MG has been contributed to oxidative DNA damage and DNA strand breakage (Kang, 2003a; Suji and Sivakami, 2007). Evidence suggests that the oxidation-dependent DNA cleavage involves in several disorders such as mutagenesis, carcinogenesis and age-related diseases (Evans et al., 2004). During the progression of MG-mediated glycation process, reactive oxygen species (ROS) such as superoxide and hydroxyl radical were generated and potentiated the DNA cleavage (Yim et al., 1995). It has been reported that MG generates free radicals and AGEs during protein cross-linking reaction through MG-radical anion and cross-linked radical cation. The formation of these intermediates leads to superoxide and hydroxyl radical generation, and AGEs formation, respectively (Yim et al., 1995; Suji and Sivakami, 2007). The DNA strand breakage is highly accelerated in the presence of transition metal ion such as Cu^{2+} and Fe^{3+} through the Fenton reaction to generate hydroxyl radical (Kang, 2003a; Kang, 2003b). In current study, co-incubation of lysine and MG leads to oxidative DNA damage representing by the elevation of open circular form of DNA. Higher amounts of OC form of DNA are found after Cu^{2+} was added to the reaction suggesting that metal ion can enhance the oxidative DNA damage. Anti-glycation activity of CTE are proved by protecting the oxidative damage mediated by MG. CTE suppressed the level of TBARS formation and maintained the reduced form of cytochrome *c* represented as hydroxyl and superoxide radical scavenging activities in respectively.

Moreover, CTE are able to inhibit protein oxidation by reducing protein carbonyl content and preventing depletion of free thiol group in BSA/MG system. Other plant extracts including Curcumin (Chan and Wu, 2006), Chaga mushroom (Najafzadeh et al., 2007), and *Moringa oleifera leaf* (Das et al., 2012) also act as free radical scavenger to prevent oxidative damage of DNA due to their high potent antioxidant activities. In addition, the metal-chelating property can be responsible for inhibiting oxidation of DNA by reducing ROS generation from Fenton reaction (Perron and Brumaghim, 2009). However, CTE show low potency to chelate metal ion in ferrous ion chelating power in this study. Therefore, it could be suggested from this study that the ability of CTE to inhibit oxidative DNA damage induced by MG is likely due to free radical scavenging activities.

It has also been reported that MG trapping capability is the one of the proposed mechanism to recognize as AGEs inhibitors (Wu et al., 2011). The reduction of MG-derived AGEs can be an effective strategy for prevention of diabetic complications. For example, aminoguanidine (AG) is an AGEs inhibitor due to its dicarbonyl scavenging activity. It is capable to rapidly react with dicarbonyl compounds such as methylglyoxal, glyoxal, and 3-deoxyglucosone to prevent AGEs formation (Thornalley, 2003b). The current study demonstrated that CTE showed the potential to directly trap MG, thereby inhibited AGEs formation and MG-induced oxidative DNA damage. The MG -trapping activity of phenolic-rich plants was positive correlation to inhibition of MG-derived AGEs (Sompong and Adisakwattana, 2015). The correlation between MG-

trapping ability and total phenolic content of red grape skin extract was also observed *(Harsha et al., 2016)*. Sugar-free phytochemicals extracted from berries were also capable to scavenge methylglyoxal indicating as a major mechanism of protein glycation inhibition (Wang et al., 2011). Catechin as a major metabolite of lotus seedpod oligomeric procyanidins exhibited anti-glycation effect which was positively correlated to carbonyl scavenging activities and antioxidant capacities (Wu et al., 2014). High quercetin fraction from *Camellia nitidissima* Chi was able to inhibit MG-mediated AGEs formation by scavenging methylglyoxal to form mono- and di-methylglyoxal quercetin adducts (Wang et al., 2016). In addition, delphinidin-3-rutinoside (D3R) and cyanidin-3-rutinoside (C3R) in blackcurrant (Chen et al., 2014) were shown as MG scavenger. The phytochemical compounds have also been reported to be able to directly trap MG. For instance, (+)-Catechin was capable to trap MG exogenous MG in a time- and dose-dependent manner to form mono-MG-catechin and di-MG-catechin adducts (Zhu et al., 2014). *In vivo*, catechin administration for 16 weeks significantly suppressed AGEs formation and proinflammatory cytokines, including tumor necrosis factor due to partial effect as MG trapping ability contributing to alleviation of diabetic nephropathy in mice (Zhu et al., 2014). Quercetin and apigenin also exert MG trapping ability at pH 7.4 and 37 °C (Shao et al., 2014). In addition, it was proved that quercetin also inhibited the formation of AGEs in a dose-dependent manner via directly trapped MG to form di-MG adducts of quercetin detected as the dominant product (Li et al., 2014). It was also shown that dietary quercetin treatment (0.067% and 0.2% in diet)

attenuated MGO-induced liver injury and inhibited the formation of AGEs in Kidney in mice due to its MG trapping ability of both quercetin and its major metabolite isorhamnetin (Zhao et al., 2016). Futhermore, the structural requirements to facilitate carbonyl trapping ability have been documented (Shao et al., 2014). The A ring is the active site of flavonoids to enhance the MG-trapping efficacy, and the hydroxyl group at C-5 on the A ring contributes to the trapping efficacy. Base on the trapping mechanism, quercetin show the best trapping efficacy of MG compared to luteolin, and epicatechin, indicating that the ketone group at the C-4 position of quercetin enhances the trapping efficacy of flavonoids. Therefore, it could be suggested that flavonoids derivatives in CTE may be responsible for anti-glycation capacities by carbonyl scavenging activity.

Furthermore, AAPH has also been widely used as a water-soluble source of free radical mediators capable of inducing lipid peroxidation and protein damage. The peroxyl radicals were initiated by thermal decomposition of azo compound of AAPH in oxygen at physiological temperature (Shiva Shankar Reddy et al., 2007). Previous study demonstrated that peroxyl radical of AAPH were initiated by oxidative damage of DNA (Zhao et al., 2007; Llorens et al., 2014). In this study, we focus on protective effect of CTE on oxidative damage induce by peroxy radical. The result showed that CTE was able to prevent oxidative DNA damage induced by AAPH in dose dependent manner. It is supported that peroxyl scavenging activity manifestation of anthocyanin-rich CTE is also capable for effectively protection on AAPH-induced hemolysis and

oxidative damage oxidation in canine erythrocytes (Phrueksanan et al., 2014). Plant extracts such as *Nardostachys jatamansi* (NJE), *Ilex spinigera* and mushroom extracts showed the protective effect against DNA damage-induced by AAPH (Mohadjerani and Vosoghi Roodgar, 2016). Grape skin anthocyanin including malvidin 3-*O*-glucoside, petunidin 3-*O*-glucoside, delphinidin 3-*O*-glucoside, and cyanidin 3-*O*-rutinoside inhibited AAPH-induced hemolysis and DNA damage (Pervin et al., 2014). Flavonoid compounds also showed protection on DNA against AAPH-induced oxidative damage in a concentration-dependent manner (Zhao et al., 2007). It could be suggested that CTE may have the potential to act as a natural antioxidant to prevent peroxyl radical induced oxidative damage of DNA *in vitro*.

5.5 Inhibitory effect of CTE on MG-induced adipogenesis *in vitro*

Obesity is one of leading factor in the metabolic syndrome caused by an imbalance between food intake and energy expenditure (Flatt, 2007). Nowadays, obesity is a growing global health problem causing the development of type 2 diabetes, cardiovascular diseases and artherosclerosis (Greenberg and McDaniel, 2002; Guilherme et al., 2008). Obesity is mainly associated with increased expansion of white adipose tissue through the activation of adipogenesis (Kahn and Flier, 2000). The process of adipogenesis involves the changes of cell morphology from fibroblast-like shape of preadipocyte to mature and increased lipid synthesis and accumulation in

adipocytes (Gall z. et al.). It has been previously reported the correlation between MG accumulation in white fat tissue and the development of obesity (Jia et al., 2012; Matafome et al., 2013). Accumulation of MG and increase of Akt1 phosphorylation were observed in obese rats (Jia et al., 2012). MG-treated 3T3-L1 preadipocytes were also increased the phosphorylation of Akt1 expression and Cdk inhibitors (p21 and p27) as well as an enhanced activity of Cdk2 and accelerated cell cycle progression (Jia et al., 2012). The possible mechanism of MG on cell proliferation may be related to the activation of Akt1 activity, resulting in regulating cell proliferation. Consequently, MG-mediated phosphorylation of Akt1 increases the phosphorylation of Cdk inhibitors (p21 and p27) which are the major regulators that arrest the cell cycle progression at the G_1/S checkpoint. The increased phosphorylation of p21 and p27 activates their degradation and Cdk2 activity leading to the entry of cells to S phase. As a result of MG-accelerated cell proliferation during early stage, the MG-treated cells finally showed more lipid accumulation as well as increased expression of adipogenic markers (Jia et al., 2012). In consistent with previous study, adipogenesis of 3T3-L1 cells was enhanced by MG treatment through Akt1 signaling pathway. Increased phosphorylation of Akt1 (T308) contributed to increase of cell cycle progression, proliferation and differentiation of preadipocytes. However, the deleterious effects of MG on different cell types including kidney mesangial cells, retinal pericytes and mouse Schwann cells were found after the treatment with high concentrations of MG (100-1,000 μM) due to oxidative stress-dependent signaling pathway (Liu et al., 2003; Ota et al., 2007; Kim et

al., 2010a). For instance, an apoptotic cell number was increased after mouse Schwann cells were treated with 500–1,000 μM MG (Ota et al., 2007). In addition, the proliferation of mesenchymal cells (smooth muscle cells and skin fibroblasts) was also reduced after 100 μM MG treatement (Cantero et al., 2007). It could be suggested that the deleterious effect is due to the acute exposure to high MG concentration, however, this concentration was not the physiological relevant concentration (Ogawa et al., 2010; Biswas et al., 2011; Jia et al., 2012). It was reported that the plasma MG level was increased from 3.34 μM in healthy subjects to 5.9 μM in type 2 diabetic patients. In this study, MG (10 μM) was used at the higher concentration than physiological concentration because of demonstrating the apparently increase of preadipocyte cell proliferation in short period of time (Wang et al., 2007).

It has been demonstrated that the inhibition of adipogenesis involves in reduction in number and lipid content of adipocytes (Rayalam et al., 2008). Suppressing differentiation and proliferation, and lipogenesis as well as stimulatory lipolysis are the strategies for prevention and treatment of obesity (Yun, 2010). It has been reported that medicinal plants and their bioactive compounds possesses anti-obesity activity (Patra et al., 2015). For example, blueberry peel, *citrus aurantium* and curcumin extracts inhibit adipogenesis through down-regulation of PPARγ and C/EBPα followed resulting in decreasing cell number and lipid accumulation of adipocytes (Kim and Kim, 2009; Kim et al., 2012; Song et al., 2013). Recent findings indicated that the blockage of cell cycle through inhibition of Akt1 and ERK1/2 signaling pathway effectively

prevents cell proliferation, expression of adipogenic transcription factors, and lipid accumulation in adipocytes (Tang et al., 2003; Xu and Liao, 2004; Bost et al., 2005; Kim et al., 2010c). Our current results demonstrated that CTE inhibited the early stage of adipogenesis mediated by MG in 3T3-L1 cells through the suppression of Akt1 signaling pathways. CTE inhibited MG-mediated proliferation of 3T3-L1 cells concomitant with increased cell cycle arrest, representing by inversion of cell cycle from G2/M to G0/G1 phase. Additionally, CTE alone showed inhibitory effect on adipogenesis through suppression of phosphorylated Akt1 at T308 and ERK1/2 at T202/Y204 contributing to inhibition of cell cycle progression and proliferation of 3T3-L1 preadipocytes. Inhibition of these pathways might result in the reduction of hyperplasia in adipocytes (Choi et al., 2012; Lee et al., 2015a). This inhibitory effect was linked to the suppression of phosphorylated Akt1 at T308 and ERK1/2 at T202/Y204. Many studies have been reported that the phosphorylation of Akt (T308 or ser473) and ERK1/2 (T202/Y204) at the active sites is required for stimulating adipogenesis (Prusty et al., 2002; Fayard et al., 2010; Tagaya et al., 2012; Humphrey et al., 2013). For instance, *Coptis chinensis* extract exerts anti-adipogeneic effects via reduction of phosphorylation of ERK1/2 (T202/Y204) and Akt1 (T308) during adipogenesis which was consistent with our results (Choi et al., 2015). Moreover, kaempferol delayed cell cycle progression by blocking the phosphorylation of Akt (Lee et al., 2015b).

After the cells were exposed to the adipogenic inducers including IBMX, insulin and dexamethasone at the late stage, 3T3-L1 cells differentiated to mature adipocytes,

resulting in the lipid accumulation. Our findings were consistent with previous studie that MG was capable to increase expression of transcription factors including PPARγ and C/EBPα was observed at both mRNA and protein levels (Jia et al., 2012). The activation of PPARγ and C/EBPα directly regulates the expression of FAS and ACC leading to conversion of acetyl-CoA to malonyl-CoA and then malonyl-CoA to saturated fatty acids driving formation of triglyceride (Desvergne et al., 2006). Furthermore, the accumulation of triglyceride increases the size of adipocytes (Rutkowski et al., 2015). There are several studies reported that suppressing mRNA or protein expression of FAS markedly prevents the accumulation of triglyceride in adipocytes (Schmid et al., 2005; Kim et al., 2012; Song et al., 2013). For example, cocoa tea water extract inhibits lipogenesis by suppressing expression of lipogenic transcription factors and their target genes such as PPARγ, C/EBPα, FAS, and ACC leading to reduced accumulation of triglyceride in 3T3-L1 cells (Li et al., 2016). Our results showed that CTE dramatically inhibited the late stage of adipogenesis in the presence and absence of MG through the inhibition of triglyceride accumulation and expression of adipocyte-associated transcriptional factors and enzymes including PPARγ, C/EBPα, FAS and ACC. Moreover, lipolysis is generally induced by hormone-sensitive lipase (HSL) and consequently released free fatty acid and glycerol and decreased the cell size of adipocytes (Duncan et al., 2007). It has been reported that black soybean enriched anthocyanin could increase the lipolysis of 3T3-L1 cells, thereby, reduction of cell mass and size (Lee et al., 2014). Additionally, polyphenol

rich-white tea extract exerts the inhibitory effect on adipogenesis through an increased lipolysis concomitant with suppression of adipogenic markers including SREBP-1c and PPARγ (Szkudelska et al., 2009). Suppression of phosphorylated Akt could stimulate HSL in 3T3-L1 cells (Fernandez-Galilea et al., 2012). The current findings indicated that CTE enhanced lipolysis related to activation of hormone sensitive lipase in mature adipocytes. The results from this effect cause a decrease in TG accumulation in mature adipocytes. As aforementioned, CTE exerts inhibitory effects on MG-mediated adipogenesis by attenuating proliferation of cell, progression of cell cycle (Akt and MAPK), expression of adipogenic transcription factors (PPARγ and C/EBPα) and lipogenic enzymes (FAS and ACC), and enhancing lipolysis. In addition, CTE was able to trap MG at the minimum concentration ratio of CTE to MG (3.47:1). However, the higher concentration ratio of CTE:MG at 347:1 was applied for investigation of the anti-adipogenesis on 3T3-L1 cells. It suggests that this ratio of CTE:MG might completely inhibit MG-mediated adipogenesis due to its ability to trap MG. However, the observed findings indicate that 100-fold higher ratio of CTE:MG could not completely suppress adipogenesis indicating that not only the ability to trap MG but CTE itself suppresses adipogenesis through Akt and ERK pathways. Therefore, it suggests that CTE exerts at least two mechanisms for inhibition of adipogenesis.

Previous studies have demonstrated that CTE contains delphinidin-3,5-glucoside, delphinidin-3β-glucoside, malvidin-3β-glucoside, kaempferol, quercetin-3-*O*-(2-rhamnosyl) rutinoside, rutin, and six major delphinidin-based ternatins (ternatins A1-

A3, B1-B4, C1-C5 and D1-D3) (Terahara et al., 1996; Kazuma et al., 2003a; Nair et al., 2015; Shen et al., 2016). In the similar pattern, the major bioactive compounds in CTE are on the basis of flavanol glycosides and delphinidin derivatives in this study. Previous works have also reported that the MG trapping ability of flavonoids including (+)-catechin, quercetin and apigenin have potential to directly trap the MG (Shao et al., 2014; Zhu et al., 2014). In addition, essential structure and glycosylation of flavonoids are required to exhibit the ability to trap MG (Shao et al., 2008; Shao et al., 2014). It has been reported that rutin, a glycosylated structure of quercetin was shown higher potency than quercetin to prevent glycation induced by MG (Wu and Yen, 2005). Moreoever, rutin also demonstrated higher MG scavenging ability than quercitrin after 24 h of incubation (Yoon and Shim, 2015). In this study, CTE contains glycones of phytochemical compounds which may be responsible for the MG trapping ability. In addition, the MG trapping ability of catechin and quercetin is a mechanism for inhibition of toxic effect mediated by MG including AGEs formation in kidney and proinflammatory cytokines (tumor necrosis factor), liver injury *in vivo* (Zhu et al., 2014; Zhao et al., 2016). In addition, it has been clearly shown that several phytochemical compounds in CTE exert the inhibitory effect on adipogenesis. For instance, dietary flavonoids including kaempferol, quercetin and myricetin suppressed the adipogenesis by inactivation of Akt1 pathway leading to inhibiting of cell cycle progression, lipid accumulation and transcriptional factor expression in 3T3-L1 cells and human adipose tissue-derived mesenchymal stem cells (Bin and Choi, 2012; Lee et al., 2015b). Rutin

could suppress the adipocyte differentiation in 3T3-L1 cells by down-regulating of PPARγ and C/EBPα (Choi et al., 2006).Therefore, it can be suggested that phytochemicals in CTE are likely responsible for inhibition of MG-mediated adipogenesis due to MG trapping ability together with anti-adipogenesis of these phytochemical compounds..

CHAPTER VI

CONCLUSION

In the present work, CTE prevents fructose and MG-induced protein glycation and oxidation-dependent damages to protein. It also exhibits an excellent scavenging ability for different forms of free radicals.

CTE inhibits oxidative DNA damage induced by AAPH and glycation of MG/lysine system indicating as suppression of DNA breakage, superoxide anion and hydroxyl production. The inhibitory effect of CTE is shown from ROS scavenging activities and MG trapping ability.

Extensively, CTE inhibits adipogenesis at both early and late stages through Akt and MAPK signaling pathway and it also inhibits MG-mediated adipogenesis through Akt signaling pathway. In early stage, CTE inhibits cell proliferation and cell cycle. In late stage, CTE reduces lipid accumulation, adipogenic transcription factors and enzymes. CTE also enhances lipolysis after differentiation to the mature adipocyte.

These findings reveal that CTE exerts the beneficial effects as an effective anti-glycating, antioxidant and anti-adipogenesis agent. Based on these beneficial effects, CTE might be considered or applied to use as a candidate extract for prevention of glycation and adipogenesis. .

REFERENCES

References

Adisakwattana S, Jiphimai P, Prutanopajai P, Chanathong B, Sapwarobol S and Ariyapitipan T 2010. Evaluation of alpha- glucosidase, alpha- amylase and protein glycation inhibitory activities of edible plants. Int J Food Sci Nutr. 61(3): 295-305.

Adisakwattana S, Ruengsamran T, Kampa P and Sompong W 2012a. *In vitro* inhibitory effects of plant- based foods and their combinations on intestinal alpha-glucosidase and pancreatic alpha-amylase. BMC Complement Altern Med. 12: 110.

Adisakwattana S, Sompong W, Meeprom A, Ngamukote S and Yibchok-Anun S 2012b. Cinnamic acid and its derivatives inhibit fructose-mediated protein glycation. Int J Mol Sci. 13(2): 1778-1789.

Adisakwattana S, Thilavech T and Chusak C 2014. *Mesona Chinensis* Benth extract prevents AGE formation and protein oxidation against fructose-induced protein glycation *in vitro*. BMC Complement Altern Med. 14: 130.

Ahmed MU, Brinkmann Frye E, Degenhardt TP, Thorpe SR and Baynes JW 1997. N-epsilon-(carboxyethyl)lysine, a product of the chemical modification of proteins by methylglyoxal, increases with age in human lens proteins. Biochem J. 324(2): 565-570.

Ahmed N 2005. Advanced glycation endproducts- - role in pathology of diabetic complications. Diabetes Res Clin Pract. 67(1): 3-21.

Ames BN, Shigenaga MK and Hagen TM 1993. Oxidants, antioxidants, and the degenerative diseases of aging. Proc Natl Acad Sci U S A. 90(17): 7915-7922.

Ardestani A and Yazdanparast R 2007. *Cyperus rotundus* suppresses AGE formation and protein oxidation in a model of fructose-mediated protein glycoxidation. Int J Biol Macromol. 41(5): 572-578.

Balu M, Sangeetha P, Murali G and Panneerselvam C 2005. Age-related oxidative protein damages in central nervous system of rats: modulatory role of grape seed extract. Int J Dev Neurosci. 23(6): 501-507.

Barja G and Herrero A 2000. Oxidative damage to mitochondrial DNA is inversely related to maximum life span in the heart and brain of mammals. FASEB J. 14(2): 312-318.

Basta G, Schmidt AM and De Caterina R 2004. Advanced glycation end products and vascular inflammation: implications for accelerated atherosclerosis in diabetes. Cardiovasc Res. 63(4): 582-592.

Beard KM, Shangari N, Wu B and O'Brien PJ 2003. Metabolism, not autoxidation, plays a role in alpha-oxoaldehyde- and reducing sugar-induced erythrocyte GSH depletion: relevance for diabetes mellitus. Mol Cell Biochem. 252(1-2): 331-338.

Beecher GR 2003. Overview of dietary flavonoids: nomenclature, occurrence and intake. J Nutr. 133(10): 3248-3254.

Beisswenger PJ, Howell SK, Nelson RG, Mauer M and Szwergold BS 2003. Alpha-oxoaldehyde metabolism and diabetic complications. Biochem Soc Trans. 31(6): 1358-1363.

Bell RC, Carlson JC, Storr KC, Herbert K and Sivak J 2000. High-fructose feeding of streptozotocin-diabetic rats is associated with increased cataract formation and increased oxidative stress in the kidney. Br J Nutr. 84(4): 575-582.

Bin H-S and Choi U-K 2012. Myricetin inhibits adipogenesis in human adipose tissue-derived mesenchymal stem cells. Food Sci Biotechnol. 21(5): 1391-1396.

Biswas UK, Banerjee S, Das A and Kumar A 2011. Elevation of serum methylglyoxal may be used as a screening marker in oral premalignant lesions. Biomed Res. 22(3): 273-278.

Bost F, Aouadi M, Caron L and Binetruy B 2005. The role of MAPKs in adipocyte differentiation and obesity. Biochimie. 87(1): 51-56.

Brownlee M, Cerami A and Vlassara H 1988. Advanced glycosylation end products in tissue and the biochemical basis of diabetic complications. N Engl J Med. 318(20): 1315-1321.

Brownlee M, Vlassara H, Kooney A, Ulrich P and Cerami A 1986. Aminoguanidine prevents diabetes- induced arterial wall protein cross- linking. Science. 232(4758): 1629-1632.

Caengprasath N, Ngamukote S, Makynen K and Adisakwattana S 2013. The protective effects of pomelo extract (*Citrus grandis* L. Osbeck) against fructose-mediated protein oxidation and glycation. EXCLI J. 12: 491-502.

Cantero AV, Portero-Otin M, Ayala V, Auge N, Sanson M, Elbaz M, Thiers JC, Pamplona R, Salvayre R and Negre- Salvayre A 2007. Methylglyoxal induces advanced glycation end product (AGEs) formation and dysfunction of PDGF receptor-beta: implications for diabetic atherosclerosis. FASEB J. 21(12): 3096-3106.

Cervantes- Laurean D, Schramm DD, Jacobson EL, Halaweish I, Bruckner GG and Boissonneault GA 2006. Inhibition of advanced glycation end product formation on collagen by rutin and its metabolites. J Nutr Biochem. 17(8): 531-540.

Chakraborty S, Karmakar K and Chakravortty D 2014. Cells producing their own nemesis: understanding methylglyoxal metabolism. IUBMB life. 66(10): 667-678.

Chan WH and Wu HJ 2006. Protective effects of curcumin on methylglyoxal- induced oxidative DNA damage and cell injury in human mononuclear cells. Acta Pharmacol Sin. 27(9): 1192-1198.

Chang T, Wang R, Olson DJ, Mousseau DD, Ross AR and Wu L 2011. Modification of Akt1 by methylglyoxal promotes the proliferation of vascular smooth muscle cells. FASEB J. 25(5): 1746-1757.

Chang T, Wang R and Wu L 2005. Methylglyoxal-induced nitric oxide and peroxynitrite production in vascular smooth muscle cells. Free Radical Biol Med. 38(2): 286-293.

Chang T and Wu L 2006. Methylglyoxal, oxidative stress, and hypertension. Can J Physiol Pharmacol. 84(12): 1229-1238.

Chen X-Y, Huang I-M, Hwang LS, Ho C-T, Li S and Lo C-Y 2014. Anthocyanins in blackcurrant effectively prevent the formation of advanced glycation end products by trapping methylglyoxal. J Funct Foods. 8: 259-268.

Cheng HM and Gonzalez RG 1986. The effect of high glucose and oxidative stress on lens metabolism, aldose reductase, and senile cataractogenesis. Metabolism. 35(4): 10-14.

Chesne S, Rondeau P, Armenta S and Bourdon E 2006. Effects of oxidative modifications induced by the glycation of bovine serum albumin on its structure and on cultured adipose cells. Biochimie. 88(10): 1467-1477.

Chinchansure AA, Korwar AM, Kulkarni MJ and Joshi SP 2015. Recent development of plant products with anti-glycation activity: a review. Rsc Advances. 5(39): 31113-31138.

Choi I, Park Y, Choi H and Lee EH 2006. Anti-adipogenic activity of rutin in 3T3-L1 cells and mice fed with high-fat diet. Biofactors. 26(4): 273-281.

Choi JS, Kim J-H, Ali MY, Jung HJ, Min B-S, Choi RJ, Kim G-D and Jung HA 2015. Anti-adipogenic effect of epiberberine is mediated by regulation of the Raf/MEK1/2/ERK1/2 and AMPKα/Akt pathways. Arch Pharm Res. 38(12): 2153-2162.

Choi KM, Lee YS, Sin DM, Lee S, Lee MK, Lee YM, Hong JT, Yun YP and Yoo HS 2012. Sulforaphane inhibits mitotic clonal expansion during adipogenesis through cell cycle arrest. Obesity. 20(7): 1365-1371.

Chuang CC, Yang RS, Tsai KS, Ho FM and Liu SH 2007. Hyperglycemia enhances adipogenic induction of lipid accumulation: involvement of extracellular signal-regulated protein kinase 1/2, phosphoinositide 3-kinase/Akt, and peroxisome proliferator-activated receptor gamma signaling. Endocrinology. 148(9): 4267-4275.

Daisy P and Rajathi M 2009. Hypoglycemic effects of *Clitoria ternatea* Linn.(Fabaceae) in alloxan-induced diabetes in rats. Trop J Pharm Res. 8(5): 393-398.

Daisy P, Santosh K and Rajathi M 2009. Antihyperglycemic and antihyperlipidemic effects of *Clitoria ternatea* Linn. in alloxan-induced diabetic rats. Afr J Microbiol Res. 3(5): 287-291.

Das N, Sikder K, Ghosh S, Fromenty B and Dey S 2012. *Moringa oleifera* Lam. leaf extract prevents early liver injury and restores antioxidant status in mice fed with high-fat diet. Indian J Exp Biol. 50(6): 404-412.

Dearlove RP, Greenspan P, Hartle DK, Swanson RB and Hargrove JL 2008. Inhibition of protein glycation by extracts of culinary herbs and spices. J Med Food. 11(2): 275-281.

Desai KM, Chang T, Wang H, Banigesh A, Dhar A, Liu J, Untereiner A and Wu L 2010. Oxidative stress and aging: is methylglyoxal the hidden enemy? Can J Physiol Pharmacol. 88(3): 273-284.

Desvergne B, Michalik L and Wahli W 2006. Transcriptional regulation of metabolism. Physiol Rev. 86(2): 465-514.

Dorsey PG and Greenspan P 2014. Inhibition of nonenzymatic protein glycation by pomegranate and other fruit juices. J Med Food. 17(4): 447-454.

Drira R, Chen S and Sakamoto K 2011. Oleuropein and hydroxytyrosol inhibit adipocyte differentiation in 3 T3-L1 cells. Life Sci. 89(19-20): 708-716.

Duncan RE, Ahmadian M, Jaworski K, Sarkadi-Nagy E and Sul HS 2007. Regulation of lipolysis in adipocytes. Annu Rev Nutr. 27: 79-101.

Dunn JA, Patrick JS, Thorpe SR and Baynes JW 1989. Oxidation of glycated proteins: age-dependent accumulation of N. epsilon.-(carboxymethyl) lysine in lens proteins. Biochemistry. 28(24): 9464-9468.

Dyer DG, Dunn JA, Thorpe SR, Bailie KE, Lyons TJ, McCance DR and Baynes JW 1993. Accumulation of Maillard reaction products in skin collagen in diabetes and aging. J Clin Invest. 91(6): 2463-2469.

Einbond LS, Reynertson KA, Luo X-D, Basile MJ and Kennelly EJ 2004. Anthocyanin antioxidants from edible fruits. Food Chem. 84(1): 23-28.

Elosta A, Ghous T and Ahmed N 2012. Natural products as anti-glycation agents: possible therapeutic potential for diabetic complications. Curr Diabetes Rev. 8(2): 92-108.

Evans MD, Dizdaroglu M and Cooke MS 2004. Oxidative DNA damage and disease: induction, repair and significance. Mutat Res. 567(1): 1-61.

Fayard E, Xue G, Parcellier A, Bozulic L and Hemmings BA 2010. Protein kinase B (PKB/Akt), a key mediator of the PI3K signaling pathway. Curr Top Microbiol Immunol. 346: 31-56.

Ferguson BS, Nam H and Morrison RF 2016. Curcumin Inhibits 3T3-L1 Preadipocyte Proliferation by Mechanisms Involving Post-transcriptional p27 Regulation. Biochem Biophys Rep. 5: 16-21.

Ferguson G and Booth I 1998. Importance of glutathione for growth and survival of *Escherichia coli* cells: detoxification of methylglyoxal and maintenance of intracellular K^+. J Bacteriol. 180(16): 4314-4318.

Fernandez-Galilea M, Perez-Matute P, Prieto-Hontoria PL, Martinez JA and Moreno-Aliaga MJ 2012. Effects of lipoic acid on lipolysis in 3T3-L1 adipocytes. J Lipid Res. 53(11): 2296-2306.

Feve B 2005. Adipogenesis: cellular and molecular aspects. Best Pract Res Clin Endocrinol Metab. 19(4): 483-499.

Finkel T and Holbrook NJ 2000. Oxidants, oxidative stress and the biology of ageing. Nature. 408(6809): 239-247.

Flatt JP 2007. Differences in basal energy expenditure and obesity. Obesity. 15(11): 2546-2548.

Freedman BI, Wuerth JP, Cartwright K, Bain RP, Dippe S, Hershon K, Mooradian AD and Spinowitz BS 1999. Design and baseline characteristics for the aminoguanidine Clinical Trial in Overt Type 2 Diabetic Nephropathy (ACTION II). Control Clin Trials. 20(5): 493-510.

Friedman EA 2010. Evolving pandemic diabetic nephropathy. Rambam Maimonides Med J. 1(1): e0005.

Frischmann M, Bidmon C, Angerer J and Pischetsrieder M 2005. Identification of DNA adducts of methylglyoxal. Chem Res Toxicol. 18(10): 1586-1592.

Gaens KH, Stehouwer CD and Schalkwijk CG 2013. Advanced glycation endproducts and its receptor for advanced glycation endproducts in obesity. Curr Opin Lipidol. 24(1): 4-11.

Gall Z., Vancea S., Mezei T. and M. K Adipocyte Triglyceride Content and Adipogenesis in Aripiprazole Treated Rats. Int J Pharm. 9(4): 251-257.

Galvis A, Marcano A, Stefancin C, Villaverde N, Priestap HA, Tonn CE, Lopez LA and Barbieri MA 2011. The effect of dehydroleucodine in adipocyte differentiation. Eur J Pharmacol. 671(1-3): 18-25.

Ghosh D and Konishi T 2007. Anthocyanins and anthocyanin-rich extracts: role in diabetes and eye function. Asia Pac J Clin Nutr. 16(2): 200-208.

Giacco F and Brownlee M 2010. Oxidative stress and diabetic complications. Circ Res. 107(9): 1058-1070.

Goh SY and Cooper ME 2008. Clinical review: The role of advanced glycation end products in progression and complications of diabetes. J Clin Endocrinol Metab. 93(4): 1143-1152.

Greenberg A and McDaniel M 2002. Identifying the links between obesity, insulin resistance and β cell function: potential role of adipocyte derived cytokines in the pathogenesis of type 2 diabetes. Eur J Clin Invest. 32(3): 24-34.

Guerin-Dubourg A, Catan A, Bourdon E and Rondeau P 2012. Structural modifications of human albumin in diabetes. Diabetes Metab. 38(2): 171-178.

Guilherme A, Virbasius JV, Puri V and Czech MP 2008. Adipocyte dysfunctions linking obesity to insulin resistance and type 2 diabetes. Nat Rev Mol Cell Biol. 9(5): 367-377.

Gunjan M, Ravindran M, Sengamalam R, Jana GK and Jha A 2010. Pharmacognostic and antidiabetic study of *Clitoria ternatea*. Int J Phytomed. 2(4).

Guo X, Yang B, Tan J, Jiang J and Li D 2016. Associations of dietary intakes of anthocyanins and berry fruits with risk of type 2 diabetes mellitus: a systematic review and meta-analysis of prospective cohort studies. Eur J Clin Nutr. 1: 1-8.

Gupta GK, Chahal J and Bhatia M 2010. *Clitoria ternatea* (L.): old and new aspects. J Pharm Res. 3(11): 2610-2614.

Harsha S, Pedapati S, Mesias M, Lavelli V and Morales FJ 2016. Grape skin extracts from winemaking by-products as a source of trapping agents for reactive carbonyl species. J Sci Food Agric. 96(2): 656-663.

Hasim S, Hussin NA, Alomar F, Bidasee KR, Nickerson KW and Wilson MA 2014. A glutathione-independent glyoxalase of the DJ-1 superfamily plays an important role in managing metabolically generated methylglyoxal in *Candida albicans*. J Biol Chem. 289(3): 1662-1674.

Hayashi T and Shibamoto T 1985. Analysis of methyl glyoxal in foods and beverages. J Agric Food Chem. 33(6): 1090-1093.

Ho C-T and Wang M 2013. Dietary phenolics as reactive carbonyl scavengers: potential impact on human health and mechanism of action. J Tradit Complement Med. 3(3): 139.

Ho S-C, Wu S-P, Lin S-M and Tang Y-L 2010. Comparison of anti-glycation capacities of several herbal infusions with that of green tea. Food Chem. 122(3): 768-774.

Hori M, Yagi M, Nomoto K, Ichijo R, Shimode A, Kitano T and Yonei Y 2012. Experimental models for advanced glycation end product formation using albumin, collagen, elastin, keratin and proteoglycan. J Anti Aging Med. 9: 125-134.

Humphrey SJ, Yang G, Yang P, Fazakerley DJ, Stockli J, Yang JY and James DE 2013. Dynamic adipocyte phosphoproteome reveals that Akt directly regulates mTORC2. Cell Metab. 17(6): 1009-1020.

Hunt JV, Dean RT and Wolff SP 1988. Hydroxyl radical production and autoxidative glycosylation. Glucose autoxidation as the cause of protein damage in the experimental glycation model of diabetes mellitus and ageing. Biochem J. 256(1): 205-212.

Jagt DLV 2008. Methylglyoxal, diabetes mellitus and diabetic complications. Drug Metabol Drug Interact. 23(1-2): 93-124.

Jain NN, Ohal CC, Shroff SK, Bhutada RH, Somani RS, Kasture VS and Kasture SB 2003. *Clitoria ternatea* and the CNS. Pharmacol Biochem Behav. 75(3): 529-536.

Jang YJ, Koo HJ, Sohn EH, Kang SC, Rhee DK and Pyo S 2015. Theobromine inhibits differentiation of 3T3-L1 cells during the early stage of adipogenesis via AMPK and MAPK signaling pathways. Food Funct. 6(7): 2365-2374.

Jariyapamornkoon N, Yibchok-anun S and Adisakwattana S 2013. Inhibition of advanced glycation end products by red grape skin extract and its antioxidant activity. BMC Complement Altern Med. 13: 171.

Jaworski K, Sarkadi-Nagy E, Duncan RE, Ahmadian M and Sul HS 2007. Regulation of triglyceride metabolism. IV. Hormonal regulation of lipolysis in adipose tissue. Am J Physiol Gastrointest Liver Physiol. 293(1): 1-4.

Jia X, Chang T, Wilson TW and Wu L 2012. Methylglyoxal mediates adipocyte proliferation by increasing phosphorylation of Akt1. PLoS One. 7(5): e36610.

Jia X, Olson DJ, Ross AR and Wu L 2006. Structural and functional changes in human insulin induced by methylglyoxal. FASEB J. 20(9): 1555-1557.

Jia X and Wu L 2007. Accumulation of endogenous methylglyoxal impaired insulin signaling in adipose tissue of fructose-fed rats. Mol Cell Biochem. 306(1-2): 133-139.

Kähkönen MP and Heinonen M 2003. Antioxidant activity of anthocyanins and their aglycons. J Agric Food Chem. 51(3): 628-633.

Kahn BB and Flier JS 2000. Obesity and insulin resistance. J Clin Invest. 106(4): 473-481.

Kamkaen N and Wilkinson JM 2009. The antioxidant activity of *Clitoria ternatea* flower petal extracts and eye gel. Phytother Res. 23(11): 1624-1625.

Kang JH 2003a. Oxidative damage of DNA by the reaction of amino acid with methylglyoxal in the presence of Fe(III). Int J Biol Macromol. 33(1-3): 43-48.

Kang JH 2003b. Oxidative damage of DNA induced by methylglyoxal *in vitro*. Toxicol Lett. 145(2): 181-187.

Kawahito S, Kitahata H and Oshita S 2009. Problems associated with glucose toxicity: role of hyperglycemia-induced oxidative stress. World J Gastroenterol. 15(33): 4137-4142.

Kazuma K, Noda N and Suzuki M 2003a. Flavonoid composition related to petal color in different lines of *Clitoria ternatea*. Phytochemistry. 64(6): 1133-1139.

Kazuma K, Noda N and Suzuki M 2003b. Malonylated flavonol glycosides from the petals of *Clitoria ternatea*. Phytochemistry. 62(2): 229-237.

Kelemu S, Cardona C and Segura G 2004. Antimicrobial and insecticidal protein isolated from seeds of *Clitoria ternatea*, a tropical forage legume. Plant Physiol Biochem. 42(11): 867-873.

Khangholi S, Majid FAA, Berwary NJA, Ahmad F and Aziz RBA 2016. The Mechanisms of Inhibition of Advanced Glycation End Products Formation through Polyphenols in Hyperglycemic Condition. Planta Med. 82(1-2): 32-45.

Kilhovd BK, Giardino I, Torjesen PA, Birkeland KI, Berg TJ, Thornalley PJ, Brownlee M and Hanssen KF 2003. Increased serum levels of the specific AGE-compound methylglyoxal-derived hydroimidazolone in patients with type 2 diabetes. Metabolism. 52(2): 163-167.

Kim CY and Kim K-H 2009. Inhibitiory role of curcumin in adipogenesis. FASEB J. 23(1): 717.724.

Kim GS, Park HJ, Woo JH, Kim MK, Koh PO, Min W, Ko YG, Kim CH, Won CK and Cho JH 2012. *Citrus aurantium* flavonoids inhibit adipogenesis through the Akt signaling pathway in 3T3-L1 cells. BMC Complement Altern Med. 12: 31.

Kim HY, Lee JM, Yokozawa T, Sakata K and Lee S 2011. Protective activity of flavonoid and flavonoid glycosides against glucose- mediated protein damage. Food Chem. 126(3): 892-895.

Kim J, Kim OS, Kim CS, Kim NH and Kim JS 2010a. Cytotoxic role of methylglyoxal in rat retinal pericytes: Involvement of a nuclear factor-kappaB and inducible nitric oxide synthase pathway. Chem Biol Interact. 188(1): 86-93.

Kim JM, Lee EK, Kim DH, Yu BP and Chung HY 2010b. Kaempferol modulates pro-inflammatory NF- kappaB activation by suppressing advanced glycation endproducts-induced NADPH oxidase. Age (Dordr). 32(2): 197-208.

Kim SP, Ha JM, Yun SJ, Kim EK, Chung SW, Hong KW, Kim CD and Bae SS 2010c. Transcriptional activation of peroxisome proliferator-activated receptor-gamma requires activation of both protein kinase A and Akt during adipocyte differentiation. Biochem Biophys Res Commun. 399(1): 55-59.

Kusirisin W, Srichairatanakool S, Lerttrakarnnon P, Lailerd N, Suttajit M, Jaikang C and Chaiyasut C 2009. Antioxidative activity, polyphenolic content and anti-glycation effect of some Thai medicinal plants traditionally used in diabetic patients. Med Chem. 5(2): 139-147.

Lee B, Lee M, Lefevre M and Kim HR 2014. Anthocyanins inhibit lipogenesis during adipocyte differentiation of 3T3-L1 preadipocytes. Plant Foods Hum Nutr. 69(2): 137-141.

Lee C, Yim MB, Chock PB, Yim HS and Kang SO 1998. Oxidation-reduction properties of methylglyoxal- modified protein in relation to free radical generation. J Biol Chem. 273(39): 25272-25278.

Lee SL, Lee HK, Chin TY, Tu SC, Kuo MH, Kao MC and Wu YC 2015a. Inhibitory Effects of Purple Sweet Potato Leaf Extract on the Proliferation and Lipogenesis of the 3T3-L1 Preadipocytes. Am J Chin Med. 43(5): 915-925.

Lee YJ, Choi HS, Seo MJ, Jeon HJ, Kim KJ and Lee BY 2015b. Kaempferol suppresses lipid accumulation by inhibiting early adipogenesis in 3T3-L1 cells and zebrafish. Food Funct. 6(8): 2824-2833.

Li KK, Liu CL, Shiu HT, Wong HL, Siu WS, Zhang C, Han XQ, Ye CX, Leung PC and Ko CH 2016. Cocoa tea (*Camellia ptilophylla*) water extract inhibits adipocyte differentiation in mouse 3T3-L1 preadipocytes. Sci Rep. 6: 20172.

Li W, Ota K, Nakamura J, Naruse K, Nakashima E, Oiso Y and Hamada Y 2008. Antiglycation effect of gliclazide on *in vitro* AGE formation from glucose and methylglyoxal. Exp Biol Med. 233(2): 176-179.

Li X, Zheng T, Sang S and Lv L 2014. Quercetin inhibits advanced glycation end product formation by trapping methylglyoxal and glyoxal. J Agric Food Chem. 62(50): 12152-12158.

Liu BF, Miyata S, Hirota Y, Higo S, Miyazaki H, Fukunaga M, Hamada Y, Ueyama S, Muramoto O, Uriuhara A and Kasuga M 2003. Methylglyoxal induces apoptosis through activation of p38 mitogen-activated protein kinase in rat mesangial cells. Kidney Int. 63(3): 947-957.

Llorens E, del Valle LJ and Puiggalí J 2014. Inhibition of radical-induced oxidative DNA damage by antioxidants loaded in electrospun polylactide nanofibers. Macromol Res. 22(4): 388-396.

Lv L, Shao X, Chen H, Ho C-T and Sang S 2011. Genistein inhibits advanced glycation end product formation by trapping methylglyoxal. Chem Res Toxicol. 24(4): 579-586.

Maessen DE, Stehouwer CD and Schalkwijk CG 2015. The role of methylglyoxal and the glyoxalase system in diabetes and other age-related diseases. Clin Sci. 128(12): 839-861.

Makynen K, Jitsaardkul S, Tachasamran P, Sakai N, Puranachoti S, Nirojsinlapachai N, Chattapat V, Caengprasath N, Ngamukote S and Adisakwattana S 2013. Cultivar variations in antioxidant and antihyperlipidemic properties of pomelo pulp (*Citrus grandis* [L.] Osbeck) in Thailand. Food Chem. 139(1-4): 735-743.

Mandavilli BS, Santos JH and Van Houten B 2002. Mitochondrial DNA repair and aging. Mutat Res. 509(1-2): 127-151.

Matafome P, Sena C and Seica R 2013. Methylglyoxal, obesity, and diabetes. Endocrine. 43(3): 472-484.

Matsuda H, Wang T, Managi H and Yoshikawa M 2003. Structural requirements of flavonoids for inhibition of protein glycation and radical scavenging activities. Bioorg Med Chem. 11(24): 5317-5323.

McCance DR, Dyer D, Dunn JA, Bailie KE, Thorpe SR, Baynes JW and Lyons TJ 1993. Maillard reaction products and their relation to complications in insulin-dependent diabetes mellitus. J Clin Invest. 91(6): 2470.

Meeprom A, Sompong W, Suantawee T, Thilavech T, Chan CB and Adisakwattana S 2015. Isoferulic acid prevents methylglyoxal-induced protein glycation and DNA damage by free radical scavenging activity. BMC Complement Altern Med. 15: 346.

Mesias M, Navarro M, Gokmen V and Morales FJ 2013. Antiglycative effect of fruit and vegetable seed extracts: inhibition of AGE formation and carbonyl-trapping abilities. J Sci Food Agric. 93(8): 2037-2044.

Miguel M 2011. Anthocyanins: Antioxidant and/or anti-inflammatory activities. J App Pharm Sci. 1(6): 7-15.

Mira L, Tereza Fernandez M, Santos M, Rocha R, Helena Florêncio M and Jennings KR 2002. Interactions of flavonoids with iron and copper ions: a mechanism for their antioxidant activity. Free Radical Res. 36(11): 1199-1208.

Mohadjerani M and Vosoghi Roodgar M 2016. *In-vitro* Evaluation of Protective Effects on DNA Damage and Antioxidative Activities of *Ilex Spinigera* Loes. Extracts. Iran J Pharm Res. 15(1): 283-292.

Monden M, Koyama H, Otsuka Y, Morioka T, Mori K, Shoji T, Mima Y, Motoyama K, Fukumoto S, Shioi A, Emoto M, Yamamoto Y, Yamamoto H, Nishizawa Y, Kurajoh M, Yamamoto T and Inaba M 2013. Receptor for advanced glycation end products regulates adipocyte hypertrophy and insulin sensitivity in mice: involvement of Toll-like receptor 2. Diabetes. 62(2): 478-489.

Mostafa AA, Randell EW, Vasdev SC, Gill VD, Han Y, Gadag V, Raouf AA and El Said H 2007. Plasma protein advanced glycation end products, carboxymethyl

cysteine, and carboxyethyl cysteine, are elevated and related to nephropathy in patients with diabetes. Mol Cell Biochem. 302(1-2): 35-42.

Mukherjee PK, Kumar V, Kumar NS and Heinrich M 2008. The Ayurvedic medicine *Clitoria ternatea*- - from traditional use to scientific assessment. J Ethnopharmacol. 120(3): 291-301.

Murphy ME and Kehrer JP 1989. Oxidation state of tissue thiol groups and content of protein carbonyl groups in chickens with inherited muscular dystrophy. Biochem J. 260(2): 359-364.

Nair V, Bang WY, Schreckinger E, Andarwulan N and Cisneros-Zevallos L 2015. Protective Role of Ternatin Anthocyanins and Quercetin Glycosides from Butterfly Pea (*Clitoria ternatea* Leguminosae) Blue Flower Petals against Lipopolysaccharide (LPS)-Induced Inflammation in Macrophage Cells. J Agric Food Chem. 63(28): 6355-6365.

Najafzadeh M, Reynolds PD, Baumgartner A, Jerwood D and Anderson D 2007. Chaga mushroom extract inhibits oxidative DNA damage in lymphocytes of patients with inflammatory bowel disease. Biofactors. 31(3-4): 191-200.

Nemet I, Varga-Defterdarovic L and Turk Z 2006. Methylglyoxal in food and living organisms. Mol Nutr Food Res. 50(12): 1105-1117.

Nicolay JP, Schneider J, Niemoeller OM, Artunc F, Portero-Otin M, Haik G, Jr., Thornalley PJ, Schleicher E, Wieder T and Lang F 2006. Stimulation of suicidal erythrocyte death by methylglyoxal. Cell Physiol Biochem. 18(4-5): 223-232.

Niemelä S, Miettinen S, Sarkanen J and Ashammakhi N 2008. Adipose tissue and adipocyte differentiation: molecular and cellular aspects and tissue engineering applications. Tissue Eng. 4(1): 26.

Nowotny K, Jung T, Hohn A, Weber D and Grune T 2015. Advanced glycation end products and oxidative stress in type 2 diabetes mellitus. Biomolecules. 5(1): 194-222.

Ogawa S, Nakayama K, Nakayama M, Mori T, Matsushima M, Okamura M, Senda M, Nako K, Miyata T and Ito S 2010. Methylglyoxal is a predictor in type 2 diabetic patients of intima-media thickening and elevation of blood pressure. Hypertension. 56(3): 471-476.

Ota K, Nakamura J, Li W, Kozakae M, Watarai A, Nakamura N, Yasuda Y, Nakashima E, Naruse K, Watabe K, Kato K, Oiso Y and Hamada Y 2007. Metformin prevents methylglyoxal-induced apoptosis of mouse Schwann cells. Biochem Biophys Res Commun. 357(1): 270-275.

Oturai PS, Rasch R, Hasselager E, Johansen PB, Yokoyama H, Thomsen MK, Myrup B, Kofoed- Enevoldsen A and Deckert T 1996. Effects of heparin and aminoguanidine on glomerular basement membrane thickening in diabetic rats. APMIS. 104(4): 259-264.

Paget C, Lecomte M, Ruggiero D, Wiernsperger N and Lagarde M 1998. Modification of enzymatic antioxidants in retinal microvascular cells by glucose or advanced glycation end products. Free Radic Biol Med. 25(1): 121-129.

Parimaladevi B, Boominathan R and Mandal SC 2004. Evaluation of antipyretic potential of *Clitoria ternatea* L. extract in rats. Phytomedicine. 11(4): 323-326.

Park YS, Koh YH, Takahashi M, Miyamoto Y, Suzuki K, Dohmae N, Takio K, Honke K and Taniguchi N 2003. Identification of the binding site of methylglyoxal on glutathione peroxidase: methylglyoxal inhibits glutathione peroxidase activity via binding to glutathione binding sites Arg 184 and 185. Free Radic Res. 37(2): 205-211.

Pasukamonset P, Kwon O and Adisakwattana S 2016. Alginate-based encapsulation of polyphenols from *Clitoria ternatea* petal flower extract enhances stability and biological activity under simulated gastrointestinal conditions. Food Hydrocolloids. 61: 772-779.

Patil A and Patil V 2011. Comparative evaluation of *in vitro* antioxidant activity of root of blue and white flowered varieties of *Clitoria ternatea* Linn. Int J Pharmacol. 7(4): 485-491.

Patra S, Nithya S, Srinithya B and Meenakshi S 2015. Review of Medicinal Plants for Anti-Obesity Activity. Transl Biomed. 6(3): 21-43.

Peng X, Cheng KW, Ma J, Chen B, Ho CT, Lo C, Chen F and Wang M 2008a. Cinnamon bark proanthocyanidins as reactive carbonyl scavengers to prevent the formation of advanced glycation endproducts. J Agric Food Chem. 56(6): 1907-1911.

Peng X, Zheng Z, Cheng K-W, Shan F, Ren G-X, Chen F and Wang M 2008b. Inhibitory effect of mung bean extract and its constituents vitexin and isovitexin on the formation of advanced glycation endproducts. Food Chem. 106(2): 475-481.

Perron NR and Brumaghim JL 2009. A review of the antioxidant mechanisms of polyphenol compounds related to iron binding. Cell Biochem Biophys. 53(2): 75-100.

Pervin M, Hasnat MA, Lee YM, Kim DH, Jo JE and Lim BO 2014. Antioxidant activity and acetylcholinesterase inhibition of grape skin anthocyanin (GSA). Molecules. 19(7): 9403-9418.

Phrueksanan W, Yibchok-anun S and Adisakwattana S 2014. Protection of *Clitoria ternatea* flower petal extract against free radical-induced hemolysis and oxidative damage in canine erythrocytes. Res Vet Sci. 97(2): 357-363.

Pietta P-G 2000. Flavonoids as antioxidants. J Nat Prod. 63(7): 1035-1042.

Price DL, Rhett PM, Thorpe SR and Baynes JW 2001. Chelating activity of advanced glycation end-product inhibitors. J Biol Chem. 276(52): 48967-48972.

Prusty D, Park B-H, Davis KE and Farmer SR 2002. Activation of MEK/ERK signaling promotes adipogenesis by enhancing peroxisome proliferator-activated receptor γ (PPARγ) and C/EBPα gene expression during the differentiation of 3T3-L1 preadipocytes. J Biol Chem. 277(48): 46226-46232.

Qatanani M and Lazar MA 2007. Mechanisms of obesity-associated insulin resistance: many choices on the menu. Genes Dev. 21(12): 1443-1455.

Rabeta M and An Nabil Z 2013. Total phenolic compounds and scavenging activity in *Clitoria ternatea* and *Vitex negundo* linn. Int Food Res J. 20(1): 495-500.

Rahbar S and Figarola JL 2003. Novel inhibitors of advanced glycation endproducts. Arch Biochem Biophys. 419(1): 63-79.

Rai KS, Murthy KD, Karanth KS, Nalini K, Rao MS and Srinivasan KK 2002. *Clitoria ternatea* root extract enhances acetylcholine content in rat hippocampus. Fitoterapia. 73(7-8): 685-689.

Ramasamy R, Vannucci SJ, Yan SS, Herold K, Yan SF and Schmidt AM 2005. Advanced glycation end products and RAGE: a common thread in aging, diabetes, neurodegeneration, and inflammation. Glycobiology. 15(7): 16-28.

Ramkissoon JS, Mahomoodally MF, Ahmed N and Subratty AH 2013. Antioxidant and anti- glycation activities correlates with phenolic composition of tropical medicinal herbs. Asian Pac J Trop Med. 6(7): 561-569.

Rao GN, Lardis MP and Cotlier E 1985. Acetylation of lens crystallins: a possible mechanism by which aspirin could prevent cataract formation. Biochem Biophys Res Commun. 128(3): 1125-1132.

Rayalam S, Della-Fera MA and Baile CA 2008. Phytochemicals and regulation of the adipocyte life cycle. J Nutr Biochem. 19(11): 717-726.

Redinger RN 2009. Fat storage and the biology of energy expenditure. Transl Res. 154(2): 52-60.

Rice- Evans C, Miller N and Paganga G 1997. Antioxidant properties of phenolic compounds. Trends Plant Sci. 2(4): 152-159.

Roche M, Rondeau P, Singh NR, Tarnus E and Bourdon E 2008. The antioxidant properties of serum albumin. FEBS Lett. 582(13): 1783-1787.

Ruderman NB, Williamson JR and Brownlee M 1992. Glucose and diabetic vascular disease. FASEB J. 6(11): 2905-2914.

Rutkowski JM, Stern JH and Scherer PE 2015. The cell biology of fat expansion. J Cell Biol. 208(5): 501-512.

Sale EM, Atkinson PG and Sale GJ 1995. Requirement of MAP kinase for differentiation of fibroblasts to adipocytes, for insulin activation of p90 S6 kinase and for insulin or serum stimulation of DNA synthesis. EMBO J. 14(4): 674-684.

Sang S, Shao X, Bai N, Lo CY, Yang CS and Ho CT 2007. Tea polyphenol (-)-epigallocatechin-3-gallate: a new trapping agent of reactive dicarbonyl species. Chem Res Toxicol. 20(12): 1862-1870.

Sasaki K, Chiba S and Yoshizaki F 2014. Effect of natural flavonoids, stilbenes and caffeic acid oligomers on protein glycation. Biomed Rep. 2(5): 628-632.

Schalkwijk CG, Stehouwer CD and van Hinsbergh VW 2004. Fructose-mediated non-enzymatic glycation: sweet coupling or bad modification. Diabetes Metab Res Rev. 20(5): 369-382.

Schlotterer A, Kukudov G, Bozorgmehr F, Hutter H, Du X, Oikonomou D, Ibrahim Y, Pfisterer F, Rabbani N and Thornalley P 2009. *C. elegans* as model for the study of high glucose–mediated life span reduction. Diabetes. 58(11): 2450-2456.

Schmid B, Rippmann JF, Tadayyon M and Hamilton BS 2005. Inhibition of fatty acid synthase prevents preadipocyte differentiation. Biochem Biophys Res Commun. 328(4): 1073-1082.

Sethi JK 2000. Obesity: Adipogenesis and Insulin Resistance. IDrugs. 3(8): 884-886.

Shao X, Bai N, He K, Ho CT, Yang CS and Sang S 2008. Apple polyphenols, phloretin and phloridzin: new trapping agents of reactive dicarbonyl species. Chem Res Toxicol. 21(10): 2042-2050.

Shao X, Chen H, Zhu Y, Sedighi R, Ho CT and Sang S 2014. Essential Structural Requirements and Additive Effects for Flavonoids to Scavenge Methylglyoxal. J Agric Food Chem. 62(14): 3202–3210.

Shen Y, Du L, Zeng H, Zhang X, Prinyawiwatkul W, Alonso-Marenco JR and Xu Z 2016. Butterfly pea (*Clitoria ternatea*) seed and petal extracts decreased HEp-2 carcinoma cell viability. Int J Food Sci Technol. 51(8): 1860-1868.

Shield JP, Poyser K, Hunt L and Pennock CA 1994. Fructosamine and glycated haemoglobin in the assessment of long term glycaemic control in diabetes. Arch Dis Child. 71(5): 443-445.

Shinohara M, Thornalley PJ, Giardino I, Beisswenger P, Thorpe SR, Onorato J and Brownlee M 1998. Overexpression of glyoxalase-I in bovine endothelial cells inhibits intracellular advanced glycation endproduct formation and prevents hyperglycemia-induced increases in macromolecular endocytosis. J Clin Invest. 101(5): 1142-1147.

Shiva Shankar Reddy CS, Subramanyam MV, Vani R and Asha Devi S 2007. *In vitro* models of oxidative stress in rat erythrocytes: effect of antioxidant supplements. Toxicol In Vitro. 21(8): 1355-1364.

Silva MS, Gomes RA, Ferreira AE, Freire AP and Cordeiro C 2013. The glyoxalase pathway: the first hundred years... and beyond. Biochem J. 453(1): 1-15.

Singh R, Barden A, Mori T and Beilin L 2001. Advanced glycation end-products: a review. Diabetologia. 44(2): 129-146.

Smith PR and Thornalley PJ 1992. Mechanism of the degradation of non-enzymatically glycated proteins under physiological conditions. Studies with the model fructosamine, N epsilon-(1-deoxy-D-fructos-1-yl)hippuryl-lysine. Eur J Biochem. 210(3): 729-739.

Solanki YB and Jain SM 2010. Antihyperlipidemic activity of *Clitoria ternatea* and *Vigna mungo* in rats. Pharm Biol. 48(8): 915-923.

Sompong W and Adisakwattana S 2015. Inhibitory effect of herbal medicines and their trapping abilities against methylglyoxal- derived advanced glycation end-products. BMC Complement Altern Med. 15: 394.

Song Y, Park HJ, Kang SN, Jang SH, Lee SJ, Ko YG, Kim GS and Cho JH 2013. Blueberry peel extracts inhibit adipogenesis in 3T3-L1 cells and reduce high-fat diet-induced obesity. PLoS One. 8(7): e69925.

Stitt AW 2001. Advanced glycation: an important pathological event in diabetic and age related ocular disease. Br J Ophthalmol. 85(6): 746-753.

Suarez G, Maturana J, Oronsky AL and Raventos-Suarez C 1991. Fructose-induced fluorescence generation of reductively methylated glycated bovine serum albumin: evidence for nonenzymatic glycation of Amadori adducts. Biochim Biophys Acta. 1075(1): 12-19.

Suarez G, Rajaram R, Oronsky AL and Gawinowicz MA 1989. Nonenzymatic glycation of bovine serum albumin by fructose (fructation). Comparison with the Maillard reaction initiated by glucose. J Biol Chem. 264(7): 3674-3679.

Suji G and Sivakami S 2007. DNA damage during glycation of lysine by methylglyoxal: assessment of vitamins in preventing damage. Amino Acids. 33(4): 615-621.

Szaleczky E, Prechl J, Feher J and Somogyi A 1999. Alterations in enzymatic antioxidant defence in diabetes mellitus--a rational approach. Postgrad Med J. 75(879): 13-17.

Szkudelska K, Nogowski L and Szkudelski T 2009. Resveratrol, a naturally occurring diphenolic compound, affects lipogenesis, lipolysis and the antilipolytic action

of insulin in isolated rat adipocytes. J Steroid Biochem Mol Biol. 113(1-2): 17-24.

Tagaya Y, Miura A, Okada S, Ohshima K and Mori M 2012. Nucleobindin-2 is a positive modulator of EGF-dependent signals leading to enhancement of cell growth and suppression of adipocyte differentiation. Endocrinology. 153(7): 3308-3319.

Talpate KA, Bhosale UA, Zambare MR and Somani R 2013. Antihyperglycemic and antioxidant activity of *Clitorea ternatea* Linn. on streptozotocin-induced diabetic rats. Ayu. 34(4): 433-439.

Tang QQ, Otto TC and Lane MD 2003. Mitotic clonal expansion: a synchronous process required for adipogenesis. Proc Natl Acad Sci U S A. 100(1): 44-49.

Tappy L and Le KA 2010. Metabolic effects of fructose and the worldwide increase in obesity. Physiol Rev. 90(1): 23-46.

Taranalli AD and Cheeramkuzhy TC 2000. Influence of *clitoria ternatea* extracts on memory and central cholinergic activity in rats. Pharm Biol. 38(1): 51-56.

Terahara N, Oda M, Matsui T, Osajima Y, Saito N, Toki K and Honda T 1996. Five new anthocyanins, ternatins A3, B4, B3, B2, and D2, from *Clitoria ternatea* flowers. J Nat Prod. 59(2): 139-144.

Terahara N, Saito N, Honda T, Toki K and Osajima Y 1990. Structure of ternatin A1, the largest ternatin in the major blue anthocyanins from *Clitoria ternatea* flowers. Tetrahedron Lett. 31(20): 2921-2924.

Terahara N, Toki K, Saito N, Honda T, Matsui T and Osajima Y 1998. Eight new anthocyanins, ternatins C1-C5 and D3 and preternatins A3 and C4 from young *clitoria ternatea* flowers. J Nat Prod. 61(11): 1361-1367.

Thilavech T, Ngamukote S, Abeywardena M and Adisakwattana S 2015. Protective effects of cyanidin-3-rutinoside against monosaccharides-induced protein glycation and oxidation. Int J Biol Macromol. 75: 515-520.

Thilavech T, Ngamukote S, Belobrajdic D, Abeywardena M and Adisakwattana S 2016. Cyanidin-3-rutinoside attenuates methylglyoxal-induced protein glycation and DNA damage via carbonyl trapping ability and scavenging reactive oxygen species. BMC Complement Altern Med. 16: 138.

Thornalley PJ 2003a. Glyoxalase I--structure, function and a critical role in the enzymatic defence against glycation. Biochem Soc Trans. 31(6): 1343-1348.

Thornalley PJ 2003b. Use of aminoguanidine (Pimagedine) to prevent the formation of advanced glycation endproducts. Arch Biochem Biophys. 419(1): 31-40.

Thornalley PJ 2005. Dicarbonyl intermediates in the maillard reaction. Ann N Y Acad Sci. 1043: 111-117.

Tsao R 2010. Chemistry and biochemistry of dietary polyphenols. Nutrients. 2(12): 1231-1246.

Tsuda T 2012. Dietary anthocyanin-rich plants: biochemical basis and recent progress in health benefits studies. Mol Nutr Food Res. 56(1): 159-170.

Uribarri J, Cai W, Woodward M, Tripp E, Goldberg L, Pyzik R, Yee K, Tansman L, Chen X, Mani V, Fayad ZA and Vlassara H 2015. Elevated serum advanced glycation endproducts in obese indicate risk for the metabolic syndrome: a link between healthy and unhealthy obesity? J Clin Endocrinol Metab. 100(5): 1957-1966.

Urios P, Grigorova-Borsos A-M and Sternberg M 2007. Flavonoids inhibit the formation of the cross-linking AGE pentosidine in collagen incubated with glucose, according to their structure. Eur J Nutr. 46(3): 139-146.

Vander Jagt DL 2008. Methylglyoxal, diabetes mellitus and diabetic complications. Drug Metabol Drug Interact. 23(1-2): 93-124.

Wallace TC, Slavin M and Frankenfeld CL 2016. Systematic Review of Anthocyanins and Markers of Cardiovascular Disease. Nutrients. 8(1): 32.

Wang H, Meng QH, Gordon JR, Khandwala H and Wu L 2007. Proinflammatory and proapoptotic effects of methylglyoxal on neutrophils from patients with type 2 diabetes mellitus. Clin Biochem. 40(16-17): 1232-1239.

Wang W, Liu H, Wang Z, Qi J, Yuan S, Zhang W, Chen H, Finley JW, Gu L and Jia AQ 2016. Phytochemicals from *Camellia nitidissima* Chi inhibited the formation of advanced glycation end-products by scavenging methylglyoxal. Food Chem. 205: 204-211.

Wang W, Yagiz Y, Buran TJ, do Nascimento Nunes C and Gu L 2011. Phytochemicals from berries and grapes inhibited the formation of advanced glycation end-products by scavenging reactive carbonyls. Food Res Int. 44(9): 2666-2673.

Wang Y and Ho CT 2012. Flavour chemistry of methylglyoxal and glyoxal. Chem Soc Rev. 41(11): 4140-4149.

Wautier J and Guillausseau P 2001. Advanced glycation end products, their receptors and diabetic angiopathy. Diabetes Metab. 27(5): 535-544.

Wongs-Aree C, Giusti M and Schwartz S 2006. Anthocyanins derived only from delphinidin in the blue petals of *Clitoria ternatea*. IV International Conference on Managing Quality in Chains-The Integrated View on Fruits and Vegetables Quality 712:437-442.

Wu CH, Huang SM, Lin JA and Yen GC 2011. Inhibition of advanced glycation endproduct formation by foodstuffs. Food Funct. 2(5): 224-234.

Wu CH and Yen GC 2005. Inhibitory effect of naturally occurring flavonoids on the formation of advanced glycation endproducts. J Agric Food Chem. 53(8): 3167-3173.

Wu HJ and Chan WH 2007. Genistein protects methylglyoxal-induced oxidative DNA damage and cell injury in human mononuclear cells. Toxicol In Vitro. 21(3): 335-342.

Wu Q, Li S, Li X, Fu X, Sui Y, Guo T, Xie B and Sun Z 2014. A significant inhibitory effect on advanced glycation end product formation by catechin as the major metabolite of lotus seedpod oligomeric procyanidins. Nutrients. 6(8): 3230-3244.

Xu J and Liao K 2004. Protein kinase B/AKT 1 plays a pivotal role in insulin-like growth factor-1 receptor signaling induced 3T3-L1 adipocyte differentiation. J Biol Chem. 279(34): 35914-35922.

Yang SJ, Chen CY, Chang GD, Wen HC, Chen CY, Chang SC, Liao JF and Chang CH 2013. Activation of Akt by advanced glycation end products (AGEs): involvement of IGF-1 receptor and caveolin-1. PLoS One. 8(3): e58100.

Yim HS, Kang SO, Hah YC, Chock PB and Yim MB 1995. Free radicals generated during the glycation reaction of amino acids by methylglyoxal. A model study of protein-cross-linked free radicals. J Biol Chem. 270(47): 28228-28233.

Yoon S-R and Shim S-M 2015. Inhibitory effect of polyphenols in *Houttuynia cordata* on advanced glycation end-products (AGEs) by trapping methylglyoxal. Food Sci Technol. 61(1): 158-163.

Yun JW 2010. Possible anti-obesity therapeutics from nature--a review. Phytochemistry. 71(14-15): 1625-1641.

Zhao F, Tang YZ and Liu ZQ 2007. Protective effect of icariin on DNA against radical-induced oxidative damage. J Pharm Pharmacol. 59(12): 1729-1732.

Zhao Y, Wang P, Chen H and Sang S 2016. Dietary quercetin inhibits methylglyoxal-induced advanced glycation end products formation in mice. The FASEB Journal. 30(1): 692.694.

Zhu D, Wang L, Zhou Q, Yan S, Li Z, Sheng J and Zhang W 2014. (+)-Catechin ameliorates diabetic nephropathy by trapping methylglyoxal in type 2 diabetic mice. Mol Nutr Food Res. 58(12): 2249-2260.

Zong H, Ward M and Stitt AW 2011. AGEs, RAGE, and diabetic retinopathy. Curr Diab Rep. 11(4): 244-252.

APPENDIX

Western blot

Chemical preparations

1. Tris-buffered saline (TBS) buffer (25X)

- NaCl (final concentration = 137 mM) 20 g

- Tris base 0.5 M (final concentration = 20 mM) 6.02 g

- dissolve in deionized water 80 mL

- adjust pH with10 N HCL to pH 7.5

- adjust the volume to 100 ml with deionized water

2. Tris-buffered saline with Tween 20 (TBST) buffer

- 450 mL of distilled water

- 50 mL of TBS

- 500 µL of tween 20 (0.1% of tween)

3. 5% BSA-TBST

- 100 mL of TBST

- 5 g of BSA fraction V

4. RIPA buffer

- 150 mM NaCl

- 1% NP40

- 0.5% Nadeoxycholate

- 0.1% SDS

- 50 mM Tris pH8.0

Procedure

Step1 cell lysis

1. Cell sample was lysed by RIPA buffer.
2. The sample was incubated at 4 ℃ for 30 mins.
3. The cell was detached by scraper.
4. The cell lysate was transferred to Eppendorf tube and then centrifuged at 12,000 rpm 4 ℃ for 5 min.
5. The supernatant was used to quantified the total protein by BCA assay kit.

Step2 gel electrophoresis

1. 100 µL of the cell lysate from step1 was mixed with 25 µL of sample buffer.
2. The sample was heat at 95 ℃ for 10 mins.
3. The sample was loaded into the gel at 125 volts for 1 h.

Step3 membrane transferring

1. The gel from step2 was put into the electric tank together with membrane, filter paper and cotton mat.
2. The membrane transferring was performed at 100 volts for 1 h

3. The membrane was then blocked by BSA-TBST at room temperature for 30 mins
4. BSA-TBST was removed and then incubated with primary antibody at 4 ℃ overnight.
5. BSA-TBST was removed and washed by TBST 3 times.
6. Secondary antibody was added and incubated at room temperature for 1 h.
7. 150 µL of luminal and peroxidase were added.
8. The membrane was exposed to the film.

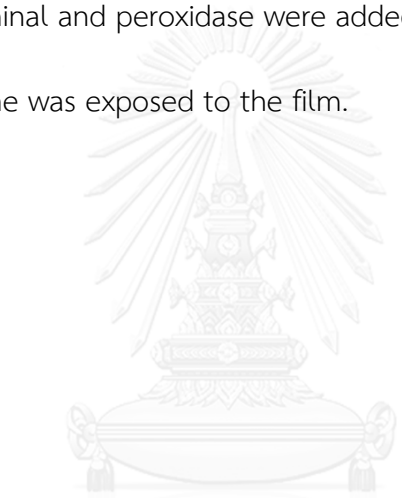

VITA

MR. Poramin Chayaratanasin was born on January 10th, 1985 in Bangkok province, Thailand. In 2009, he graduated with a Bachelor's degree in Doctor of Veterinary Medicine (D.V.M., First class Honors) from the Faculty of Veterinary Science, Chulalongkorn University, Thailand. He is interested about beneficial effects of herbal medicines on diabetes. Then, he enrolled in Doctor of Philosophy program in Veterinary Biosciences, Department of Veterinary Anatomy, Faculty of Veterinary Science, Chulalongkorn University.